Dissertation

submitted to the
Combined Faculties for the Natural Sciences and
for Mathematics of the
Ruperto-Carola University of Heidelberg, Germany
for the degree of
Doctor of Natural Sciences

submitted by
Diplom-Biol. Martin Wurst
born in Konstanz, Germany
Oral examination: 31.5.2011

# Characterization of the RNA binding protein RBP10 in *Trypanosoma brucei*

**Supervisor:** **Prof. Dr. Christine Clayton**
Zentrum für Molekulare Biologie (ZMBH)
Universität Heidelberg
Im Neuenheimer Feld 282
69120 Heidelberg

**Co- Supervisor:** **Prof. Dr. Luise Krauth-Siegel**
Biochemie-Zentrum (BZH)
Universität Heidelberg
Im Neuenheimer Feld 328
69120 Heidelberg

**Danksagung**

Ich möchte mich zuerst bei Prof. Christine Clayton bedanken: nicht nur für die Betreuung meiner Doktorarbeit, sondern auch für die offenen und produktiven Diskussionen.

Bei Luise Krauth-Siegel möchte ich mich für die Übernahme des Koreferats sowie interessante Seminare bedanken.

Den Mitgliedern des Clayton-Labors möchte ich für eine tolle Arbeitsatmosphäre und den sonstigen Aktivitäten wie Kubb bedanken. Es war stets schön im Labor von netten Menschen wie Stuart, Mhairi, Doro, Conny, Valentin, Praveen, Theresa, Abeer, Conny, Diana, Ute, Claudia, Esteban, Julius, Bhaskar, Bernard und Aditi umgeben zu sein. Vielen Dank für eine schöne Zeit.

Ein spezieller Dank an Doro und Theresa für das Korrekturlesen meiner Arbeit.

# Table of Content

## Summary

*Trypanosoma brucei* is the causative agent of the African sleeping sickness. Between mammalian hosts it is transmitted by the tsetse fly. Due to the different environments of the hosts the parasite has to adapt its metabolism quickly. *T. brucei* RNA polymerase II lacks transcriptional control; therefore the control of gene expression is exerted mainly at the level of mRNA stability and translation. RNA stability is influenced by the binding of RNA binding proteins (RBPs), which thereby can play a crucial role in gene expression.

This work focused on the characterization of the RNA binding protein RBP10. A polyclonal antibody was raised which showed that RBP10 is only expressed in the BS of the parasite. A knockdown of RBP10 by RNAi in the bloodstream form (BS) of the parasite was lethal after four days. Microarray studies comparing RBP10 knockdown RNA to BS WT RNA revealed a widespread effect on the transcriptome with many BS-specific mRNAs decreased, including many mRNAs encoding proteins involved in glucose metabolism. Further, the effect of the inhibition of glucose uptake by phloretin treatment on the transcriptome was explored and compared to the effect of RBP10 RNAi.
The ectopic expression of RBP10-myc in the PC resulted in a defect in proliferation and also in the expression of endogenous RBP10. Microarray studies showed that in the PC the artificial expression of RBP10 lead to a strong increase of many BS specific mRNAs and a simultaneous decrease of PC specific mRNAs. It could also be shown that the forced expression of RBP10 inhibited differentiation of BS to PC trypanosomes.
Putative direct RNA targets were identified by IP with subsequent purification of bound RNA and deep-sequencing. However, these results do not overlap with the mRNAs affected after RPB10 RNAi. Also using IP probable protein interaction partners were detected revealing among others RBP29, which is known to be on polysomes, and PABP2. In a sucrose gradient RBP10 was not found in the fractions of the heavy polysomes but could be detected in fractions of the free proteins to the fractions of proteins in trisomes.
These findings show that RBP10 is necessary for the expression of many BS specific mRNAs.

# Zusammenfassung

*Trypanosoma brucei* ist der Erreger der Afrikanischen Schlafkrankheit. Die Parasiten werden von der Tsetse Fliege zwischen den menschlichen Wirten übertragen. Deshalb ist es notwendig, dass sie ihren Stoffwechsel schnell an neue Umgebungen anpassen können. Allerdings verfügen diese Parasiten über keine transkriptionelle Kontrolle der Genexpression, weshalb die Kontrolle über Translation und die Stabilität der RNA sehr wichtig sind. Die Lebensdauer einer RNA wird bestimmt durch RNA-bindende Proteine, die daher eine entscheidende Rolle in der Genexpression einnehmen.

In dieser Arbeit wird das RNA bindende Protein RBP10 charakterisiert. Mit Hilfe eines polyklonalen Antikörpers konnte gezeigt werden, dass RBP10 ausschließlich in der Blutstromform (BS) des Parasiten exprimiert wird und eine Reduktion der Proteinmenge für den Parasiten letal ist. Microarray Analysen ergaben dass RBP10 notwendig für die Expression vieler BS spezifischen mRNAs ist, darunter sind viele mRNAs die für Proteine der Glykolyse kodieren. Deshalb wurde der Effekt von Phloretin, das die Aufnahme von Glukose in die Zellen verhindert, ebenfalls mittels Mikroarray Analyse untersucht und mit den Daten der RBP10 Reduktion verglichen.
Eine Expression von RBP10 in Zellen im prozyklischen Stadium hatte eine Verringerung der Wachstumsrate zur Folge. Zudem wurden viele BS spezifische mRNAs verstärkt exprimiert. Eine Expression von RBP10 in BS Trypanosomen verhinderte zudem die Differenzierung in das prozyklische Stadium.
Durch die Isolierung von an RBP10 gebunden RNAs und deren Sequenzierung konnten potentielle Ziele von RBP10 identifiziert werden. Allerdings konnte keine Übereinstimmung mit den Ergebnissen der Mikroarray Analyse gefunden werden. Mögliche Bindungspartner von RBP10 konnten mittels Massenspektroskopie ermittelt werden. Unter anderem wurde RBP29, welches in Polysomen gefunden wurde, wie auch PABP2 identifiziert.
Die Ergebnisse zeigen, dass RBP10 für die Expression für viele BS spezifische mRNAs benötigt wird.

# 1. Introduction

## 1.1 Kinetoplastids

*Trypanosoma brucei* is an extracellular parasite which belongs to the class of Kinetoplastida. As seen by the analysis of the 16S rRNA, Kinetoplastids have branched early from the eukaryotic lineage [1]. They have developed several unique features not seen in other eukaryotes like the kinetoplast from which they derived their name. The kinetoplast is a microscopically visible structure containing the mitochondrial DNA. It is unique in terms of structure and replication [2], [3]. Research has focused on three different species of Kinetoplastida: *Trypanosoma brucei*, *Leishmania major* and *Trypanosoma cruzi*. *T. cruzi* is transmitted by the reduviid bug and causes the Chagas disease mainly in Mexico, Central and South America. *Leishmania major* is responsible for leishmaniasis and is transferred by the sandfly. *Trypanosoma brucei* is transmitted by the tsetse fly vector and has three subspecies: *T. b. brucei*, *T. b. gambiense* and *T. b. rhodesiense*. *T. b. gambiense* causes a chronic infection and can be found mainly in central and West Africa. For these parasites humans are thought to be the reservoir [4] since the infection may be unnoticed for a long time. An infection with *T. b. rhodesiense* in contrast causes a quite rapid illness and is spread in southern and east Africa. Here animals and livestock are thought to be the reservoir [4]. *T. b. gambiense* accounts for 95% of the reported cases of sleeping sickness. Currently there are 30,000 people infected (www.who.int). *T. b. brucei* on the other hand causes animal African trypanosomiasis and is not infectious for humans because it is susceptible to lysis in human blood by the human apolipoprotein L1 [5]. Since *T. b. brucei* is both not pathogenic to humans and also accessible to genetic manipulations it serves as a model organism for other kinetoplastids and is commonly studied in laboratories.

## 1.2 Life cycle of *T. brucei*

Trypanosomes undergo a full life cycle (**Fehler! Verweisquelle konnte nicht gefunden werden.**) when they are transmitted between humans by the tsetse fly, *Glossina* spp. After a bloodmeal of the fly from an infected person the parasites accumulate in the midgut as a proliferative form. Here the parasites are called procyclic trypanosomes (PC). Then they arrest their cell cycle and migrate to the salivary glands where they continue their replication as epimastigotes. At last the parasites differentiate into metacyclin trypomastigotes, which are non-proliferative and have adapted their surface coat to the mammalian host by expressing Variant Surface Glycoproteins (VSGs). Then they can be transmitted to the mammalian host after a bite of the fly. During their life cycle trypanosomes have to change both their morphology and their metabolism drastically in order to adapt to the different environments of their hosts. PC trypanosomes have a fully functional mitochondrion which is larger than in trypanosomes of the bloodstream form (BS). PC mainly utilize proline as the energy source [6] but are also able to use glucose if available [7]. The surface of PC trypanosomes is covered by acidic and proline-rich EP/GPEET proteins. These are linked to the cell surface by a glycosylphosphatidylinositol (GPI) anchor [8]. This protects the parasite from proteolysis in the midgut of the tsetse fly [9].

In the BS the surface coat consists of a dense layer of VSGs. VSGs are massively expressed and constantly recycled [10]. Additionally, there are ~ 1000 different copies of VSG in the genome, from which only one is expressed from the active expression site [11]. By antigenic variation of the expressed VSG, trypanosomes can escape the human immune system [12] since the few parasites, that have switched the surface protein are not recognized by the existing antibodies. BS trypanosomes depend on the glucose of the host's blood and generate all ATP by glycolysis. The mitochondrion is not fully functional in this life stage. As the number of parasites increases in the human blood the trypanosomes start to differentiate into the stumpy form. Stumpy parasites are non-proliferative and cell-cycle arrested in G1 phase but are prepared to be transmitted into the tsetse fly.

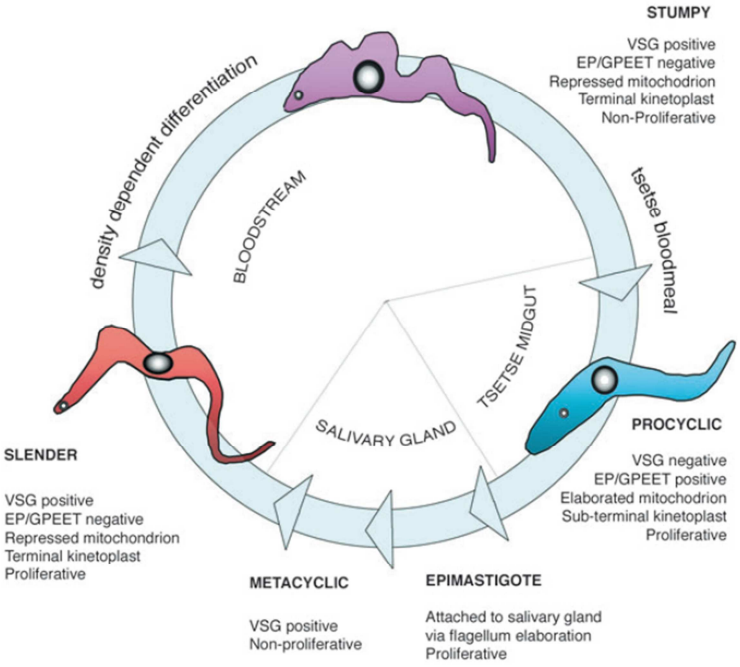


**Fig. 1**: Life cycle of *T. brucei*, from [13].

## 1.3 Differentiation of *T. brucei*

During differentiation of BS to the PC, trypanosomes have to control their gene expression tightly in order to adapt to the different environments. Up to 25 % of all transcripts are regulated during transformation from BS to PC [14] [15] [16] [17]. The amount of mRNAs that are found to be regulated depends on the technique used and also on the applied thresholds. Some of the gene regulation that is seen during differentiation is required in order for the parasites to adapt to new energy sources. In the human host, the bloodstream form of the parasite derives its ATP from glucose catabolism by glycolysis. The glucose is taken up into the cell mainly by the glucose transporter THT1 [18] and utilised in the glycosomes, which are microbodies containing most of the glycolytic enzymes. In vitro, the differentiation from BS to PC can by triggered by the addition of *cis*-aconitate to the medium [19] and a shift from 37°C to 27°C; differentiation is facilitated by *cis*-aconitate transporters [20], and involves a signalling pathway that includes protein phophatases [21]. Interestingly, the removal of glucose alone is also sufficient for the cells to start differentiation [22] and a similar effect is seen after inhibition of the glucose transporter using phloretin [23]. During differentiation, the trypanosomes' surface coat of variant surface glycoprotein (VSG) is replaced by EP and GPEET procyclins [24].

## 1.4 Gene expression in trypanosomes

### 1.4.1 Transcription and splicing

Trypanosomes indeed are special in the way they express their genes. Most of the mRNAs are transcribed by RNA-polymerase II (RNAP II), but in contrast to higher eukaryotes the search for promoters has been elusive so far. Furthermore transcription by RNAP II leads to very long polycistronic precursor RNAs including sometimes more than 100 genes which are not functionally clustered. Neighboring units of polycistronic transcription can be convergent or divergent; the region between the units is called strand switch region (SSR) [25]. Certain histone variants are enriched at RNAP II transcription start sites while other variants are enriched at transcription termination sites [26] and mark the boundaries of the transcription units. It seems as if transcription initiation by RNAP II would be regulated by the histone modifications instead by transcription factors. The transcribed precursors are subsequently *trans*-spliced into the single mRNAs, whereupon a 39 nucleotide long spliced leader RNA is added to the 5' end of each mRNA. This spliced leader itself is transcribed by RNAP II and has a cap structure. *Trans*-splicing also is the preceding step for polyadenylation; these two reactions seem to be coupled [27], [28]. However, not all mRNAs are transcribed by RNAP II: The mRNAs encoding the surface proteins VSG and EP/procyclins are transcribed by the RNA polymerase I [29], [30]. With a few exceptions, mRNAs in trypanosomes do not contain introns: The gene encoding the poly-A polymerase [31] was found to have an intragenic region which is *cis*-spliced. A further search for genes containing introns revealed only a putative RNA helicase [32]. A characterization of the *T. brucei* transcriptome by RNA sequencing showed no additional genes harboring introns.

### 1.4.2 RNA degradation in *T. brucei*

The regulation of gene expression is crucial for *T. brucei* in order to adapt to the environments of the different hosts. Since transcription seems not to be regulated mRNA degradation and translation exert the main control over gene expression as suggest by [33], but also mRNA localization, mRNA export, posttranslational modification and the efficiency of *trans*-splicing could have an influence. A lot of research has focused on the degradation on mRNAs. In yeast and in mammalian cells, deadenylation is usually the first and rate limiting step in RNA decay. The degradation then can occur by two different pathways: either in the 3' to 5' direction by the exosome [34], or in the 5' to 3' direction by XRN1. For the 5' to 3' degradation the cap has to be removed first, which is done by the decapping enzymes Dcp2 [35] or, in mammalian cells, also Nudt16 [36]. Trypanosomes don't differ very much in terms of RNA degradation from mammalian cells: the first step in RNA degradation is deadenylation [37]. Then the exosome degrades RNA from the 3' end [38]. It has an exonuclease and an endonuclease activity and is thought to be associated with unstable RNAs like *EP*. The alternative pathway for degradation takes place from the 5' end, which requires a preceding decapping of the mRNA. However, the decapping enzymes of *T.brucei* have not yet been identified. The *T. brucei* genome encodes for four homologs of the 5' to 3' exoribonuclease XRN1 named XRNA, XRNB, XRNC and XRND. Only XRNA it has been shown to be important in mRNA degradation [39], (Manful et al, unpublished data). XRNA depletion also affects transcripts that are unstable or developmentally regulated as *EP* or *PGKC*, but also seems to have a small effect on more stable mRNAs. In mammalian cells RNA degradation via XRN1 is assumed to take place in cytosolic granules called P-bodies [40]. The presence of these structures have also been shown in trypanosomes [41], but their influence on mRNA degradation still needs to be investigated.

### 1.4.3 Regulation of mRNA stability by RNA binding proteins via motifs in the 3' untranslated region

In mammals the stability of mRNAs encoding for example for cell cycle regulators or cytokines is mediated by AU-rich elements in the 3' UTR (untranslated region) of the mRNA. An estimated 5-8% of all human mRNAs contain AU-rich elements (ARE). Proteins that can bind to these elements are called ARE-BPs and have RNA binding domains like the RNA recognition motif (RRM), Zink finger motif or the K Homology (KH) domain. The bound proteins can then determine the stability of the mRNA. A well characterized protein is HuR, which stabilizes its target [42] [43]. HuR is an RBP containing three RRMs, which mediate the binding to single stranded RNA [44], [45]. Other proteins like TTP and BRF-1 [46][47] have a destabilizing effect on mRNAs containing an ARE sequence.

In trypanosomes proteins bearing these RNA binding motifs are present, too. In *T. brucei* 75 RNA binding proteins (RBPs) with at least one RRM have been identified [48]. The RRM motif contains about 90 amino acids, including the canonical RNP1 motif. In a recent *in silico* screen 48 RBPs with a Zinc finger motif have been found [49]. At least 10 RBPs with PUF-domains were identified in *T.brucei* [50].

The sequences within the trypanosome mRNAs that mediate degradation are, at least in some cases, present in form of U-rich elements (URE), which are similar to AREs of mammalian cells. In *T. cruzi* the RBP UBP1 has been shown to bind to UREs of SMUG mucin mRNAs [51]. The binding of UBP1 is achieved by a complex formation with the RBP UBP2 and the Poly-A-binding protein TcPABP1 [52] and destabilizes the target. Homologues of TcUBP1 and TcUBP2 are also expressed in *T. brucei*; they bind to an mRNA encoding for an F-box domain protein [53], although the binding to the mRNA was proposed to have little specificity. Also the expression of the human HuR in *T. brucei* had an effect: mRNAs containing AREs like *EP* and *PGKB*, which are normally unstable in the BS, showed an increase in abundance [54]. In this case the ARE is responsible for the stage-specific degradation of mRNAs. Previously it already had been shown by the usage of reporter constructs that sequences in the 3'UTR are responsible for the strong developmental regulation of the phosphoglycerate kinases mRNAs [55]. Also the mRNAs encoding the glucose transporters THT1 and THT2 are regulated by sequences in their 3' UTR [56]. It is not yet known how RBPs influence the stability of their targets. It is possible that destabilizing RBPs could interact with the mRNA degradation machinery. Stabilizing RBPs could in the opposite way compete with destabilizing factors.

Since the stabilities of mRNAs of all genes in the genome have to be regulated permanently due to the lack of transcriptional control, it is quite unlikely that an RBP only acts on a single mRNA. Rather it is probable that RBPs bind to a subset of RNAs which are regulated in the same manner. Indeed transcriptome analysis of differentiating cells revealed clusters of RNAs which are both functionally related and whose RNA abundance is changed in the same way [15], although they are not derived from the same precursor RNA. The mRNAs encoding proteins involved in glucose metabolism could be shown to be similarly regulated, together with the RNA binding protein RBP10. This would mean it is likely that those mRNAs may have similar sequences in their 3' or 5' UTR, but the search for motifs has not been successful so far. However, [57] showed that the RNA binding protein DRBD3 binds to a subset of developmentally regulated mRNAs encoding membrane proteins. The protein-RNA interaction could be narrowed down to a certain region in the 3' UTR of the mRNA. Also in *Leishmania* the existence of two specific motifs *Lm*Sider1 and *Lm*Sider2 was shown to be responsible for stage-specific regulation [58]. In *T. brucei* Puf9, an RBP with a Puf RNA

binding domain, has been shown to have a stabilizing effect on mRNAs encoding for proteins that are cell-cycle regulated, such as LIGKA [59].

Since RBPs seem to influence mRNAs on a large range the regulation of the RBPs themselves is crucial. A fast response, for example to environmental changes, can be achieved by posttranslational modifications like phosphorylation. In humans a well-studied protein is HuR: upon phosphorylation it is transported from the nucleus to the cytoplasm and stabilizes several target mRNAs [60]. In trypanosomes regulation of RBPs by phosphorylation is possible: According to [61] *T. brucei* has 182 predicted protein kinases which is twice as many as in mammalian cells in relation to percentage of the proteome. In this study the phosphoproteome of BS trypanosomes has been investigated. It revealed a significant number of phosphorylated proteins involved in DNA/RNA processing. This makes it likely that phosphorylation might play a role in the regulation of the activity of RBPs. For other events phosphorylation has already been shown to be essential: The differentiation from the BS to PC, which is triggered by *cis*-aconitate [19], is mediated by the transporter PAD1 [20] and the tyrosine phosphatase PTP1 [62], which regulates a second phosphatase named PIP39 [21].

## 1.5 Glucose metabolism in BS trypanosomes

BS trypanosomes rely on glucose taken up from the host's blood to generate ATP [63]. Glucose is taken up by the glucose transporter THT1, whose expression is increased in the BS compared to the PC [64], [18]. Utilization of glucose takes place in the glycosomes, which are peroxisome like organelles only found in trypanosomes and related Kinetoplastida [65]. Glycosomes are enclosed by one phospholipid bilayer and currently it is not known how the glucose is transported into the organelle. In the BS more than 90% of glycosomal proteins are involved in glycolysis, this percentage is decreased in the PC [66, 67]. However, only the first seven steps of glycolysis take place in the glycosomes; the stepwise degradation of 3-phosphoglycerate to pyruvate, which is the only end product under aerobic conditions, takes place in the cytosol [68]. Under anaerobic conditions a small amount of glycerol is produced and excreted. The last enzymatic step in the glycosome differs between BS and PC: In the BS the phosphoglycerate kinase PGKC is expressed, which is localized to the glycosome, while PC express PGKB, which is found in the cytosol. An expression of the wrong isoform is lethal in BS trypanosomes [69]. The control over glycolytic flux depends on the concentration of glucose in the blood: At the normal blood glucose concentration of 5 mM the flux control coefficient of the glucose transporter is between 0.3 and 0.5 [70], leaving the remaining control to aldolase, glyceraldehyde-3-phosphate dehydrogenase, phosphoglycerate kinase, and glycerol-3-phosphate dehydrogenase [71]. The flux control coefficient of the transporter increases with decreasing glucose concentration. Inhibition of glycolytic flux is feasible by either 2-deoxy-D-glucose (2-DOG) [72] or phloretin [70]. 2-DOG acts as inhibitor of glucose import and also on Hexokinase activity if inside the glycosome. Phloretin is not imported into the cell and inhibits the uptake of glucose by the transporter. It has been shown that a decrease of the glycolytic flux of 30 - 50% is sufficient to block growth of trypanosomes [23].

## 1.6 Aims of the thesis

The objective of this thesis is the characterization of the RNA binding protein RBP10. Furthermore I want to assess its impact on the RNA metabolism in the cell, to identify the direct mRNA targets, possible protein interaction partners and investigate a possible phosphorylation detected by [61].

# 2. Materials and Methods

## 2.1 Trypanosome culture

Except for two experiments all cells used in this study were derived from the Lister 427 strain. BS Trypanosomes which were kept in culture for a long time have lost the ability to undergo a complete differentiation and are called monomorphic. For the differentiation experiment (chapter 3.6) and the investigation of the effect of phloretin on RBP10 (chapter 3.7), EATRO1125 (clone AnTat 1.1) pleomorphic trypanosomes were used which still have the ability to undergo complete differentiation. All BS are kept in modified HMI9 medium [73] at 37°C, PC in MEM [74] at 27°C. For stable transfections $2x10^7$ cells were transfected by electroporation with 10-12 µg of Not1 linearized plasmid. After addition of the drug the cells were diluted to obtain single clones. Antibiotics were used in the following concentrations: phleomycin 0.2 µg/ml (BS) and 0.5 µg/ml (PC); hygromycin B 10 µg/ml (BS) and 50 µg/ml (PC). The induction of RNAi or overexpression of a protein was started 24 h before the cells were collected using 100 ng/ml tetracycline. During proliferation assays cells were diluted every day to $2x10^5$ cells / ml. For differentiation assays pleomorphic cells were used. 24 h before beginning the differentiation the overexpression of RBP10 was induced. At $t_{0\ h}$ cells were at a density of $1.5x10^6$ cells / ml or higher. Then 6 mM *cis*-aconitate was added and cells were shifted to 27°C. At $t_{24\ h}$ cells were centrifuged at 2000 g for 10 min and suspended in preheated MEM medium without tetracycline or *cis*-aconitate.

## 2.2 Inhibition of glucose uptake

Phloretin was purchased from Sigma. It was dissolved in 70% ethanol and added in a concentration of 100 µM to cells at a density of approximately $5x10^5$ cells / ml. This resulted in a slow but reproducible growth to ~$8x10^5$ cells / ml in 24 h.

## 2.3 Cell fractionation, Western blotting and immunofluorescence

Cell fractionation was performed as described in [75]. For standard Western blot analysis $3x10^6$ cells were harvested by centrifugation at 2000 g for 10 min, washed with 1ml PBS and suspended in 13 µl 2x protein loading buffer. Western blots were probed with RBP10 antibody (1:500, α rat), EP repeat (Cedar Lane, 1:2000, α mouse), XRND (1:1000, α rabbit), V5 (1:1000, α mouse) and Tubulin (1:2000, α mouse). Immunofluorescence was done as described in [75]. Additionally z-stacks with a distance of 0.14 µm were taken for 3d-deconvolution using the wiener filter.

## 2.4 Pulse labeling with $^{35}$S-methionine

2 x $10^6$ BS cells were grown to a density of ~5x$10^5$ cells /ml, centrifuged and suspended in 400 µl labeling medium. After one hour 125 µCi of [35S]-methionine$^{35}$S was added and was incorporated into newly synthesized proteins for one hour. Then cells were washed twice in PBS, lysed in 20 µl protein loading buffer and run on a SDS gel. Afterwards the gel was fixed for 45 min in a mix of 10% acidic acid, 30% methanol and 60% $H_2O$ and incubated in en$^3$hance solution (Perkin Elmer) for 45 min. The gel was washed with $H_2O$ and dried for 3 hours at 65 °C. The gel then was exposed to an x-ray film at -80 °C.

## 2.5 RNA preparation and Nothern blotting

RNA was prepared from cells not exceeding 1.5 x $10^6$ cells/ml (BS) or 2 x $10^6$ cells/ml (PC). Cells were harvested and either suspended in PeqGold Trifast (Peqlab) or the RNA was extracted using the RNeasy mini kit (Qiagen). For Nothern blot analysis 10 µg of total RNA were separated by formaldehyde gel electrophoresis as described in [59], blotted onto a nylon membrane (GE Healthcare) and hybridized with α-[$^{32}$P] radioactive DNA probes (Prime-IT RmT Random Primer Labelling Kit, Stratagene), which were made according to manufacturer's protocol. The signals were measured with a phosphoimager and normalized to the signal of the *7SL* probe (signal recognition particle RNA).

## 2.6 Microarray analysis

cDNA synthesis and slide hybridisations were performed as described in [15] with the following changes: 12 µg of total RNA were used per hybridisation; the cDNA synthesis was performed with 400 U RevertAid™ H Minus Reverse Transcriptase (Fermentas), the appropriate reaction buffer and 40 U Ribolock (Fermentas). The reaction was incubated for 2 hours at 43 °C. DNAse treatment, cDNA purification and scanning of the slides were done as in [15]. The microarray slides (version 3 of *Trypanosoma brucei*) were obtained from the Pathogen Functional Genomics Resource Center – J. Craig Venter Institute.

Data analysis was done using ExpressConverter and MIDAS software (freely available at http://www.tm4.org). Files obtained from the scan were background-substracted and transformed into .mev – files using ExpressConverter. Using MIDAS the signal intensities were normalized by locally weighted linear regression and duplicate spots on each slide were merged. $Log_2$ transformed data were exported to SAM as described [76]. All RNAs with a change of 1.5 fold or higher and a p-value of $\leq 0.5$ were considered to be significantly regulated.

## 2.7 Immunoprecipitation (IP)

4 x$10^8$ BS cells expressing RBP10-myc were harvested with a maximal density of 1.5 x$10^6$ cells/ml. The same amount of BS WT cells was used as control. The cells were lysed in 1ml lysis buffer consisting of 10 mM NaCl, 10 mM TRIS pH 7.5, 0.1% Igepal and 1 Complete Inhibitor (Roche; 1 minitablet was dissolved in 7 ml buffer). Cell debris was pelleted at 17.000g for 20 min and supernatant was adjusted to 100 mM NaCl. 50 µl of myc-agarose beads (Sigma) were added and incubated for 90 minutes. Afterwards the beads were washed

4x 10 min in lysis buffer adjusted to 100 mM NaCl. Then 30 µl of NaCl adjusted lysis buffer and 30 µl protein loading buffer were added and the samples boiled for 5 min.

## 2.8 RNA – IP

$4x10^8$ cells expressing RBP10- myc were grown to a density of 1.2 $x10^6$ cells/ml, washed once in ice-cold PBS, UV crosslinked with 400 mJ and a wavelength of 254 nm, centrifuged again and snap-frozen. All following steps were carried out at 4°C or on ice. Cells were lysed in 400 µl lysis buffer containing 10 mM NaCl, 10 mM TRIS pH 7.5, 0.1% Igepal, 8 mM Ribonucleoside-Vanadyl Complexes and 1000 U RNasin (Promega). Cell debris was pelleted at 17.000 g and supernatant was adjusted to 150 mM NaCl. 50 µl of myc-agarose beads (Sigma) were added, and incubated for one hour. Afterwards beads were separated by centrifugation and washed three times with cold PBS. Proteinase K (Sigma) was added and degradation of proteins occurred at room temperature for 15 min. Then RNA was extracted using the Trifast FL (Peqlab) according to manufacturer's protocol.

## 2.9 Expression of recombinant RBP10 for polyclonal antibody

Full length open reading frame (ORF) of RBP10 (Tb927.8.2780) was cloned into the vector pQE-38 (Qiagen). The resultant plasmid pHD1990 was used for transformation of the *E. coli* strain BL21(DE3)pLysS (Stratagene). Bacteria were grown to $OD_{600}$ of 0.6 and induced with 1 mM isopropyl - β - D – thiogalactopyranoside for two hours at 37°C. The recombinant protein was purified using Ni-NTA agarose (Qiagen) according to the manufacturer's protocol (Qiagen expressionist) for purification under denaturing conditions. RBP10-HIS was eluted once with pH 5.9 and four times with pH 4.5 (Fig. 2.1). The "elution 2 pH 4.5", in total 2 mg, was dialyzed against 1xPBS at 4°C over night and sent to Charles River Laboratories for inoculation of a rat.

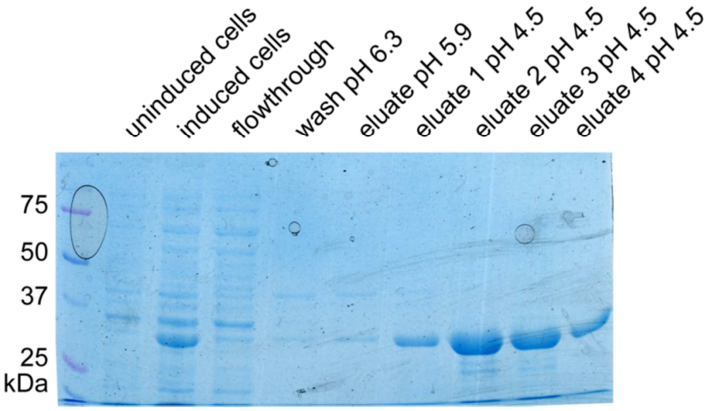


**Fig. 2**: Purification of recombinant HIS-tagged RBP10 under denatured conditions.

The obtained serum recognized both the recombinant protein and the endogenous RBP10 of *T. brucei* with a dilution of 1: 500 in 5% (W/V) milk powder in PBS-T (Fig. 4 and Fig. 19)

## 2.10 Dephosphorylation assay

The dephosphorylation was performed with lambda phosphatase and the respective buffers from New England Biolabs (NEB). All steps were carried out at 4°C or on ice. $2x10^7$ BS cells were lysed in 47 µl lysis buffer (50 mM TRIS, 50 mM NaCl, 2 mM $MgCl_2$ and 0.1% Igepal). For 7 ml of lysis buffer 1 minitablet of complete protease inhibitor (Roche) was added. Cells were centrifuged for 10 min with 17.000g, and then the supernatant was transferred to a new tube. Afterwards 6 µl 10x reaction buffer (NEB), 6 µl $MnCl_2$ (NEB) and 1 µl lambda phosphatase were added and incubated on ice for 20 min. Reaction was terminated by the addition of 60 µl protein loading dye and heating to 95°C prior to separation of proteins by SDS-PAGE.

## 2.11 Used plasmids and primers

Primers and Plasmids used in this thesis are listed in **Table 1**and **Table 2**, respectively.

**Table 1**: Primers used for cloning the vectors listed in table 2.

| Primer | Sequence 5' to 3' |
|---|---|
| cz3309 | ATC CAA GCT TAT GCG TAA CGT TTA TGT C |
| cz3309 | ATC CAA GCT TAT GCG TAA CGT TTA TGT C |
| cz3312 | ATA TGG ATC CGG CGT CTG CTA TTC GT |
| cz3313 | ATA TGG ATC CGT GAA TTG GCG CTT GCA |
| cz3389 | TAT AGG ATC CTC ACT CCA TTC GAA CCG GA |
| cz3469 | GCA ATC AGC AGC GGA AGC GGT CCT CTC GAC A |
| cz3470 | AGC ATC GCA AGC GGA AGC GGT CCT CTC GAC A |
| cz3471 | AGC ATC AGC GCA GGA AGC GGT CCT CTC GAC A |
| cz3472 | AGC ATC AGC AGC GGA GCA GGT CCT CTC GAC A |
| cz3473 | GCA ATC GCA GCA GGA GCA GGT CCT CTC GAC A |
| cz3474 | TGC TCC TGC TGC GAT TGC TGC GCC AAG CTG T |
| cz3475 | GCTTCCGCTGCTGATTGCTGCGCCAAGCTGT |
| cz3476 | GCTTCCGCTTGCGATGCTTGCGCCAAGCTGT |
| cz3477 | GCTTCCTGCGCTGATGCTTGCGCCAAGCTGT |
| cz3478 | TGCTCCGCTGCTGATGCTTGCGCCAAGCTGT |
| cz3481 | TAG CAA GCT TTC ACT CCA TTC GAA CCG G |
| cz3746 | TAT AGG ATC CCT CCA TTC GAA CCG GA |
| cz4110 | GCG CAA GCT TAT GGG AGA CTC GAT ATC ACC T |
| cz4111 | ATA TGG CGC GCC CTC CAT TCG AAC CGG AGG ATA |
| RBP10 Stem for | GAG AAG ATC TCT CGA GGG AGA CTC GAT ATC ACC TTC |
| RBP10 Stem rev | AGA GGA ATT CGT CGA CTT TCA TTC CCT GAC GCG TG |

**Table 2**: Properties of the cloned vectors

| Construct | Used for | Promoter | Integration target | Selection | Parent construct | Insert | forward primer | reverse primer |
|---|---|---|---|---|---|---|---|---|
| 2098 | expression RBP10-2x-myc | PARP Tet Op | rDNA intergenic | Hygromycin | pHD 1700 | RBP10 ORF | cz4110 | cz3746 |
| 1984 | RBP10 RNAi | PARP Tet Op | rDNA intergenic | Hygromycin | pHD 1445 | RBP10 ORF fragment | RBP10 stem for | RBP10 stem rev |
| 1945 | expression RPB10-TAP | PARP Tet Op | rDNA intergenic | Hygromycin | pHD 918Δ | RBP10 ORF | cz4110 | cz4111 |
| 2104 | expression 4x mutated RBP10 | PARP Tet Op | rDNA intergenic | Hygromycin | pHD 1700 | 4x mutated RBP10 | cz3473 | cz3474 |
| 2105 | expression RBP10 S159G | PARP Tet Op | rDNA intergenic | Hygromycin | pHD 1700 | RBP10 S159G | cz3469 | cz3475 |
| 2106 | expression RBP10 S161G | PARP Tet Op | rDNA intergenic | Hygromycin | pHD 1700 | RBP10 S161G | cz3470 | cz3476 |
| 2107 | expression RBP10 S162G | PARP Tet Op | rDNA intergenic | Hygromycin | pHD 1700 | RBP10 S162G | cz3471 | cz3477 |
| 2108 | expression RBP10 S164G | PARP Tet Op | rDNA intergenic | Hygromycin | pHD 1700 | RBP10 S164G | cz3472 | cz3478 |
| 1990 | expression of recombinant RBP10 in E.coli | | | Ampicillin | pQE 38 (Quiagen) | RBP10 ORF | cz4110 | cz3481 |
| 2053 | expression Fragment 1 of RBP10-2x-myc | PARP Tet Op | rDNA intergenic | Hygromycin | pHD 1700 | RBP10 ORF fragment 1 | cz3309 | cz3312 |
| 2054 | expression Fragment 2 of RBP10-2x-myc | PARP Tet Op | rDNA intergenic | Hygromycin | pHD 1700 | RBP10 ORF fragment 2 | cz3309 | cz3746 |
| 2055 | expression Fragment 3 of RBP10-2x-myc | PARP Tet Op | rDNA intergenic | Hygromycin | pHD 1700 | RBP10 ORF fragment 3 | cz4110 | cz3313 |
| 2056 | expression Fragment 4 of RBP10-2x-myc | PARP Tet Op | rDNA intergenic | Hygromycin | pHD 1700 | RBP10 ORF fragment 4 | cz4110 | cz3312 |
| 1514 | expression RBP10-myc (N-term) | PARP Tet Op | rDNA intergenic | Hygromycin | pHD 1484 | RBP10 ORF | cz4110 | cz3746 |
| 1518 | expression RPB10-myc (C-term) | PARP Tet Op | rDNA intergenic | Hygromycin | pHD 1485 | RBP10 ORF | cz4110 | cz3746 |

The plasmids pHD 2104-2108 are cloned using site directed mutagenesis. The mutations were introduced using the specified primers, the second primer pair was cz4110 and cz3389.

# 3. Results

## 3.1 Expression of RBP10 in BS

RBP10 was found in the *T. brucei* genome in a screen for proteins with the RRM motif [48]. RBP10 is a protein of 32 kDa with one RRM from amino acid 49 to 121 close to its C-terminus. I found that RNAi against RBP10 was lethal in the BS of the parasite while no effect of its depletion could be seen in the PC [77]. In this screen the vector for RNAi had two opposing T7- promoters. Since cell lines transfected with these vectors tend to show unstable RNAi phenotypes I cloned an RNAi vector for an inducible expression of an RNA stemloop, which is generally a more stable system. A 400bp fragment from the ORF of RBP10, which was blasted against the *T. brucei* genome to ensure the absence of off-target effects, was amplified by PCR and cloned into pHD 1146. The resulting vector was transfected into BS 1313 cells, which constitutively express the tet repressor protein. The BS 1313 cell line will be referred to as BS WT in the subsequent text. Positively transfected clones were selected using hygromycin B. The knockdown of RBP10 was induced with 100 ng/ml tetracycline. The decrease of *RBP10* was monitored by Northern blot analysis and, when the antibody against RBP10 was available, the depletion of the protein was measured by Western blot. The decrease of *RBP10* is shown in **Fig. 3**, for the loading control the rRNA levels are displayed. The mRNA of RBP10 has a length of approximately 9kb due to its very long 3'UTR. Fortunately the uninduced RNAi sample does not show a reduction of *RBP10*; the cell line could be maintained in culture without an unintended induction of RNAi.

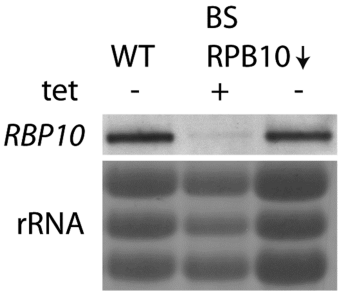


**Fig. 3**: Northern blot showing the RNAi against RBP10 in the BS. The staining of the rRNA serves as loading control.

The depletion of the protein can be seen in **Fig. 4**. RBP10 is almost completely removed after 24 h of RBP10 RNAi while in the BS WT it can easily be detected at the expected size of ~32 kDa. Interestingly RBP10 protein was not expressed in the PC WT in a detectable amount, which could explain the ineffectiveness of RBP10 RNAi in the PC seen in [77]. However, attempts to knock out the RBP10 gene in PC were not successful (work done by B. Seliger). This could either be due to technical problems or could indicate a residual function of the protein in the PC.

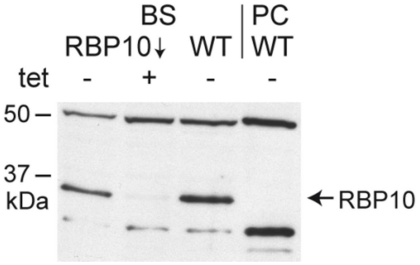


**Fig. 4**: Western blot probed with RBP10 antibody showing the expression of RBP10 in BS WT, BS RBP10 RNAi and PC WT.

The knockdown of RBP10 in the BS had a strong effect on proliferation of the parasite (**Fig. 5**). A decline in growth could be seen after the second day, two days later the RNAi induced cells were dead.

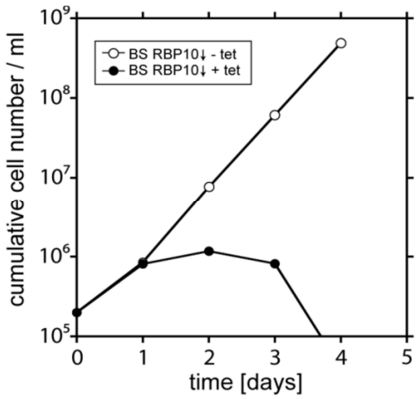


**Fig. 5**: Cumulative growth curve of BS RBP10 RNAi +/- tetracycline. Open circles - tet, filled circles + tet. The cells were diluted to $2x10^5$ cells/ml every day.

## 3.2 Localization of RBP10

To investigate in which step of RNA metabolism RBP10 could be involved in, the localization of the protein was important. Two different approaches were used to address this question. First, subcellular fractionation was done (**Fig. 6**) and showed RBP10, which has been myc-tagged at its C-terminus, in the cytosolic fraction. XRND, which is known to be localized to the nucleus, served as control [39]. For immunofluorescence the TAP-tagged RBP10 was used because two cross-reactions precluded us from using the RBP10 antibody. Attempts at purification to purify the antibody failed. RBP10-TAP was detected with the protein A antibody (**Fig. 7**), BS WT cells served as control. Here RBP10 could also be seen excluded from the nucleus and in distinct particles in the cytosol.

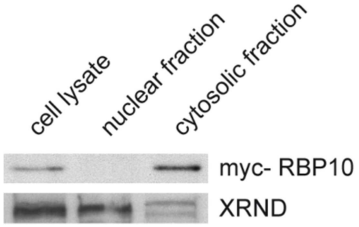


**Fig. 6**: Western blot showing subcellular cell fractionation probed with myc and XRND antibody in BS trypanosomes. XRND serves as a nuclear marker protein.

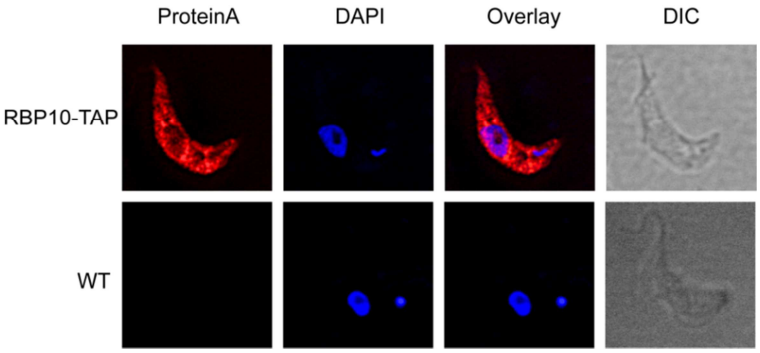


**Fig. 7**: Immunofluorescence against RBP10 TAP in BS using Protein A Antibody for the detection of RBP10-TAP and DAPI for staining the DNA. Z-stacks were taken and deconvolution was done using the wiener filter.

## 3.3 Effect of RBP10 on translation

Since RBP10 is localized to the cytosol it was possible that the protein acts as a factor required for global translation. To investigate whether this is the case I performed a pulse-labelling assay using $^{35}$S- methionine. Exponentially growing cells were removed from the medium and put into labelling medium for one hour. Afterwards they were suspended in medium containing the $^{35}$S methionine which would then be incorporated into newly synthesized proteins. The knockdown of RBP10 was induced 24 hours before. The uninduced RBP10 RNAi strain served as negative control. **Fig. 8** shows that after RBP10 RNAi the translation of a few abundant proteins was decreased (like proteins 2-4), while others were unaffected (for instance number 1). The proteins were not experimentally characterized probably protein 1 was HSP70 and 2-4 were VSG, Aldolase and GAPDH because those proteins are very abundant in the cell and migrate at the corresponding sizes. This outcome ruled out the possibility that RBP10 was a general factor needed for translation, but it didn't reveal whether it acts on the level of translation or any other step of gene regulation such as RNA degradation.

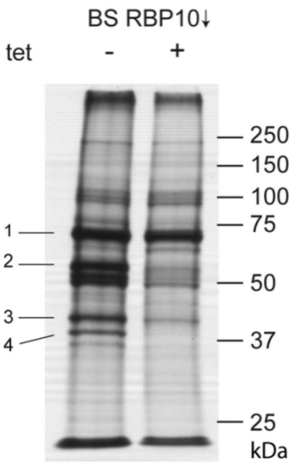


**Fig. 8**: SDS- gel autoradiogram showing the $^{35}$S labelled extracts of RBP10 knockdown cells -/+ tet. RNAi against RBP10 was induced for 24h; after one hour in labeling medium the radioactively labelled $^{35}$S-methionine was added and incorporated into newly synthesised proteins.

## 3.4 Effect of RBP10 RNAi on the BS transcriptome

To examine the effect of RBP10 RNAi on the whole transcriptome, microarray analysis was used. RNA samples of BS cells depleted of RBP10 and of BS WT cells were reverse transcribed into cDNA using Cy3 or Cy5 labeled dCTP. The mixture of both RNA samples was hybridized onto an oligonucleotide microarray slide; after several washes the bound cDNA on the slide could be measured by excitation of the fluorophores. 5 slides including 3 biological replicates and dye-swap were analyzed. Changes of a minimum of 1.5-fold with a p-value of $\leq 0.5$ were considered to be significantly regulated.

595 RNAs were affected by RBP10 RNAi: 275 increased and 320 decreased. The most striking changes in mRNA level were observed for genes involved in sugar metabolism and transport (**Fig. 9** and supplementary Table S1). 21 mRNAs encoding glycosomal proteins or proteins involved in glucose metabolism, and also the major glucose transporter of the BS,

THT1, were decreased. Also broadly affected were genes encoding proteins of the flagellum and the cytoskeleton. A few of the obtained results were confirmed by Northern blotting (**Fig. 10** A-C). Additionally an increase of the mRNA encoding EP and a decrease of *VSG* mRNA could be seen after induction of RBP10 RNAi.

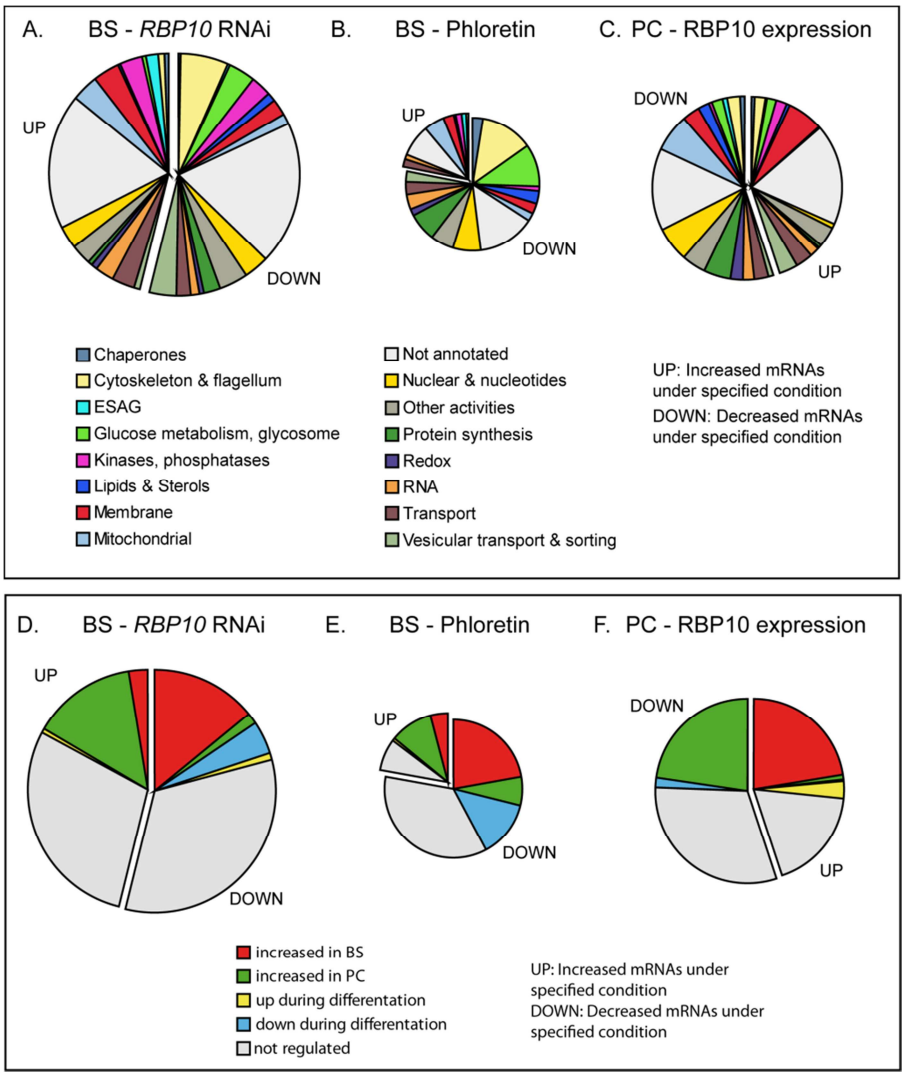


**Fig. 9** A-F: Effects of RBP10 RNAi and phloretin treatment on the BS transcriptome and of RBP10 expression on the PC transcriptome. Exponentially growing bloodstream-form trypanosomes ($2x10^5$/ml for BS RNAi and PC RBP10 expression; $6x10^5$/ml for phloretin treatment) were treated with 100 ng/ml tetracycline or 100 mM phloretin, respectively, for 24 h. Subsequently their RNA was prepared for microarray analysis using untreated cells as a control. The forced expression of RPB10 in PC was induced for 24 h with 100 ng/ml tet; the RNA was compared to PC WT cells.
For each condition the results shown are for five slides including three biological replicates, including dye-swap, with all spots showing significant $P \leq 0.05$ differences of at least 1.5-fold. The colour key is in the figure.
A./B./C. Regulated RNAs of BS RBP10 RNAi/ phloretin / PC RBP10 expression classified according to regulation during differentiation, as seen in [15].
D./E./F. Regulated mRNAs of BS RBP10 RNAi/ phloretin / PC RBP10 expression classified according to the function of the encoded protein [automated and manual annotation, as in [15]].

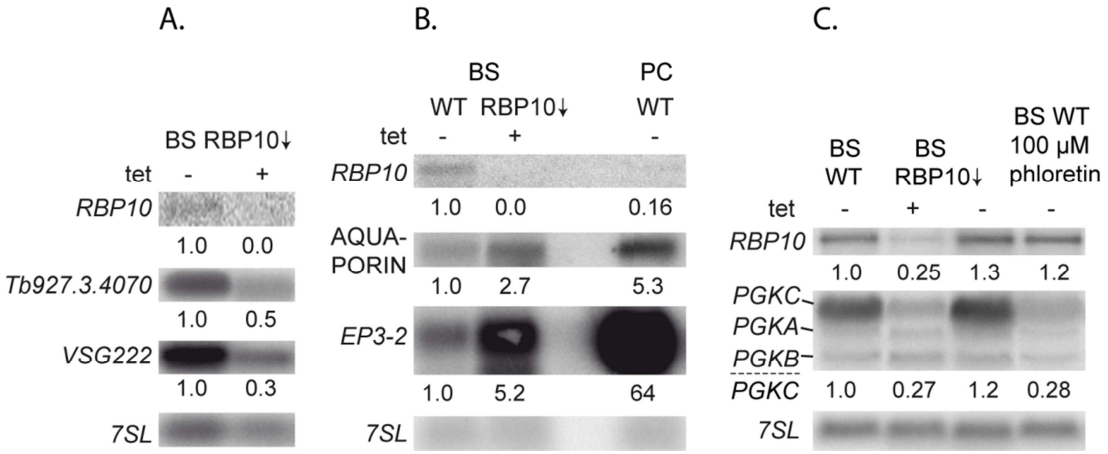


**Fig. 10** A-C: Northern blots showing the effect of RBP10 RNAi on different mRNAs. RNAi was induced for 24 h before RNA was extracted from exponentially growing cells. *7SL* serves as loading control for quantification for each membrane.
A: RBP10 RNAi sample was compared to RNA from uninduced RBP10 knockdown cells. The membrane was probed against the Tb927.3.4070 and the currently expressed *VSG222*.
B: The RNA of RBP10 knockdown cells was compared to BS WT and PC WT RNA. The membrane was probed against Aquaporin and *EP3-2*.
C: The RNA of BS WT cells was compared to RPB10 RNAi and phloretin treated cells. The membrane was probed against the 5' end of the ORF of PGKC which recognizes the mRNA of all PGK isoforms.

Several of the effects seen after RBP10 RNAi in the BS can also be seen after in the beginning of differentiation or after an inhibition of growth. To evaluate whether there was an overlap with the changes in the transcriptome seen during differentiation, I compared the results of RBP10 RNAi to the dataset of [15]. The methodology used in this analysis is very similar to mine and allows a quantitative comparison. The effect of inhibition of glucose uptake by phloretin also had certain similarities to the effect of RBP10 RNAi. Hence the effect of phloretin treatment on the transcriptome was evaluated (published in [23]) and compared to the effect of RBP10 RNAi. For an easier discussion I will use the "PC specific" to mean that an mRNA is more abundant in the PC than in the BS, but not that this according mRNA is only present in PC.
320 mRNAs are decreased after RBP10 RNAi. Among them are 85 BS and only eight PC specific (Fig. 9D). The treatment with phloretin has a smaller effect with 153 mRNAs decreased. Some mRNAs also show a developmental regulation: 44 were BS and 13 PC specific (Fig. 9E). A subset of 71 mRNAs was decreased after both phloretin treatment and RBP10 RNAi. Here, 18 mRNAs encoding proteins of the glucose metabolism or glycosomal proteins and 16 mRNAs encoding proteins of the cytoskeleton or the flagellum could be found. This is most likely a result of a decline in growth which can also be seen in the beginning of differentiation where mRNAs encoding cytoskeletal and flagellar proteins are down-regulated [15].
275 mRNAs increased after RBP10 RNAi (Fig. 9A). Of these, 84 were PC specific and 15 BS specific. In this group several mRNAs encoding mitochondrial and transmembrane proteins were found. The mRNA encoding the transporter PAD1, which is known to be increased in the stumpy form of the parasite [20], was also increased. This also accounts for the developmentally regulated phosphatase PIP39 (Tb10.70.4080) [21]. However, the increase of the mRNA under both conditions, RBP10 RNAi and phloretin, was lower than 1.5 fold and thereby filtered out. A total of 44 mRNAs were increased after phloretin treatment; 20 mRNAs were PC- and 8 BS specific (Fig. 9E). Overall, 91 mRNAs were affected by both RBP10 RNAi and phloretin; the correlation coefficient within this subset is 0.9 (Supplementary table 1). Thus this subset of mRNAs is affected very similarly under both conditions.

## 3.5 Expression of RBP10 induces BS specific mRNAs in PC

RBP10 protein was not detectable in PC. I therefore investigated a possible effect of an ectopic expression of myc-tagged RBP10 in that stage. The *RBP10* 3'UTR has a length of ~8 kilobases (kb), while the 3'UTR of the transgenic mRNA was only ~ 500 nucleotides short. Therefore the two transcripts could be distinguished by Nothern blotting (**Fig. 11**A). It could be seen that ectopic expression of RBP10-myc caused an increase in endogenous *RBP10* mRNA and protein (**Fig. 11**B). Moreover, a defect in proliferation (**Fig. 11**C) was seen; in several experiments the effect was ranging from growth arrest to cell death.

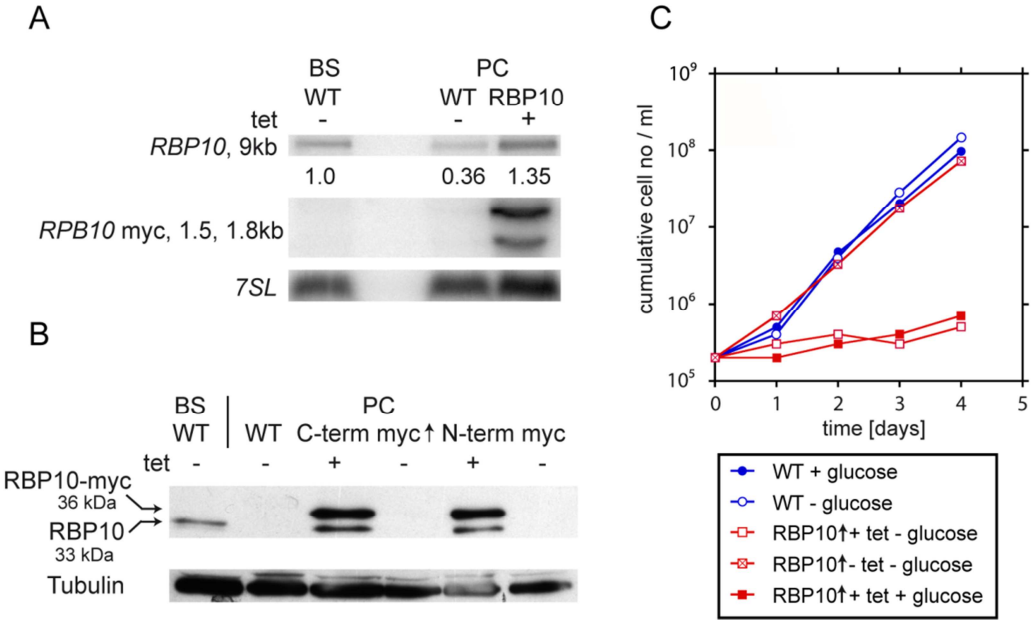


**Fig. 11**: A. Nothern blot showing the forced expression of RPB10-myc in PC which can be detected at 1.5/1.8 kb. The endogenous RBP10 mRNA has a length of ~9kb. *7SL* was used as loading control for quantification. B. Western blot showing the forced expression of RBP10-myc in the PC, the membrane was probed with the RBP10 antibody. Probing against Tubulin served as loading control. C. Cumulative growth curve of PC RBP10 expression. The figure legend is displayed below the graph.

It was of interest whether the anomalous expression of RBP10 had an effect on the mRNAs that were affected by RBP10 RNAi in the BS. The BS specific *THT1* mRNA was decreased to about 30% by RBP10 RNAi in BS trypanosomes (**Fig. 12**A). In PC WT cells, *THT1* is hardly detectable by Northern blotting. Here, the ectopic expression of RBP10-myc raised the amont of *THT1* to the abundance of the BS WT. *THT2*, which is normally higher expressed in the PC compared to the BS, decreased after the expression of RBP10 in PC (**Fig. 12**B). A similar effect could be seen for the developmentally regulated *PGKB* and *PGKC* mRNAs (**Fig. 12**C). Usually, BS trypanosomes express PCKC and display a higher level of *PGKC* than *PCKB*. In PC, PGKB is expressed and *PGKB* is more abundant than *PGKC*. The expression of RBP10 in PC led to an increase of *PCKC* and a decrease in *PCKB*. However, the effect on *THT1* was stronger than on the *PGK* mRNAs.

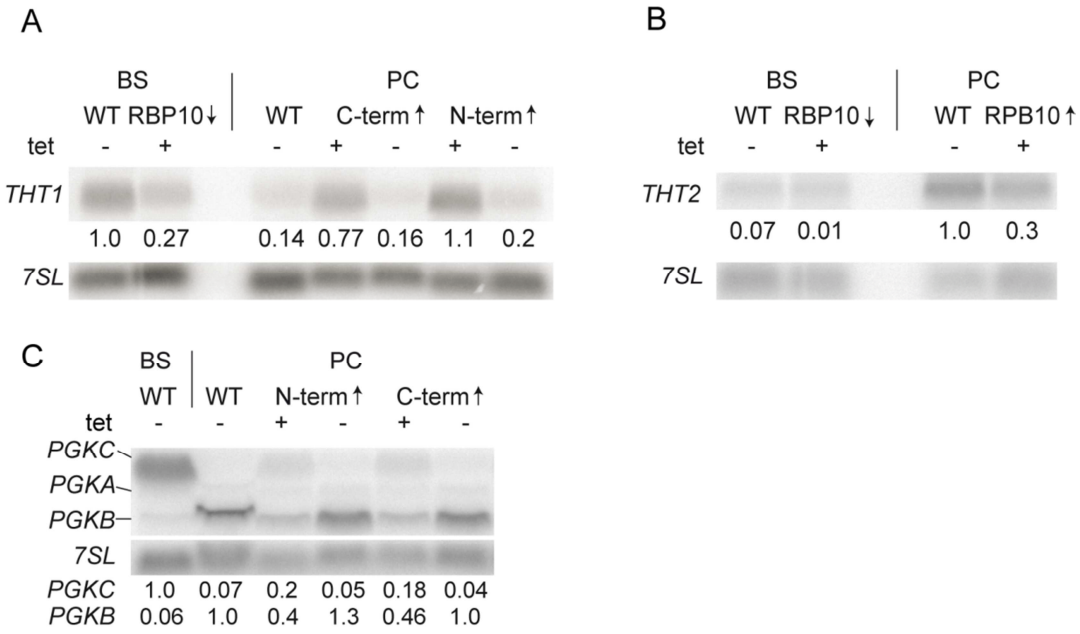


**Fig. 12**: Nothern blots showing the effect of the forced expression of RBP10 in PC on different mRNAs. Expression of RBP10 was induced with tetracycline 24 h before RNA was harvested. *7SL* served as loading control for quantification. A. RNA of PC expressing RBP10 with a myc-tag at the N- or the C-terminus was compared to RNA of PC WT, BS WT and BS RBP10 RNAi. The membrane was probed against a specific region of the 3'UTR of THT1 [56]. B. PC RBP10 expression RNA was compared to RNA of PC WT, BS WT and BS RBP10 RNAi. The membrane was probed against *THT2*. C. RNA of PC expressing RBP10 bearing a myc-tag at the N- or the C-terminus was compared to RNA of PC WT and BS WT. The membrane was probed against the 5' end of the PGKC ORF which is able to detect mRNAs of all PGK isoforms.

To investigate the effect of RPB10 on the transcriptome, microarray analysis was used to compare RNA samples of PC WT with RNA of PC which expressed RBP10. It showed that the expression of RBP10 in PC had, in many ways, an opposite effect compared to RBP10 RNAi in the BS. In total 346 mRNAs were changed (**Fig. 9**C), and again there was a correlation with developmental regulation (**Fig. 9**F). I could not only confirm the increase of the glucose transporter *THT1*, but also increases in mRNAs encoding for 5 proteins involved in glucose metabolism: glucose-6-phosphate isomerase, glycerol kinase, ATP-dependent phosphofructokinase, fructose-bisphosphate aldolase and aquaglyceroporin. Additional mRNAs encoding glycosomal proteins were also increased but had a p-value higher than the cut-off. Several mRNAs that encoded for transporters and other transmembrane proteins were also increased (**Fig. 9**C and Supplementary table 1), indicating that the change in glucose transport was not the only effect on metabolite uptake.

Of the 190 mRNAs that decreased during RBP10 expression, 79 were normally PC-specific, while none was BS-specific (**Fig. 9**F). A broad decrease of mRNAs encoding mitochondrial components (**Fig. 9**C) was the inverse of the increase seen during BS RNAi. There were seven mRNAs encoding glycosomal components, but three of them were not BS but PC specific. For HK2, which mRNA also was found to be decreased upon RBP10 expression, it was proposed that the protein might not have a hexokinase activity [78]. The decrease in mRNAs involved in protein synthesis was most likely a secondary effect of the growth inhibition.

Since the expression of RBP10 in PC caused many effects in energy metabolism it was possible that the proliferation defect was due to an inability of the cells to generate energy from the sources present in the medium. Hence I tried to rescue the growth defect by adding 4.6 g/l glucose to the medium. However, this had no effect (Fig. 11C).

## 3.6 Inhibition of differentiation by forced expression of RBP10

Expression of RBP10 correlated with the expression of BS-specific transcripts. Therefore it was interesting to know whether BS trypanosomes that constitutively express RBP10 would be able to differentiate into PC. I therefore transfected pleomorphic, differentiation-competent AnTat 1.1 cells with the RBP10 overexpression plasmid. RBP10 expression was induced with tetracycline 24 hours before I induced differentiation by adding *cis*-aconitate and decreasing the temperature to 27°C. Since RBP10 expression would kill PC, the medium was changed to MEM without tetracycline or *cis*-aconitate 24 hours later. The amount of RBP10 decreased during differentiation in the WT, while in the overexpression strain the endogenous protein level remained stable up to $t_{24h}$ (**Fig. 13**). After tetracycline removal both RBP10 proteins disappeared in the overexpression strain. As an indicator that the cells were transforming into PC the expression of EP procyclin was monitored. In the WT cell population, 24h after *cis*-aconitate addition, EP procyclin expression had begun, though not to the full procyclin level, while RBP10 had decreased but was still detectable. It is nevertheless possible that RBP10 and EP procyclin expression were mutually exclusive, since this was an asynchronous population, in which cells differentiated at varying rates [15]. Indeed, forced expression of RPB10 during the first 24h of differentiation completely prevented induction of EP procyclin. Moreover, the parasites overexpressing RBP10 died 1-3 days after the change of the medium even though tetracycline and RBP10 were absent. Again, addition of glucose to the procyclic medium didn't rescue the parasites (data not shown).

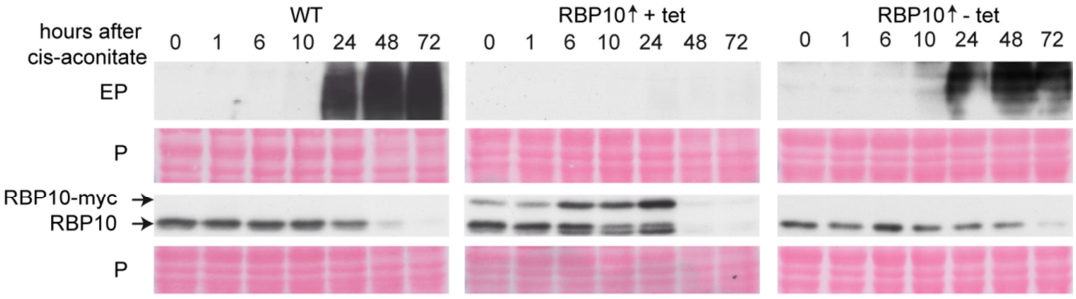


**Fig. 13**: Western blots showing the levels of EP, RBP10 and RBP10-myc of AnTat 1.1 cells during differentiation. Forced expression of RBP10-myc was induced 24 h before start of differentiation. Differentiation was performed as described by [15]. The membranes were probed with RBP10 and EP antibody. Staining of total protein with Ponceau S (P) served as loading control.

Since PIP39 is known to be an important switch controlling differentiation [21] I used immunoprecipitation to look for an interaction between RBP10 and PTP1; no interaction was detected (data not shown).

## 3.7 Can RBP10 override the effect of phloretin?

The treatment of BS cells with phloretin is known to induce changes in RNA metabolism also seen in the beginning of differentiation [23]. In contrast to this it could be seen that the expression of RBP10 correlated with a BS phenotype. Therefore it was important to know if phloretin treatment has an effect on the expression of RPB10. I also wanted to investigate whether BS trypanosomes with a forced expression of RBP10 still respond to phloretin and start to express *EP*. After the addition of phloretin the cells grow very slowly due to the lack of available energy, I therefore induced the expression of RBP10-myc 24 h before phloretin treatment.

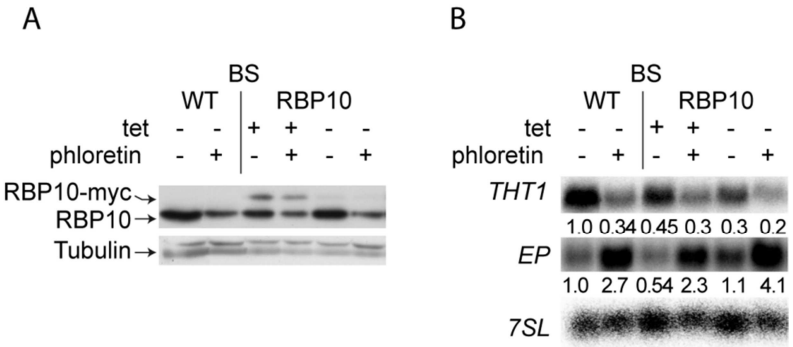


**Fig. 14** A: Western blot showing the levels of RBP10 and RBP10-myc after treatment of phloretin with preceding induction of RBP10-myc forced expression. The membrane was probed with the RBP10 antibody. Detection of tubulin served as loading control. B: Northern blot showing the levels of *THT1* and *EP* mRNA of the same cells as in 14A. *7SL* mRNA was used as loading control for quantification.

The expression of RBP10-myc was detected by Western blotting (Fig. 14A) using the RBP10 antibody. After phloretin treatment it could be seen that the level RBP10-myc decreased slightly. This could be due to the reduced protein synthesis after phloretin treatment or due to other regulatory mechanisms. Phloretin is known to reduce the level of *THT1* and increase the amount of *EP* in the BS. **Fig. 14**B shows a Northern blot with the levels of both mRNAs. It can be seen that in the WT the level of *THT1* decreases after phloretin treatment. This was also the case for the BS RBP10 forced expression cells. Notably the overexpression strain showed a reduced level of *THT1* even in the absence of phloretin. However, the results for *EP* mRNA were clear: Both BS WT and the RBP10 forced expression cell lines displayed a strong increase of *EP*, indicating that the treatment with phloretin was able to overrule RBP10 expression.

## 3.8 Direct mRNA targets of RBP10

To address the question of possible direct mRNA targets of RBP10 the myc-tagged protein was expressed in the BS. After harvesting the cells, protein – DNA or RNA interactions were cross-linked by UV radiation, followed by the purification of the protein using myc-agarose. The bound proteins were degraded by a Proteinase K treatment, afterwards the RNA was extracted using Trifast FL (Peqlab). Aliquots of the total cell lysate, the flow-through and the eluate were collected for Western blotting. **Fig. 15** shows the pull-down of RBP10-myc. There is a strong decrease in the level of RBP10-myc in the flow-through compared to the input, indicating that most of the tagged protein was bound to the beads.

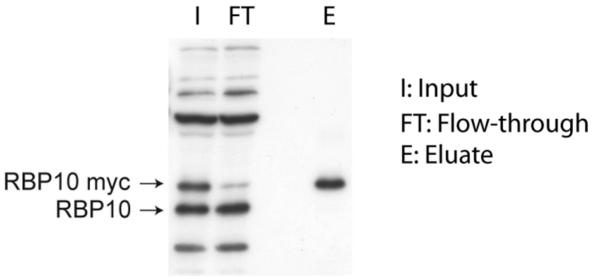


**Fig. 15**: Western blot showing the levels of RBP10 and RBP10-myc during the IP. The membrane was probed with the RBP10 antibody. Cell lysates of the input and flow-through corresponded to $3x10^6$ cells, the eluate corresponds to $5x10^7$ cells.

The isolated eluate RNA and the flow-through RNA, which was depleted of rRNA using the Ribominus kit (Invitrogen), were sent for deep-sequencing using the Illumina sequencing system. However, the sequencing results were ambiguous. There were only few reads for the

eluate, which might not be surprising and be explainable by the little amount of RNA found in the eluate. However, the number of average reads in the flow-through RNA was also quite low.
Therefore I applied several filters: First all mRNAs with less than five reads were removed. The remaining mRNAs were sorted for a minimum of 2-fold increase in rpkm (reads per kilobase of gene length per million mapped reads) of the eluate compared to the flow-through for both the ORF and the 3'UTR. The result of this filtering can be seen in supplementary table 2. Several mRNAs encoding RBPs are enriched in the eluate, but also the mRNAs encoding for the large subunit of RNA polymerase IIA, PEX11, a component of the glycosomal membrane and an RNA helicase were increased.
A comparison with the microarray datasets (**Fig. 9**) showed on overlap of 8 mRNAs which are also affected by RBP10 RNAi in the BS and 5 mRNAs that are changed after RBP10 expression in the PC. Only one mRNA encoding a hypothetical protein was increased after RBP10 expression in the PC, decreased after RBP10 knockdown in the BS and enriched in the eluate of the RNA-IP. However, a knockdown by RNAi showed no effect in any life stage [79].

## 3.9 Protein interaction partners

The knockdown of RBP10 in the BS has strong effects on various mRNAs, but we could not find evidence for binding of those mRNAs by RBP10. It was shown that RRM motives can also function in protein-protein interactions [80]. Tandem Affinity Purification (TAP) was used as a first attempt to look for proteins interacting with RBP10 but could not reveal any specific interactions (data not shown). However, only distinct bands of the eluate were analysed by mass spectrometry. Potentially interacting, but less abundant proteins may have been missed. For this reason an immunoprecipitation was done; BS cells expressing RBP10-myc and WT cells as control were lysed and incubated with myc-agarose beads. The binding of RBP10-myc to the beads worked well since most of the protein could be found not in the flow through but in the eluate as seen in Fig. 16A. As expected no protein can be detected by the RBP10 antibody in the WT eluate. Fig. 16B shows the image of the gel from which the samples were taken for mass spectrometry.
Table 3 shows the identified proteins which potentially interact with RBP10 but which were not detected in the WT control. As expected, RBP10 itself could also be identified in the eluate of the RBP10-myc expression cell line.

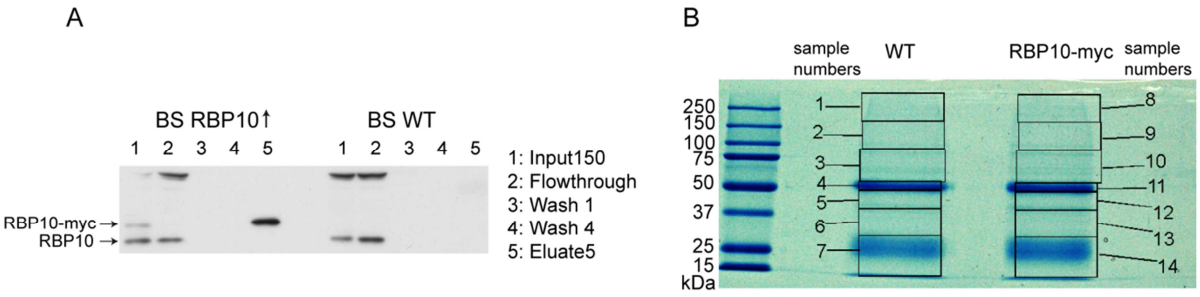


**Fig. 16** A: Western blot showing the control for the IP of RBP10-myc. $4x10^8$ cells of both RBP10-myc expression and WT were used. Lanes 1 and 2 correspond to $3x10^6$ cells; in lane 5 ~$5x10^7$ cells equivalents are loaded. The membrane was probed with the RBP10 antibody. B: SDS gel analysed by mass spectrometry. For the analysis the lanes were divided into the specified sample.

**Table 3**: Identified proteins potentially interacting with RBP10. Gray highlighted proteins are considered as false positives. "TAP" means that the proteins have previously been detected by Tandem-Affinity-Purification of RBP10-TAP.

| Identified Proteins | Accession | TAP | MW | 1 | 8 | 2 | 9 | 3 | 10 | 4 | 11 | 5 | 12 | 6 | 13 | 7 | 14 | sample number |
|---|---|---|---|---|---|---|---|---|---|---|---|---|---|---|---|---|---|---|
| RBP10 | Tb927.8.2780 | YES | 32 kDa | 0 | 0 | 0 | 0 | 0 | 0 | 0 | 0 | 0 | 10 | 0 | 7 | 0 | 1 | Number of identied peptids |
| dynamin | Tb927.3.4720 | | 73 kDa | 0 | 0 | 0 | 0 | 0 | 7 | 0 | 0 | 0 | 0 | 0 | 0 | 0 | 0 | |
| RBP29 | Tb927.10.13720 | YES | 41 kDa | 0 | 0 | 0 | 0 | 0 | 0 | 0 | 4 | 0 | 0 | 0 | 0 | 0 | 0 | |
| Polyadenylate-binding protein 2 | Tb09.211.2150 | | 62 kDa | 0 | 0 | 0 | 0 | 0 | 5 | 0 | 0 | 0 | 0 | 0 | 0 | 0 | 0 | |
| U2 splicing auxiliary factor | Tb927.10.3200 | | 29 kDa | 0 | 0 | 0 | 0 | 0 | 0 | 0 | 0 | 0 | 0 | 0 | 4 | 0 | 0 | |
| hypothetical protein | Tb927.4.2030 | | 23 kDa | 0 | 0 | 0 | 0 | 0 | 0 | 0 | 0 | 0 | 0 | 0 | 2 | 0 | 1 | |
| SCD6 | Tb11.03.0530 | | 31 kDa | 0 | 0 | 0 | 0 | 0 | 0 | 0 | 0 | 0 | 0 | 0 | 2 | 0 | 0 | |
| hypothetical protein | Tb11.02.4300 | YES | 49 kDa | 0 | 0 | 0 | 0 | 0 | 3 | 0 | 0 | 0 | 0 | 0 | 0 | 0 | 0 | |
| 60S acidic ribosomal subunit protein | Tb11.46.0001 | | 35 kDa | 0 | 0 | 0 | 0 | 0 | 0 | 0 | 0 | 0 | 0 | 0 | 2 | 0 | 0 | |
| glucose-regulated protein 78 | Tb11.02.5450 | YES | 71 kDa | 0 | 0 | 0 | 0 | 0 | 11 | 0 | 0 | 0 | 0 | 0 | 0 | 0 | 0 | |
| alpha tubulin | Tb927.1.2340 | YES | 50 kDa | 0 | 0 | 0 | 0 | 0 | 0 | 0 | 7 | 0 | 0 | 0 | 0 | 0 | 0 | |
| 40S ribosomal protein SA | Tb11.01.2560 | YES | 28 kDa | 0 | 0 | 0 | 0 | 0 | 0 | 0 | 0 | 0 | 0 | 0 | 5 | 0 | 0 | |

Grey highlighted proteins were considered as false positive candidates since they appear frequently in purifications of other proteins and are not known to be related to RBPs. One potential interaction partner, RBP29, has already been detected in the TAP. RBP29 was found to be on polysomes (Cornelia Klein, unpublished data). SCD6, which is a quite abundant protein in the cell and which is a part of P-bodies, was also found in other purifications, but since it is involved in RNA metabolism it is doubtful whether it should be considered as contaminant. Verifications of the interactions by reverse IP or by yeast-two-hybrid test are necessary for a reliable statement.
None of the putative interaction partners are developmentally regulated as RBP10. There is also no change in the mRNAs encoding the proteins after BS RBP10 RNAi.

## 3.10 Verification of RBP29-RBP10 interaction

To verify a result of the mass spectrometry, a co-IP with RBP29 was done. RBP29, which was endogenously expressed with a V5 tag (cell line obtained from C. Klein), was immunoprecipitated using V5 agarose beads (Biomol). BS WT cells were used as controls. In total $2x10^8$ cells were used for each experiment. Afterwards a sample of the input, the flow-through and the whole eluate were analysed by Western blotting. The membrane was probed with the RBP10 and the V5 antibody.

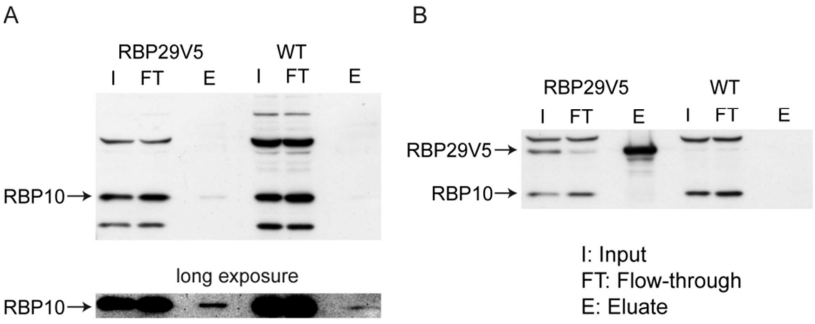


**Fig. 17**: Western blots showing the fractions of the Co-IP of RBP29-V5 and WT cell lysates. Input and flow-through correspond to $4.4x10^6$ cells; the eluate corresponds to ~$1.9x10^8$ cells. The membrane was probed with A: RBP10 antibody and B: V5 antibody.

**Fig. 17**A shows the pull-down of RBP29-V5 probed with the RBP10 antibody. Most likely the counting of the cells was imprecise, because more cells seem to be loaded for the WT control. However, a thin band can be detected for RBP10 in the eluate of the RBP29-V5 cell line. Also in the WT control this band can be seen, though it was weaker despite the uneven amount of cells used for the experiment. **Fig. 17**B shows the same membrane probed with the V5 antibody. It confirms that the pulldown of RBP29-V5 was successful. It could also be seen that most of the RBP29-V5 was bound to the beads since there was a decline of the RBP29-

V5 signal in the flow-through compared to the input. This experiment confirms the binding of RBP10 to RBP29, though it could be that only a small portion of the proteins interact.

## 3.11 Structural analysis of RBP10

To gain insight in the important parts of the protein RBP10 I expressed four truncated versions (**Fig. 18**A) of RBP10 with a myc-tag at their C-terminus in the PC. Since RPB10 is normally not present in PC and the artificial expression of the full protein has a strong effect on several mRNAs like *THT1* (**Fig. 12**A), the functionality of the different fragments could easily be measured by an observation of *THT1*.

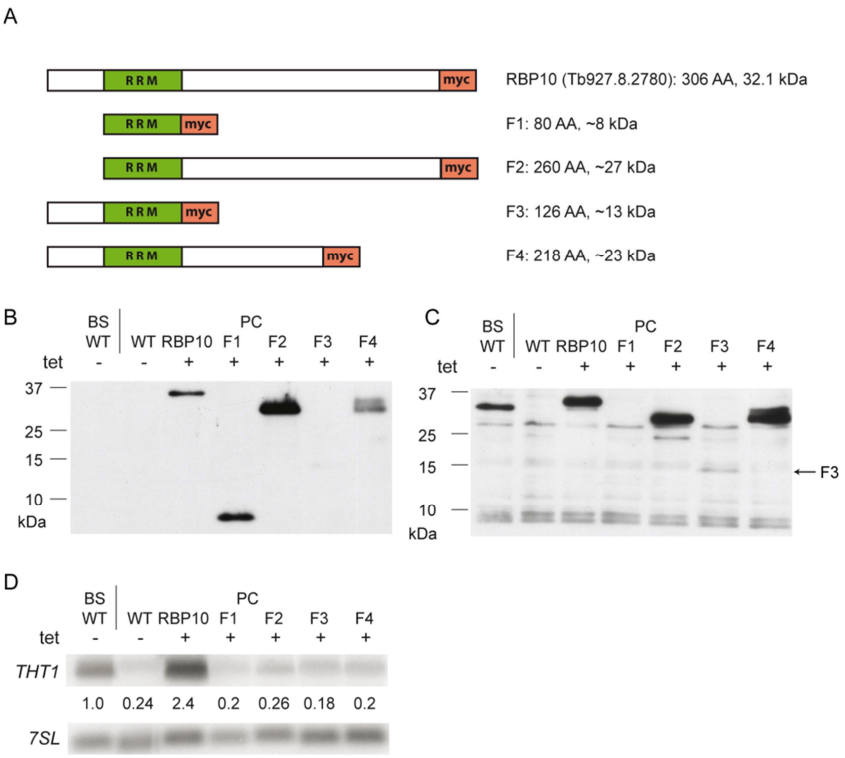


**Fig. 18** A: Illustration of the five myc-tagged proteins expressed in PC: Full length RBP10 and the four shortened versions bearing deletions at either the C- and / or the N-terminus. B and C: Western blots showing the expression of the proteins in PC. The membranes were probed with the myc antibody (B) or RBP10 antibody (C). D: Northern blot showing the levels of *THT1* in BS WT, PC WT and PC expressing the five proteins seen in 15A. *7SL* served as loading control for quantification.

The expression of the truncated proteins was verified by Western blotting using the myc antibody (Fig. 18B) and the RBP10 antibody (Fig. 18C). All the different fragments migrated at the expected sizes. Notably the expression of the fragment F3 was quite weak but could be detected by the RBP10 antibody, while F1 could only be detected by the myc- and not with the RBP10 antibody. The effect of the forced expression was measured by detection of the *THT1* mRNA (Fig. 18D) and was normalized to the signal of the *7SL* mRNA. The amount of *THT1* is strongly inceased in PC expressing the full length RBP10 protein (labelled “RBP10”) compared to the PC WT and even to the BS WT. However, none of the truncated RBP10 proteins caused an increase of the *THT1* mRNA; instead the abundance of *THT1* was in the same range as the PC WT.

## 3.12 Quantification of RBP10 in the BS

To investigate the number of molecules of RBP10 per BS cell, various numbers of cells were compared to different amounts of recombinant protein. In Fig. 19 $0.5x10^6$, $2x10^6$ and $4x10^6$ cells were compared to 50 ng and 100 ng of recombinant RBP10.

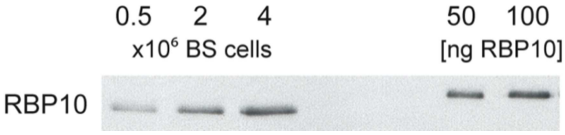


**Fig. 19**: Western blot comparing different amounts of recombinant RBP10 with endogenous protein of BS cells. The membrane was probed with the RBP10 antibody.

$2x\ 10^6$ and $4x\ 10^6$ cells match with 50 ng and 100 ng of recombinant RBP10 protein, respectively. One molecule of RBP10 has a mass of 32.2 kDa, resulting in a rough estimate of $4x10^5$ RBP10 molecules per cell. This corresponds to 0.0004% of total cell protein, taking in account that $1.94x10^8$ cells contain 1 mg of protein [81].

## 3.13 Phosphorylation of RBP10

RBP10 was found to be phosphorylated by [61] at the four serines S159, S161, S162 and S164. To confirm the phosphorylation and see whether it had an effect on the functionality of RBP10 I expressed five different mutated RBP10 proteins in the PC where a possible phosphorylation of the protein at the serine residues was abolished. Four proteins had a single mutation of one serine to glycine and one protein was bearing all four mutations (named "4xG"). The expression of the proteins in PC is shown in Fig. 20A. It can be seen that some of the different mutations influenced the migration of the proteins in the gel. S159G was detected above the other mutated proteins. The "WT" RPB10 protein was expressed with a myc-tag, therefore both the endogenous and the myc-tagged protein were seen here. For both clones of 4xG an additional band can slightly be seen, also a higher band can be detected at S162G C2. A possible impact of the mutations was measured by detection of the mRNA encoding the glucose transporter THT1. Normally this mRNA is decreased in the PC compared to the BS; the forced expression of RBP10 in the PC increased the amount of *THT1* (Fig. 12A). If the function of RBP10 was depended on phosphorylation, the mutated proteins would not increase the *THT1* level and hence the amount of *THT1* would be lower compared to PC expressing the normal RBP10.

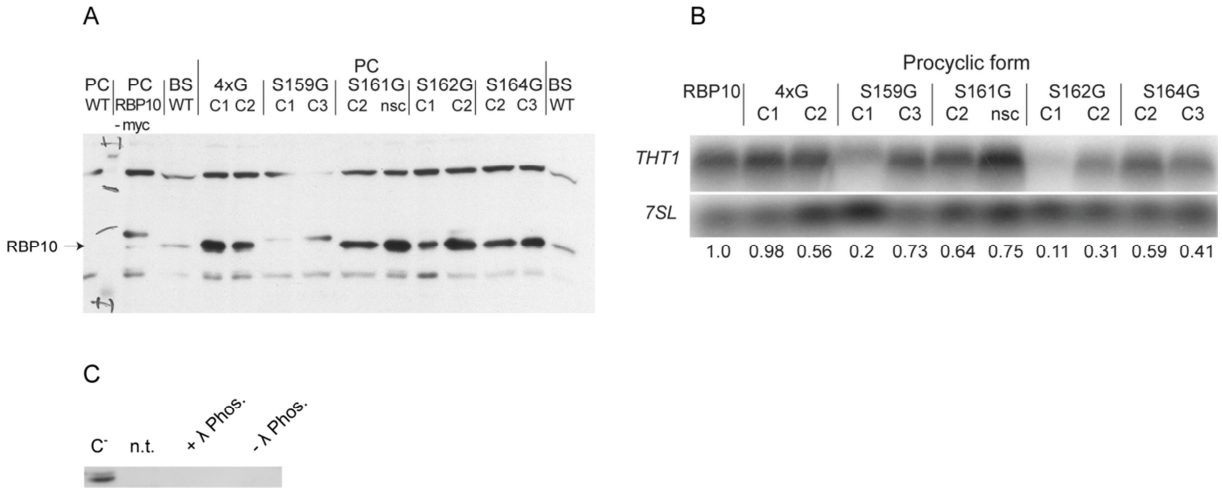


**Fig. 20** A: Western blot showing the expression of mutated RBP10 proteins in PC. The membrane was probed with the RBP10 antibody. The "RBP10" cells expressed the not mutated protein. "C1" stands for "clone1", while "nsc" are cells not derived from a single clone. B: Northern blot showing the levels of *THT1* of different PC cell lines expressing the mutated or the not normal RBP10. *7SL* served as loading control for quantification.

Fig. 20B shows the *THT1* levels of the PC expressing the regular RBP10 ("RBP10") and the five different mutated versions, two different clones each. Generally the level of *THT1* is very little in PC and the expression of RBP10 leads to a strong increase (**Fig. 12**) of *THT1*. 4xG C2 displayed the same increase of *THT1* as the not mutated protein; 4xG C1 showed a lower increase of *THT1* which can be explained by the low expression seen by Western blotting (Fig. 20A). This indicates that the phosphorylation of RBP10 is not important for the functionality of RBP10 in the PC. Also both clones of S162G display a reduced increase of *THT1*.

As seen in Fig. 13 AnTat 1.1 cells showed a double band recognized by the RBP10 antibody. This indeed could indicate a possible phosphorylation of the protein. However, the double band was not seen in all experiments and the conditions, under which the extra band was detectable, could not be clarified.
To investigate whether RBP10 is phosphorylated in these cells a dephosphorylation assay was performed using the λ-phosphatase. The trypanosomes were lysed in the appropriate buffer for the enzyme and the supernatant was treated with the phosphatase for 20 min. Fig. 20C shows the assay with the AnTat 1.1 cells; for the control the cells were lysed directly in protein loading dye. "n.t." means that the cells were lysed in the dephosphorylation buffer and frozen immediately after the addition of protein loading dye. In the control cells the double band could slightly be seen. Though in all samples that were lysed in phosphatase buffer no RBP10 was detectable any more. Even in the sample that was not incubated on ice for 20 min the protein was degraded. Hence the possible phosphorylation of RBP10 could not be confirmed.

# Additional results

## 3.14 Polysome gradient

Cornelia Klein, a co-worker in the lab, ran a sucrose gradient with cell lysates of BS to investigate the protein composition on polysomes (**Fig. 21**A). I separated the obtained protein fractions by SDS-PAGE and analysed them by Western Blotting (**Fig. 21**B). It can be seen that RBP10 is mainly detectable in the fraction of the unbound proteins. Though, a minor part of the protein is associated with ribosomes and can be detected in the fractions from the 40S subunits up to trisomes. Also with a longer illumination of the ECL film RBP10 was not seen in the fractions of the heavy polysomes.

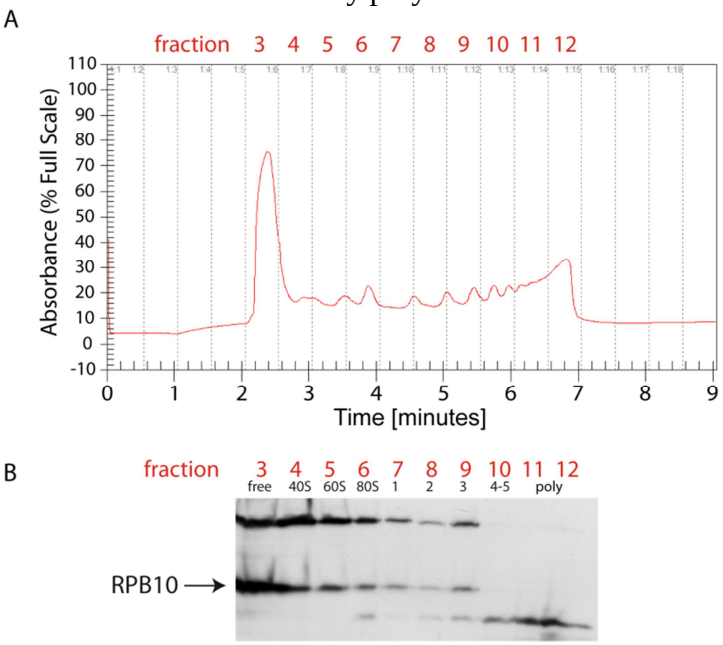


**Fig. 21** A: Polysome profile showing the absorbance at $OD_{254}$ of the proteins in the different fractions of the gradient. B: Western blot of the proteins obtained from the sucrose gradient. The membrane was probed with the RBP10 antibody.

# 4. Discussion

## 4.1 Effect of RBP10

RBP10 was shown to be a BS specific protein (**Fig. 4**). In the PC the protein is not detectable, although *RBP10* mRNA is still present at a low level (**Fig. 11**A). This makes it likely that the expression of RBP10 is regulated not only at the level of RNA stability but also affected by downstream events. The knockdown of RBP10 by RNAi (**Fig. 4**) resulted in an almost entire depletion of the protein and a severe defect in proliferation of the parasite (**Fig. 5**). The decrease of RBP10 was accompanied by strong changes in the transcriptome: The abundance of a large number of BS specific transcripts was decreased, while many PC specific mRNAs were increased after RBP10 RNAi. Using reporter constructs with 3'UTRs of two BS specific mRNAs, THT1 and PGKC 3'UTR, we could show that the regulation of RNA abundances occurred at posttranscriptional level via those 3'-UTRs (data from Beate Seliger).
RBP10 RNAi affected the levels of many RNAs encoding proteins involved in glycolysis and the glucose transporter THT1. Though it is difficult to show that this affected protein levels, too, since there are no antibodies available against THT1. If RBP10 RNAi would have an effect on THT1 protein this could already be sufficient to explain the lethality of the knockdown. The reduction of glucose uptake would lead to a decrease of the glycolytic flux since the glucose transporter has a strong flux control coefficient [70]. A reduction of the flux of 30-50% as a consequence of glucose uptake inhibition is sufficient to block growth [23], a stronger inhibition of glycolysis leads to cell death. In this study was also shown that a decrease of intracellular glucose does not lead to a higher expression of the glycolytic components, but in the contrary to an even stronger down regulation of the glucose transporter and the glycolytic enzymes. This effect could also be seen after RBP10 knockdown: most mRNAs encoding for glycolytic enzymes were decreased in a very similar way as after phloretin treatment. There were 91 transcripts affected under both conditions with a correlation coefficient of 0.9 including several of those transcripts mentioned (supplementary table 1).
An inhibition of glucose uptake also leads to a partial differentiation [23]: several BS specific mRNAs are decreased and PC specific transcripts are increased. This can be seen after RBP10 RNAi, too. However, the overlap between phloretin treatment and RBP10 knockdown is not large enough to say that the two conditions are the same and claim that the whole effect of RBP10 RNAi can be reduced to the inhibition of glucose uptake. RBP10 RNAi has a much more widespread effect on the transcriptome than phloretin treatment. A more severe inhibition of proliferation is unlikely to be the reason for the broader effect of RBP10 RNAi since the decline in growth was not stronger than after treatment with phloretin. The inhibition of growth is also displayed in the transcriptome under both conditions: several mRNAs encoding for proteins of the cytoskeleton and the flagellum are decreased, some of these transcripts are also part of the 91 mRNAs whose regulation overlap between RBP10 RNAi and phloretin. Nevertheless, it is unclear to which extent the growth defect has affected the microarray results. Knockdowns of many proteins lead to a defect in growth, but not all induce the expression of *EP*. The inhibition of growth by the reduction of glucose uptake evokes an increase of *EP* and other PC specific mRNAs [23]. RNAi against the RNA helicase DHH1 has an effect on developmentally regulated mRNAs [82]. However, DHH1 is assumed to be involved in a pathway to regulate many stage specific mRNAs. Therefore this effect would not be related to a growth defect. On the other hand, the knockdown of UBP1 or UBP2 also results in a defect in proliferation but has no effect on *EP* [53], same as RNAi against ZC3H11 (Droll et al, unpublished). Eventually this could mean that either there are different kinds of growth defects in the BS and only some induce the expression of PC specific

mRNAs; or each growth inhibition leads to the expression of mRNAs like *EP* but under some conditions, for example after a knockdown of a specific protein, the cells are not able any more to start the expression.

The changes in the transcriptome caused by the expression of RBP10 in the PC indicate that the developmental regulations are not only due to growth arrest. PC expressing RBP10 showed almost the opposite effect in comparison to BS RBP10 RNAi. The expression of RBP10 in PC displayed an even stronger correlation to developmental regulation. Large portions of the increased mRNAs were BS specific, while several of the decreased mRNAs were PC specific. Among the increased mRNAs was also the BS specific *RBP10* followed by the expression of RBP10 protein (**Fig. 11**B). If RBP10 would only control the glucose transporter THT1 and the glycolysis, one could speculate that with the expression of RBP10 in PC the defect in proliferation could be rescued by the addition of glucose to the medium. This was however not the case. Though, also in the PC the expression of RBP10 came along with a BS phenotype. This raised the question whether fully differentiation competent AnTat 1.1 cells were still able to undergo differentiation if expression of RBP10 was constantly forced. As seen in **Fig. 13** this was not the case, the cells died and showed no expression of *EP*. Since the forced expression of RBP10 was induced only in the first 24 hours it can be excluded that the cells first differentiated into PC and died afterwards, but the precise mechanism how the differentiation was inhibited is not known.
Normally differentiation is triggered by the PAD transporters, which are localized on the cell surface of stumpy form parasites and sense *cis*-aconitate [20]. The tyrosine phosphatase PTP1 is responsible for maintenance of the stumpy form until the start of differentiation [62]. PTP1 prevents differentiation by dephosphorylating another phosphatase, PIP39, whose presence is required for differentiation [21]. Both PTP1 and RBP10 are necessary for the maintenance of the BS state. Since RRM motifs can function in protein-protein interactions [80], an interaction between the two proteins might have been possible. However, no such interaction was detected by immunoprecipitation.

Glucose starvation is also able to induce at least partial differentiation as seen in [23]. A full, but slower differentiation by removal of glucose from the medium is possible [22]. The expression of RBP10 was shown to be sufficient for the expression of many BS specific mRNAs. There is a weak decline of RBP10 protein after treatment with phloretin (**Fig. 14**). Even with an additional expression of RBP10-myc, phloretin treatment was able to override the expression of RBP10 and induce the expression of *EP* (**Fig. 14**). This leads to the conclusion that there could be two different pathways to start differentiation. A differentiation by *cis*-aconitate was shown to be inhibited by the artificial expression of RBP10-myc, while differentiation via glucose uptake inhibition was unaffected by RBP10 expression. One could speculate the two routes are independent pathways to induce differentiation.

## 4.2 Functionality of RBP10

RBP10 was found to be localized to the cytosol by immunofluorescence and subcellular fractionation (**Fig. 6** and **Fig. 7**). This makes it unlikely that RBP10 is involved in processes like pre-mRNA processing, which takes place in the nucleus. Rather, it would be probable that RBP10 binds to, and stabilizes, BS specific transcripts. However, this cannot be confirmed since the transcripts that were seen to be affected by RBP10 RNAi in the BS or RBP10 expression in the PC could not be found enriched in the eluate of the RNA IP. After filtering the putative direct mRNA targets 90 mRNAs remained (supplementary table 2). The filtering leads to a small bias for long mRNAs since all transcripts with less than 5 reads in

the ORF in the eluate and the flow-through were removed. This was necessary because even in the flow-through there was a poor coverage of reads alignment. This raises the question whether the RNA used had a low quality and maybe was mostly degraded or whether the sequencing itself worked as designed.
Most of the putative mRNA targets which showed at least 2-fold increases in the eluate compared to the flow-through were diverse and could not be clustered. However, there were three mRNAs encoding proteins involved in glucose metabolism (PEX11, fructose-bisphosphate aldolase and glycosomal phosphoenolpyruvate carboxykinase). These mRNAs were not affected by RBP10 RNAi which questions the reliability of this outcome. If RBP10 would stabilize those mRNAs one would expect it to be on polysomes. RBP10 was not found in the heavy polysome fractions (**Fig. 21**), which excludes a constant binding to the mRNAs during translation. Most of the protein was detected in the fraction of the free proteins. This confirms the results of the glycerol gradient (work of Valentin Färber) which showed that most RBP10 protein is not involved in large complexes (data not shown).
However, in the sucrose gradient the signal of RBP10 was detectable in the fractions from the free proteins to the fractions of the trisomes, which could mean that RBP10 transiently binds to mRNAs and can be found in a complex with ribosomes, but dissociates after translation initiation or after the first round of translation.

Immunoprecipitation of RBP10-myc revealed several potential interaction partners (Table 3). Besides PABP2, three of these potential interaction partners have been shown to be involved in RNA metabolism. The U2 splicing auxiliary factor seems to be an unlikely interaction partner since splicing takes place in the nucleus. This nevertheless could be a valid interaction if RBP10 would, under certain stress conditions, shuttle to the nucleus as seen for UBP1 after arsenite treatment [83]. Shuttling to the nucleus has also been shown for PABP2. Inhibition of transcription, but not arsenite stress, leads to migration of PABP2 to the nucleus. However, the role of PABP2 is not clear yet. Its homologue in *L.major* has a weak affinity to Poly-A and binds to the translation initiation factor LmEIF4G3 only *in vitro* and not *in vivo*. It was suggested that the protein either acts as a general factor for RBPs in posttranscriptional control or for it could be associated with mRNA export.
Another identified protein which is associated with RNA is SCD6, which is known to be a marker for P-bodies. P-bodies are proposed to be the sites of RNA decay and SCD6 thereby a possible interaction partner. On the other hand SCD6 is quite abundant and could also be a false positive like many chaperones. Immunofluorescence to look for an overlap of RBP10 and SCD6 could show colocolization; a reverse IP or a yeast-2-hybrid experiment could confirm the interaction.
Another protein potentially interacting with RBP10 was RBP29, which also was found to be associated with polysomes (Klein et al, unpublished). Knockdown of RBP29 is lethal in the BS [79]. The interaction of RBP10 and RBP29 was confirmed by pulldown of RBP29 and subsequent detection of RBP10 in the eluate (**Fig. 17**), though only a minor part of the proteins are interacting. It can be speculated that the contact of the two proteins takes place on mRNPs (ribonucleoproteins). If this would be the case a stronger interaction might be detectable if the IP was performed in the presence of RNAse inhibitors.

## 4.3 Structural analysis of RBP10

RBP10 protein is normally not expressed in PC but its forced expression evokes changes in several mRNAs like *THT1*. This gave the possibility to investigate which parts of RBP10 were necessary and also to study a possible role of phosphorylation of the protein. For the structural analysis, four different truncated versions of RBP10 were expressed in PC, none of them showed an increase in *THT1* mRNA. This could be due to improper folding of the fragments; this could only be confirmed by X-ray crystallography. It is also possible that indeed the whole protein is necessary for its functionality though the only know motif of RBP10 is the RRM.
Also the phosphorylation seen in the phosphoproteome [61] was studied first in PC by expressing proteins with mutation at the serine residues 159,161,162 and 164. Especially the expression of the RBP10 with all four serines exchanged was expected to show no effect on THT1 in PC if the phosphorylation was crucial for its function. However, most of the investigated clones in **Fig. 12**A showed the same effect as RBP10. This indicates that the phosphorylation is not important in terms of the function of RBP10. However, in most Western blots with PC or BS trypanosomes only a single band was detectable. An extra band for RBP10 was seen occasionally in AnTat 1.1 cells (**Fig. 13**) and even less often in monomorphic BS. To investigate a possible phosporylation in BS, I performed a dephosphorylation assay using the λ-phosphatase. However, RBP10 was extremely unstable in the buffer used for the assay because even without phosphatase treatment and incubation the protein was degraded after lysis of the cells. Another way to examine a possible phosphorylation in BS would be to knock down the endogenous RBP10 by RNAi targeting the 3'UTR of *RBP10* and simultaneously express the mutated versions of the protein.

## 4.4 Future perspectives

In this work I could show the effect of RBP10 expression and depletion in *T.brucei*. For a better understanding how the regulations are achieved several experiments could be done. The search for direct mRNA target revealed some candidates. Although these mRNAs are not affected by RBP10 RNAi in the BS, they could be valid targets and the results of the microarray studies a subsequent regulation. A direct interaction between RBP10 and an mRNA target could be confirmed by RNA-IP with a following semi-quantitative RT-PCR or quantitative RT-PCR. If the outcome would be negative it would be important to investigate whether RBP10 binds to RNA at all using the PAR-CLIP method (Photoactivatable-Ribonucleoside-Enhanced Crosslinking and Immunoprecipitation) [84]. This would need a preceding setup of the used system in *T. brucei*. If this result would show that RBP10 actually binds to RNA, a repetition of the deep-sequencing of the bound RNA should be done since it is possible that the first sequencing did not work as designed.
Several protein interaction partners for RBP10 were found by IP and the binding to RBP29 was confirmed. The Co-IP with RBP29 could be repeated in the presence of RNAse inhibitors to see whether the interaction is RNA dependent. For the remaining potential interaction partners a reverse IP would be necessary to show the specificity of the interactions. This could clarify in which pathway RBP10 is involved in. PABP2, which is known to shuttle to the nucleus under transcription inhibition, was also detected as potential interaction partner. Therefore a possible change in the localization of RBP10 under different stress conditions like block of transcription or arsenite addition could be investigated.

## 5. Supplementary material

**5.1.**

# An RNAi screen of the RRM-domain proteins of *Trypanosoma brucei*

Martin Wurst, Ana Roblesa, June Poa, Van-Duc Luu, Stefanie Brems, Mari Marentije, Savrina Stoitsova, Luis Quijada, Jörg Hoheisel, Mhairi Stewart, Claudia Hartmann, Christine Clayton

Molecular & Biochemical Parasitology 163 (2009) 61–65

Contents lists available at ScienceDirect

Molecular & Biochemical Parasitology

Short communication

# An RNAi screen of the RRM-domain proteins of *Trypanosoma brucei*

Martin Wurst[a,1], Ana Robles[a,1], June Po[a], Van-Duc Luu[a], Stefanie Brems[b], Mari Marentije[a], Savrina Stoitsova[a], Luis Quijada[a], Jörg Hoheisel[b], Mhairi Stewart[a], Claudia Hartmann[a], Christine Clayton[a,*]

[a] Zentrum für Molekulare Biologie der Universität Heidelberg (ZMBH), Im Neuenheimer Feld 282, D69120 Heidelberg, Germany
[b] Section for Functional Genome Analysis, Deutsches Krebsforschungszentrum, Im Neuenheimer Feld 580, D-69120 Heidelberg, Germany

ARTICLE INFO

*Article history:*
Received 21 February 2008
Received in revised form 15 August 2008
Accepted 3 September 2008
Available online 18 September 2008

*Keywords:*
RNA binding protein
Trypanosoma
RRM

ABSTRACT

In eukaryotes, proteins containing RNA Recognition Motifs (RRMs) are involved in many different RNA processing reactions, RNA transport, and mRNA decay. Kinetoplastids rely extensively on post-transcriptional mechanisms to control gene expression, so RRM domain proteins are expected to play a prominent role. We here describe the results of an RNA interference screen targeting 37 of the 72 RRM-domain proteins of *Trypanosoma brucei*. RNAi targeting 8 of the genes caused clear growth inhibition in bloodstream trypanosomes, and milder effects were seen for 9 more genes. The small, single-RRM protein *Tb*RBP3 specifically associated with 10 mRNAs in trypanosome lysates, but RBP3 depletion did not affect the transcriptome.



## 1. Introduction, results and discussion

The genomes of Kinetoplastids are made up of polycistronic transcription units [1]; individual mRNAs are generated by *trans* splicing and polyadenylation. As a consequence of this genomic organisation, trypanosomes and Leishmanias are highly dependent on post-transcriptional mechanisms to regulate gene expression [2]. In addition, the mitochondrial mRNAs are extensively edited [3] and, as in other eukaryotes, the stable catalytic and structural RNAs are subject to processing and modification. All of these processes require the participation of RNA binding proteins. Prominent among these are proteins containing an RNA Recognition Motif (RRM). In a previous survey we described 72 *Trypanosoma brucei* genes encoding RRM-containing proteins. We predicted possible functions for some of them based on sequence homologies or published experimental data [4]. We describe here the results of an RNA interference screen that was designed to find out which of the remaining proteins were important in trypanosome survival.

For RNAi we used a vector in which dsRNA is synthesised from opposing T7 promoters [5,6] (Supplementary Table S1). We transfected 35 plasmids into either bloodstream-form trypanosomes, procyclic-form trypanosomes or both, with a bias towards bloodstream forms. The day after transfection, selecting drug was added and the cultures were cloned by limiting dilution [5]. If no parasites survived the selection, we attempted the transfection once more; failure to get live cells occurred more often for bloodstream forms than for procyclic forms. Overall we obtained clones for 32 genes (Table 1). Failure to get clones is uninformative: although it could be caused by leakage of a lethal RNAi, other technical problems cannot be excluded.

To test the effects of RNAi, we added tetracycline (0.1–0.5 μg/ml) and cultivated the parasites for up to 7 days, diluting as required, and assessed mRNA levels by Northern blotting. The results are summarised in Tables 1 and 2, illustrated in Fig. 1, and presented more fully in Supplementary Table S1. If Northern blotting results demonstrated that tetracycline addition did not cause a decrease in the amount of the target mRNA, clones were not investigated further. Eight of the genes tested were required for normal growth of bloodstream forms (Table 2); in several more cases, transient or mild effects were seen, including decreased growth whether or not tetracycline was added (Table 2 and Fig. 1). The doubling time of the bloodstream trypanosomes used in our experiments, in the absence of deleterious mRNA depletion, is about 7 h [7] (see panels for *DRBD9* and *TRRM3* in Fig. 1) and for procyclics, about 10 h. Most of the bloodstream RNAi lines illustrated in Fig. 1 grew slower than the wild type even in the absence of tetracycline, with even slower growth upon tetracycline addition. Similar observations were made for some of the procyclic lines (see Table 2). These cell lines may have some dsRNA effect on either translation or mRNA levels even in the absence of tetracycline. It is important to note that the less dramatic differences were apparent only if growth was monitored

* Corresponding author. Tel.: +49 6221 546876; fax: +49 6221 545894.
*E-mail address:* cclayton@zmbh.uni-heidelberg (C. Clayton).
[1] These authors contributed equally to this manuscript.

0166-6851/$ – see front matter © 2008 Elsevier B.V. All rights reserved.
doi:10.1016/j.molbiopara.2008.09.001

**Table 1**
RNAi screen statistics. (1) The plasmid was transfected into the relevant form at least once. (2) Cells resistant to the selecting drug obtained. (3) No cells survived the selection. (4) A decrease of at least 50% in the target mRNA was seen by Northern blot after tetracycline induction. (5) The Northern blot revealed no difference between cells with and without RNAi induction. (6) The mRNA for the RRM protein was not detected in cells without RNAi. (7) "Mild" growth effects were either transient or resulted in an increase in division time of two-fold or less relative to cells without RNAi induction. (8) "Clear growth effect" in bloodstream forms indicates a division time of 12 h or more in the presence of tetracycline. No conclusions can be drawn from any of the negative results.

| | | Procyclic | Bloodstream |
|---|---|---|---|
| 1 | Plasmid transfected | 24 | 30 |
| 2 | Clones obtained | 19 | 23 |
| 3 | No live cells obtained | 5 | 7 |
| 4 | mRNA decrease confirmed | 6 | 11 |
| 5 | No RNAi effect on mRNA | 1 | 5 |
| 6 | RNA not detected | 6 | 8 |
| 7 | Mild growth effect | 7 | 9 |
| 8 | Clear growth effect | 0 | 8 |

**Table 3**
Protein location studies. A sequence encoding a V5 tag was integrated in frame with the open reading frame, at the 5′-end; alternatively, the protein with a C-terminal myc tag was over-expressed from a procyclin promoter. For the immunofluorescence (IFA), proteins in parentheses gave low signals, not very different from background, so the assignments are tentative. Data for RBPs 20, 25 and 38 are shown in Supplementary Figure 2. Data for the locations of DRBD7, DRBD9 and TRRM3 (Table 2) were obtained by cell fractionation.

| | V5 *in situ* | Myc inducible expression |
|---|---|---|
| Not detected on Western blot | RBP10 | RBP8, RBP9 |
| Detected on Western blot | RBP3, RBP6, RBP20, RBP21, RBP28, RBP38, RBP28, DRBD7, DRBD9, TRRM3 | RBP3, RBP6, RBP10, RBP25 |
| IFA: cytoplasm | RBP3, RBP38 (RBP28, DRBD7) | (RBP6) |
| IFA: nucleus | RBP20 (DRBD9, TRRM3) | |
| IFA: nucleus and cytoplasm | | RBP25 |
| IFA: negative | RBP21 | RBP10 |

over at least 5 days and cumulative growth curves were plotted. Two cell lines with *RBP23* RNAi behaved strangely: they grew extremely slowly in the absence of tetracycline but recovered somewhat in the presence of tetracycline (Fig. 1); the basis for this has not been investigated. Inducible over-expression of RBP3 increased the division time from 8.2 to 12.6 h (Supplementary Figure S1A,B).

Two of the RRM-protein mRNAs were known, from microarray analyses, to be more abundant in bloodstream forms than procyclic forms (R. Queiroz and C. Clayton, in preparation). For both of these – *RBP9* and *RBP10* – RNAi in procyclic trypanosomes did not affect growth. A bloodstream cell line with *RBP10* RNAi showed severe growth inhibition; we have not yet succeeded in generating a bloodstream line with *RBP9* RNAi. Bloodstream trypanosomes with a T7-driven RNAi against *TRRM3* showed no growth effect, but a stem-loop construct revealed growth inhibition (Fig. 1).

Our RNAi methods have two major limitations: the system may be leaky in the absence of tetracycline, and it does not completely remove a gene product. In the "Trypanofan" RNAi screen 197 open reading frames were targeted [8]. Effects on growth were detected for 38% of all genes tested, and 29% of those with a Pfam annotation. These are clearly likely to be under-estimates: on top of the incomplete penetrance of RNAi, the cells were not cloned, so the methodology selected strongly against parasites with leaky RNAi. Our results for RNAi targeting RRM protein mRNAs, in contrast, suggested that 60–70% of the individual gene products were required for normal growth. The difference between these numbers and those seen in Trypanofan could be due to technical differences, but might also reflect the essential role of RNA metabolism.

We next wished to investigate the subcellular distributions of some of the essential proteins. After checking the protein sequences for targeting signals (to rule out the presence of a mitochondrial pre-sequence) we either tagged genes *in situ*, to give proteins with an N-terminal V5 tag [9], or inducibly expressed proteins with a myc tag at the N- or C-terminus (see e.g. [10]). Four proteins were found in the cytoplasm, three were restricted to the nucleus and one was in both compartments. Some tagged proteins that were detectable by Western blotting gave no signal by immunofluorescence; a few were not detected at all. The results are summarised in Table 3 and some data shown in Supplementary Figure S2.

**Table 2**
Effects of RNAi on trypanosome growth. Data are shown only for genes whose growth of RNAi lines was affected by tetracycline addition, or the lines had defective growth even without tetracycline. Numbers are the division time in hours. Where several numbers are given for one gene, they represent the results for independent cloned cell lines, and the numbers are given in order: the first number is for clone 1, the second number is for clone 2, etc. "Transient" means that an effect was seen in the 24-well plates but not after transfer to 5 ml flasks; this must be regarded with extreme caution. Bloodstream *DRBD5* lines (stem-loop construct, not included in the table) showed poor growth independent of tetracycline addition; quantitation was difficult because of clumping.

| | PC −tet | PC +tet | BS −tet | BS +tet | Location |
|---|---|---|---|---|---|
| *RBP3* | 8.4 | 8.7 | 8.2 | 12.6 | Cytoplasm |
| *RBP10* | [a] | No effect[a] | 11 | Dead[b] | Cytoplasm |
| *RBP14A* | ND | ND | 7.4, 7.5 | 8.0, 7.9 | ND |
| *RBP20* | 13.0 | 13.5 | [a] | No effect[a] | Nucleus (spots) |
| *RBP21* | [a] | Transient[a] | 9.5, 9.6 | 10.0, 10.2 | ND |
| *RBP23* | ND | ND | 19, 17 | 13, 10 | ND |
| *RBP25*[c] | ND | ND | 11.5 | 23 | Nucleus and cytoplasm |
| *RBP26* | ND | ND | 12 | 14 | ND |
| *RBP28* | 11.7, 10.8 | 13.1, 12.2 | ND | ND | Unclear |
| *RBP30* | [a] | Transient[a] | 9.2 | 9.8 | ND |
| *RBP31* | ND | ND | 9.8 | 17 | ND |
| *RBP38* | 11.8, 12.5, 12.6 | 12.7, 12.6, 12.8 | 9.1, 9.5, 8.9 | 10.0, 9.8, 9.6 | Cytoplasm |
| *DRBD6 A/B, 11* | NC | | 10.2, 9.5 | 12.0, 12.7 | ND |
| *DRBD7* | ND | ND | 9.8, 9.5, 10.1 | 13.1, 13.9, 16.8 | Cytoplasm |
| *DRBD9* | ND | ND | 7.4 | 8.4 | Nucleus |
| *DRBD12* | NC | | 10.0, 12.6, 11.7 | 11.5, 13.7, 13.4 | ND |
| *DRBD14* | [a] | No effect[a] | [a] | Transient[a] | ND |
| *TRRM3* | 10.5 | 13.5[b] | 7.0 | Dead[b] | Nucleus |

[a] Not measured in detail. ND: not done; NC: no clones obtained.
[b] Using p2T7 derivatives, no effect or clones not obtained; results are for a stem-loop.
[c] Results for *RBP25* were very variable, ranging from no effect to complete growth inhibition.

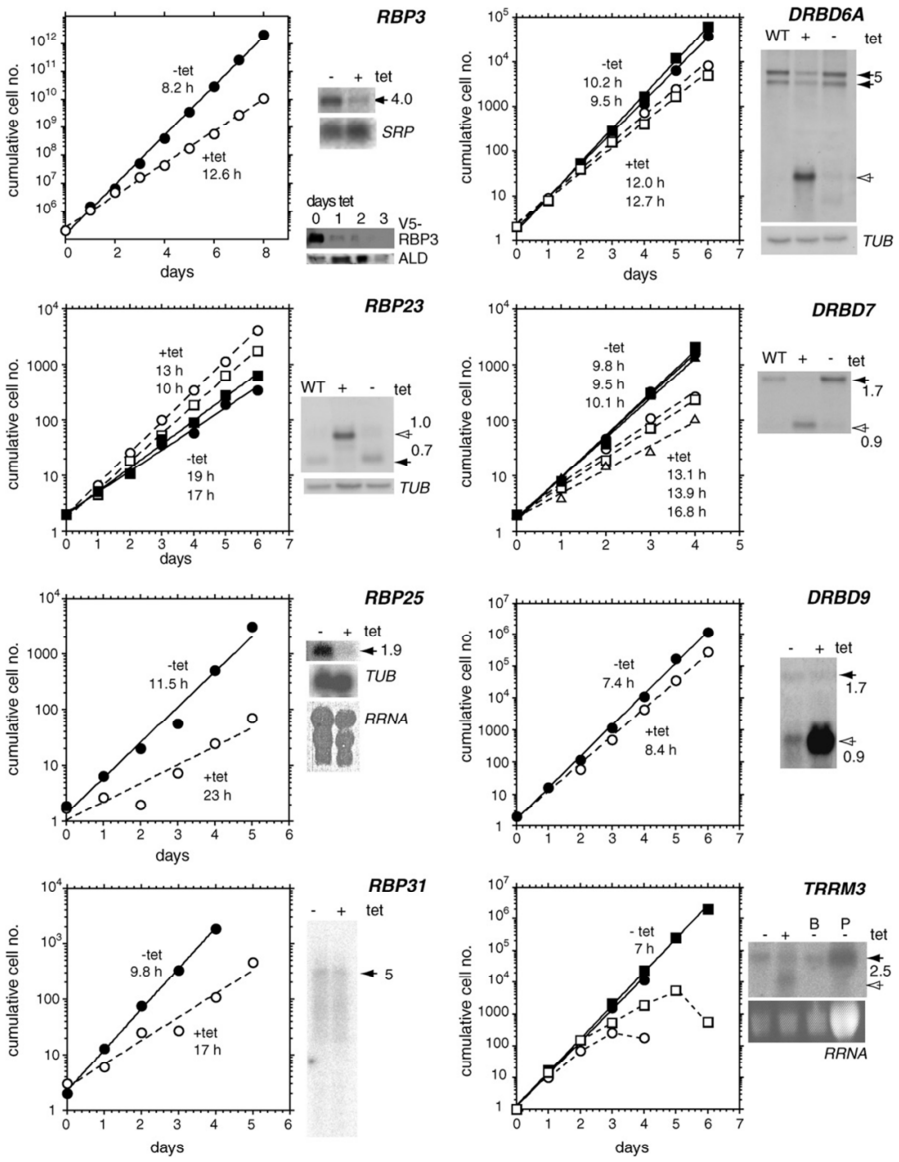


**Fig. 1.** Growth data for bloodstream trypanosomes with RNAi. The targeted protein is indicated. Cells were grown with (+) or without (−) tetracycline and diluted as required to maintain exponential growth; cumulative growth curves are shown along with division times calculated using Kaleidograph. RNA was prepared on day 3 after tetracycline addition, except for *DRBD9* (day 2). Sizes of mRNAs in kb are indicated next to the blots (solid arrow); the open arrow indicates the dsRNA. *TUB*: tubulin control probe. The Northern for *TRRM3* is from the clone with the less severe effect. All RNAi plasmids were based on p2T7 except those for *RBP3* and *TRRM3*, which were stem-loops (Supplementary Table S1). For RBP3 we also induced RNAi in cells expressing V5-tagged RBP3; the lower panel shows depletion of V5-RBP3 1, 2 and 3 days after RNAi induction, with aldolase (ALD) as a control.

We have previously shown that over-expression of the abundant small RRM proteins UBP1 and UBP2 affects gene expression in *T. brucei* [11]. RBP3 is related to UBP1 and UBP2 [4] and was reported to colocalise with the helicase DHH1 and polyA + RNA in granules in stressed procyclic trypanosomes [12]. In bloodstream forms, V5-*in situ* tagged RBP3 was all over the cytoplasm but also showed some concentration in regions containing DHH1 (Fig. 2A). In other respects V5-RBP3 behaved similarly to UBP1 and UBP2 [11]:

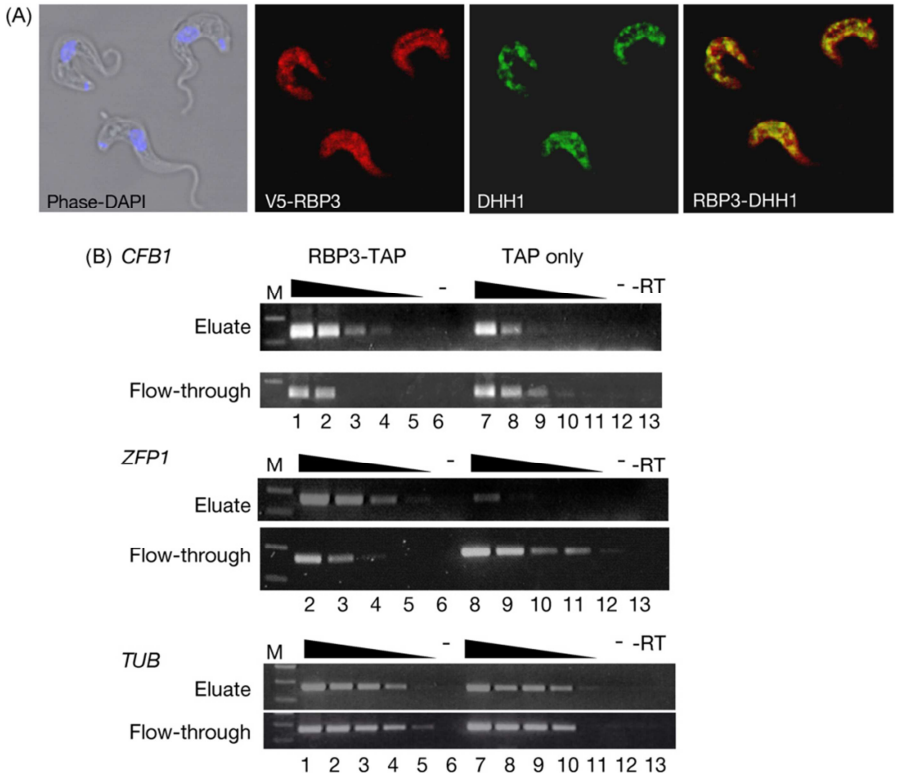


**Fig. 2.** Localisation and RNA binding assays for RBP3. (A) Immunofluorescence of bloodstream-form trypanosomes with *in situ* V5-tagged *Tb*UBP3 (red) counterstained for *Tb*DHH1 (green) and for DNA (DAPI). (B) Cells expressing *Tb*RBP3-TAP and the TAP tag alone were bound to IgG sepharose, and the bound complexes were released by TEV protease [14]. RNA was prepared from the entire eluate, and from 0.3 ml out of the 1 ml flow-through fraction [14], and reverse transcribed using an oligo-dT primer. 1:10 serial dilutions (until 1:10,000) of the cDNA generated were used as a template for the PCR, using specific primers for each transcript. After 30 amplification cycles, 10 μl of each sample were run into an agarose gel. The photograph shows the ethidium bromide stain. Lanes 1 and 7 represent cDNA from $3 \times 10^6$ cells for the eluate, and $9 \times 10^5$ cells for the flow-through; lanes 2 and 8, 10 times less, and so on. Thus the flow-through lanes represent four times less cDNA than the eluate lanes immediately above them.

it showed a similar abundance by Western blotting, was predominantly cytoplasmic after cell fractionation, and was not associated with polysomes on sucrose gradients (not shown).

To find out whether RBP3 is able to bind to specific RNAs, we expressed TAP-tagged RBP3 in bloodstream trypanosomes, pulled down RBP3-TAP from cell lysates, and identified the bound mRNAs using microarrays. The method ([13,14], see Supplementary Methods) did not distinguish between RNAs bound *in vivo*, and RNAs bound subsequent to cell lysis, but could nevertheless reveal whether RBP3 binds preferentially to specific RNA sequences. The microarrays used contain random genomic fragments, so many genes are represented more than once. Only 10 sequences reproducibly showed more than three-fold enrichment in the RBP3-bound sample (Table S2); of these, five were represented twice or more. They encode the cyclin F-box protein CFB1 [7]: two CCCH zinc finger proteins, ZFP1 [15] and ZC3H11 (Tb927.5.810); and two proteins with no annotation (loci Tb927.4.1000 and Tb927.8.7820). To find out what proportions of the *CFB1* and *ZFP1* mRNAs co-purified with RBP3-TAP, we compared their abundances in the bound and flow-through fractions by reverse transcription and PCR. The highly abundant tubulin (*TUB*) mRNA, and a purification using TAP tag alone, served as controls: these suggested non-specific binding of 10–15% of *TUB* RNA to either the tag, or the resin used for purification. In contrast, at least 25% of *CFB* and *ZFP1* RNAs were reproducibly specifically selected by RBP3-TAP; moreover, these RNAs were depleted in the RBP3-TAP flow-through fraction (Fig. 2B). A full tandem affinity purification of RBP3-TAP, in contrast, revealed no stably-associated protein binding partners (not shown).

To find out whether RBP3 depletion affects mRNA abundances, we compared the transcriptomes of RBP3-depleted cells with those of normal cells by microarray. No differences were seen, and Northern blots for some of the RBP3-selected mRNAs also showed little effect, apart from a slight increase in *ZC3H11* mRNA upon RBP3 overexpression (Figure S1C). Another possible role of RBP3 might be in translation. Antibodies are available for CFB1 [7] or ZFP1 [16] but we were unable to detect either in our cells, whether or not RBP3 levels were altered (not shown). Thus the biological role of RBP3 remains unknown.

**Acknowledgements**

This work was mainly supported by the Deutsche Forschungsgemeinschaft, SFB 544, project B13. The work on RBP3 was done

mainly by Ana Robles. who was supported by the Deutsches Akademisches Austauschdienst; Van-Duc Luu, Stefanie Brems and Jörg Hoheisel were all involved in the microarray analysis. The work in the Figures and Tables was done mainly by Martin Wurst, Ana Robles and June Po, with contributions by Mari Marentije and Savrina Stoitsova. Mhairi Stewart was responsible for some supervision and cloning, and Luis Quijada, who was supported by a long-term EMBO fellowship, did most of the experiments with DRBD13. The project was partially supervised by Claudia Hartmann (who also did a lot of the cloning work), and administered by Christine Clayton, who wrote the manuscript. We thank all of the students who assisted with this project during lab practicals: Maria Liebert, Katherina Rauschenberger, Maren Emmerich, Mohit Kumar, Theresa Manful, Sabrina Schmitt. We also thank the students of the practical "E1: nucleic acids" for PCRs and some Northern results. We thank all other members of the lab for assisting the students.

## Appendix A. Supplementary data

Supplementary data associated with this article can be found, in the online version, at doi:10.1016/j.molbiopara.2008.09.001.

## References

[1] Martinez-Calvillo S, Yan S, Nguyen D, Fox M, Stuart K, Myler PJ. Transcription of *Leishmania major* Friedlin chromosome 1 initiates in both directions within a single region. Mol Cell 2003;11:1291–9.
[2] Clayton C, Shapira M. Post-transcriptional regulation of gene expression in trypanosomes and leishmanias. Mol Biochem Parasitol 2007;156:93–101.
[3] Simpson L, Sbicego S, Aphasizhev R. Uridine insertion/deletion RNA editing in trypanosome mitochondria: a complex business. RNA 2003;9:265–76.
[4] De Gaudenzi JG, Frasch ACC, Clayton C. RNA-binding domain proteins in Kinetoplastids: a comparative analysis. Eukaryot Cell 2006;4:2106–14.
[5] Clayton CE, Estévez AM, Hartmann C, Alibu VP, Field M, Horn D. Downregulating gene expression by RNA interference in *Trypanosoma brucei*. In: Carmichael G, editor. RNA interference. Humana Press; 2005.
[6] Alibu VP, Storm L, Haile S, Clayton C, Horn D. A doubly inducible system for RNA interference and rapid RNAi plasmid construction in *Trypanosoma brucei*. Mol Biochem Parasitol 2004;139:75–82.
[7] Benz C, Clayton C. The cyclin F box protein CFB2 is required for cytokinesis of bloodstream-form *Trypanosoma brucei*. Mol Biochem Parasitol 2007;156:217–24.
[8] Subramaniam C, Veazey P, Redmond S, et al. Chromosome-wide analysis of gene function by RNA interference in the African trypanosome. Eukaryot Cell 2006;5:1539–49.
[9] Shen S, Arhin GK, Ullu E, Tschudi C. In vivo epitope tagging of *Trypanosoma brucei* genes using a one step PCR-based strategy. Mol Biochem Parasitol 2001;113:171–3.
[10] Colasante C, Alibu VP, Kirchberger S, Tjaden J, Clayton C, Voncken F. Characterisation and developmentally regulated localisation of the mitochondrial carrier protein homologue MCP6 from *Trypanosoma brucei*. Eukaryot Cell 2006;5:1194–205.
[11] Hartmann C, Benz C, Brems S, et al. The small trypanosome RNA-binding proteins TbUBP1 and TbUBP2 influence expression of F box protein mRNAs in bloodstream trypanosomes. Eukaryot Cell 2007;6:1964–78.
[12] Cassola A, De Gaudenzi J, Frasch A. Recruitment of mRNAs to cytoplasmic ribonucleoprotein granules in trypanosomes. Mol Microbiol 2007;65:655–70.
[13] Luu VD, Brems S, Hoheisel J, Burchmore R, Guilbride D, Clayton C. Functional analysis of *Trypanosoma brucei* PUF1. Mol Biochem Parasitol 2006;150:340–9.
[14] Archer S, Queiroz R, Stewart M, Clayton CE. Trypanosomes as a model to investigate mRNA decay pathways. In: Maquat LE, Kiledjian M, editors. RNA turnover in eukaryotes. Elsevier; in press.
[15] Hendriks EF, Robinson DR, Hinkins M, Matthews KR. A novel CCCH protein which modulates differentiation of *Trypanosoma brucei* to its procyclic form. EMBO J 2001;20:6700–11.
[16] Hendriks EF, Matthews KR. Disruption of the developmental programme of *Trypanosoma brucei* by genetic ablation of TbZFP1, a differentiation-enriched CCCH protein. Mol Microbiol 2005;57:706–16.

**5.2**

# A domino effect in drug action: from metabolic assault towards parasite differentiation

Jurgen R. Haanstra, Eduard J. Kerkhoven,
Arjen van Tuijl, Marjolein Blits, Martin Wurst,
Rick van Nuland, Marie-Astrid Albert,
Paul A. M. Michels, Jildau Bouwman,
Christine Clayton, Hans V. Westerhoff1, and
Barbara M. Bakker

Molecular Microbiology (2011) 79(1), 94–108 ■

doi:10.1111/j.1365-2958.2010.07435.x
First published online 5 November 2010

# A domino effect in drug action: from metabolic assault towards parasite differentiation

**Jurgen R. Haanstra,[1†‡] Eduard J. Kerkhoven,[2†] Arjen van Tuijl,[1] Marjolein Blits,[1] Martin Wurst,[3] Rick van Nuland,[1§] Marie-Astrid Albert,[4] Paul A. M. Michels,[4] Jildau Bouwman,[1] Christine Clayton,[3] Hans V. Westerhoff[1,5] and Barbara M. Bakker[1,6*]**

[1]*Department of Molecular Cell Physiology, Faculty of Earth and Life Sciences, Vrije Universiteit Amsterdam, De Boelelaan 1085, NL-1081 HV Amsterdam, the Netherlands.*
[2]*Institute of Biomedical and Life Sciences, Division of Infection and Immunity, University of Glasgow, Glasgow, UK.*
[3]*Zentrum für Molekulare Biologie, Universität Heidelberg, Heidelberg, Germany.*
[4]*Research Unit for Tropical Diseases, de Duve Institute and Laboratory of Biochemistry, Université catholique de Louvain, Brussels, Belgium.*
[5]*AstraZeneca Chair for Systems Biology, Manchester Centre for Integrative Systems Biology, Manchester, UK.*
[6]*Department of Pediatrics, Centre for Liver, Digestive and Metabolic Diseases University Medical Centre Groningen, University Groningen Hanzeplein 1, NL-9713 GZ Groningen, the Netherlands.*

## Summary

**Awareness is growing that drug target validation should involve systems analysis of cellular networks. There is less appreciation, though, that the composition of networks may change in response to drugs. If the response is homeostatic (e.g. through upregulation of the target protein), this may neutralize the inhibitory effect. In this scenario the effect on cell growth and survival would be less than anticipated based on affinity of the drug for its target. Glycolysis is the sole free-energy source for the deadly parasite *Trypanosoma brucei* and is therefore a possible target pathway for anti-trypanosomal drugs. Plasma-membrane glucose transport exerts high control over trypanosome glycolysis and hence the transporter is a promising drug target. Here we show that at high inhibitor concentrations, inhibition of trypanosome glucose transport causes cell death. Most interestingly, sublethal concentrations initiate a domino effect in which network adaptations enhance inhibition. This happens via (i) metabolic control exerted by the target protein, (ii) decreases in mRNAs encoding the target protein and other proteins in the same pathway, and (iii) partial differentiation of the cells leading to (low) expression of immunogenic insect-stage coat proteins. We discuss how these 'anti-homeostatic' responses together may facilitate killing of parasites at an acceptable drug dosage.**

Accepted 7 October, 2010. *For correspondence. E-mail: B.M. Bakker@med.umcg.nl; Tel. (+31) 503611542; Fax (+31) 503611746. †These authors contributed equally. ‡Present address: Department of Hematology, ErasmusMC, Rotterdam, the Netherlands. §Present address: Department of Physiological Chemistry, UMCU, Utrecht, the Netherlands.



## Introduction

Living organisms combat external perturbations through homeostatic response mechanisms. For example, if a substrate becomes limiting, the transporter that takes it up might be upregulated, through either increased expression or post-translational mechanisms. Similarly, during treatment with a drug that inhibits an enzyme, the enzyme activity might be increased, neutralizing drug action.

Much current research is devoted to validation of new molecular targets for antimicrobial drugs. The major criteria for such targets include (i) that they should be essential for microbial growth or survival and (ii) that there should be a sufficient difference between the host and the pathogen to allow specific inhibition of the pathogen target. Since a large proportion of microbial proteins may fulfil both conditions, it is useful also to add additional criteria. For example, high concentrations of an enzyme substrate will out-compete substrate analogues; and if the target is present in huge excess, then very high levels of inhibition will be required to kill the pathogen. Either of these situations would hinder development of a specific inhibitor that can be given at acceptable doses. The ability of the microbial system to homeostatically adapt to inhibition adds an additional complication.

To deal with these issues, it is useful to apply a systems biology approach, including metabolic modelling, when choosing potential targets for antimicrobial drugs. Because adaptation may involve various aspects of regulation,

target validation ideally should integrate not only metabolic, but also signalling and gene-expression networks (Alberghina and Westerhoff, 2005). So far, however, of the few successful network-based drug design studies that exist (Noble, 2006), none addresses the potential adaptation of the network.

*Trypanosoma brucei* causes deadly African sleeping sickness in humans, and the related disease 'Nagana' in cattle. As currently available drugs are inadequate and toxic while drug resistance is increasing rapidly, new and more selective medication is needed (Barrett *et al.*, 2003).

*T. brucei* is transmitted by tse-tse flies. After growing to a certain density in the mammalian bloodstream, the proliferating 'long-slender' bloodstream forms differentiate into non-dividing 'short-stumpy' trypanosomes. The short-stumpy trypanosomes differentiate further into the 'procyclic' (insect-form) cells in the midgut of the tse-tse fly after the latter has taken a blood meal (Matthews, 2005). The most prominent differences between the life-cycle stages inside the mammalian host and inside the insect vector are at the level of metabolism and surface-protein expression. The long-slender bloodstream-form trypanosome relies merely on the glycolytic pathway with pyruvate as the main end-product. Metabolism in procyclic trypanosomes is more complex: they can utilize more substrates and, in contrast to bloodstream form cells, they use extensive mitochondrial metabolism (Hellemond *et al.*, 2005). The bloodstream-form cells are shielded from the mammalian immune system by a dense layer of variant surface glycoproteins (VSG) (Cross, 1975; Borst and Ulbert, 2001). Upon ingestion by the tse-tse fly, or transfer to procyclic culture conditions, the VSG coat is shed and replaced by a coat of EP and GPEET proteins of the procyclin family (Vassella *et al.*, 2001; Urwyler *et al.*, 2005; Gruszynski *et al.*, 2006). The short-stumpy cells undergo some minor metabolic changes in the direction of procyclic forms. Both stumpy forms and non-dividing trypanosomes in the early stages of differentiation *in vitro* express lower levels of many mRNAs required for growth, and show upregulation of plasma-membrane tricarboxylic acid transporters that are involved in sensing the differentiation signal (Dean *et al.*, 2009; Jensen *et al.*, 2009; Kabani *et al.*, 2009; Queiroz *et al.*, 2009). Bloodstream-form trypanosomes that have been cultured continuously are called 'monomorphic' because they have lost the ability to develop into stumpy forms; in some cases they are no longer able to differentiate into growing procyclic forms (Fenn and Matthews, 2007).

The reliance of bloodstream-form *T. brucei* on glycolysis suggests that this pathway could be an excellent drug target, should selective inhibition be possible (Verlinde *et al.*, 2001). Previously, we combined Metabolic Control Analysis (Kacser and Burns, 1973; Heinrich and Rapoport, 1974; Groen *et al.*, 1982), a theoretical framework to analyse the relative importance of each protein for cellular fluxes, with computer modelling and experimentation (Bakker *et al.*, 1999a,b; Albert *et al.*, 2005; Caceres *et al.*, 2010) to study which enzyme(s) control(s) glycolytic flux in trypanosomes. We demonstrated that glucose transport across the plasma membrane is the dominant factor controlling the free-energy metabolism (the ATP synthesis flux) of African trypanosomes. The amino acid sequence of the trypanosome glucose transporter (THT1) is only ~19% identical and 42% similar to that of the human erythrocyte glucose transporter GLUT1 (Bringaud and Baltz, 1992): thus it may be possible to find a highly specific inhibitor of THT1, and to capitalize on the unique dependence of the parasites upon its transport activity. This made the glucose transporter a promising candidate drug target. However, the possibility of homeostatic adaptation via gene expression had not been addressed.

Trypanosomes do not regulate transcription of individual genes by RNA polymerase II, since transcription is polycistronic. Yet they do regulate mRNA processing, mRNA degradation and translation (Clayton and Shapira, 2007; Haile and Papadopoulou, 2007). Gene-expression changes in trypanosomes have almost exclusively been studied in the context of differentiation. There have, however, been a few studies investigating the responses to glucose availability. In bloodstream-form trypanosomes, glucose deprivation induced the expression of procyclic surface-coat proteins (Milne *et al.*, 1998). And in procyclic forms, which can obtain energy either from glucose or from proline, inhibition of the glucose transporter by *N*-acetyl D-glucosamine caused a shift towards proline-dependent metabolism (Ebikeme *et al.*, 2008). In procyclic forms, also, RNAi targeting of either the glucose transporter or hexokinase caused a switch from one procyclic-specific surface protein to another (Morris *et al.*, 2002).

In the present study we aim to quantitatively link the metabolic response of trypanosomes to glucose transport inhibition with adaptations in gene expression, growth and differentiation. We show that while high concentrations of glucose transport inhibitors kill trypanosomes, sublethal concentrations evoke a multilayered adaptation of the network. Unexpectedly, this adaptation is not homeostatic: instead, it potentiates the effect of the primary inhibition. This anti-homeostatic response enhances the status of the trypanosome glucose transporter as a potential drug target.

## Results

### *Chemical inhibition of glucose transport leads to a decrease of glycolytic flux and growth rate of trypanosomes*

To study the effects of glucose-transport inhibition beyond metabolism, we inhibited glucose transport with either

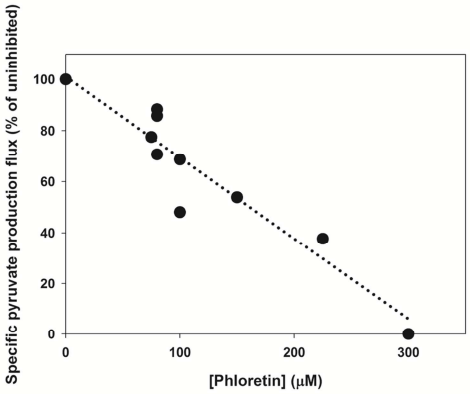


**Fig. 1.** Glycolytic flux upon inhibition by phloretin. Glycolytic flux (measured as the specific pyruvate production flux) in bloodstream-form trypanosomes after 24 h exposure to various phloretin concentrations. Each point in the graph is based on an independent culture and its control. The uninhibited pyruvate flux, i.e. in the absence of phloretin, was 373 ± 57.1 nmol $min^{-1}$ ($10^8$ $cells)^{-1}$ (SEM, $n = 5$). At the beginning of each experiment we split cultures into one that remained untreated and was used as control, and another that was treated with the indicated concentration of phloretin. The measured flux in the untreated control culture was used as the 100% reference, to correct for variations between experiments. The dotted line is a linear fit to the data ($R^2 = 0.92$).

phloretin (Bakker *et al.*, 1999b) or 2-deoxy-D-glucose (2-DOG) (Tetaud *et al.*, 1997), two chemically unrelated inhibitors. Phloretin is a general inhibitor of facilitated diffusion transporters and has been shown to be a competitive inhibitor of the trypanosome glucose transporter (Bakker *et al.*, 1999b). 2-DOG is a glucose analogue that cannot be metabolized beyond phosphorylation by hexokinase. 2-DOG therefore acts as a competitive inhibitor of glucose transport, and – depending on its intracellular concentration – also of hexokinase (HXK). As far as side-effects are known, they are quite different for the two compounds. Phloretin remains outside cells, but may hit other transporters (Krupka and Deves, 1980) while intracellular 2-DOG affects HXK. Effects that are seen for both inhibitors are therefore likely to be due to the inhibition of glucose transport specifically. The inhibitors have the advantage that they act very rapidly on the transporter; in contrast to RNAi, their use allows assessment of changes of the transporter itself. All of our studies were conducted with a monomorphic trypanosome line 449 derived from strain Lister 427. These trypanosomes were chosen because their glycolytic metabolism has been exhaustively characterized; they are however unable to undergo complete differentiation to procyclic forms.

Phloretin reduced the glycolytic flux, measured as the pyruvate production flux (Fig. 1), and the specific growth rate (Fig. 2A) of bloodstream-form trypanosomes. 2-DOG gave similar results (Fig. 2B). At all inhibitor concentrations we found production of only small amounts of glycerol and neither succinate nor acetate. Above 100 μM phloretin the cells started dying within the first 24 h, although the glycolytic flux was only inhibited by 50% (Fig. 1). The latter result is not specific for inhibition of glucose transport, but was also previously found for various glycolytic enzymes. A compilation of results obtained with RNAi of various glycolytic targets and those of the phloretin and 2-DOG experiments shows that a partial (30–50%) inhibition of the glycolytic flux sufficed to block growth (Fig. 3). A further inhibition of the pathway

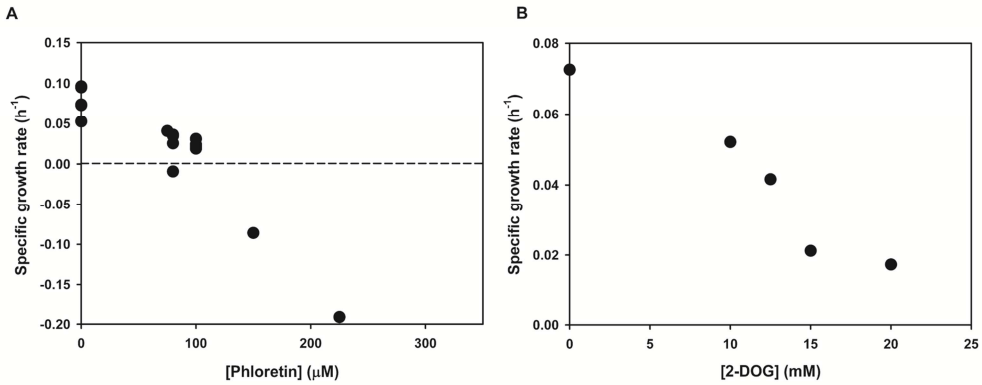


**Fig. 2.** Effect of inhibition of glucose transport on the specific growth rate of trypanosomes. Specific growth rate ($\mu$, see *Experimental procedures*) as determined in the first 24 h after inhibition by various concentrations of phloretin (A) or 2-DOG (B). The negative growth rates should be interpreted as death rates. Further experiments were all performed at 100 μM phloretin or 12.5 mM 2-DOG, doses at which the cells remain alive but hardly grow. Each point in the graph is based on an independent culture.

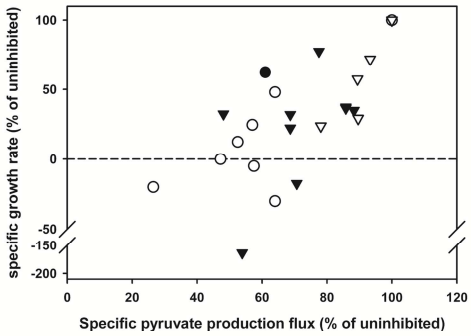


**Fig. 3.** Relation between growth rate and glycolytic flux in trypanosomes with impaired activities of glycolytic enzymes or glucose transport. Specific growth rates plotted against specific pyruvate production flux (– glycolytic flux) after 24 h inhibition with various concentrations of phloretin (▼) or 2-DOG (▽) (this article), RNAi against several glycolytic enzymes (○) (Albert *et al.*, 2005; Caceres *et al.*, 2010) and a knockout of the alternative oxidase (●) (Helfert *et al.*, 2001). Percentages were calculated relative to control cultures in the same experiment. For phloretin, data of Figs 1 and 2A were combined. Each point in the graph shows an independent experiment.

caused cell death. Unlike phloretin, 2-DOG was only tested at sublethal concentrations. Over the tested concentration range the relation between specific growth rate and pyruvate production flux was similar for the two inhibitors (open and closed triangles in Fig. 3). Growth inhibition by phloretin was reversible during the first 24 h (Fig. S1).

### *Inhibition by phloretin or 2-DOG evokes a gene-expression response in bloodstream-form* T. brucei

We next studied mRNA levels in cells treated with sublethal concentrations of phloretin and 2-DOG, concentrating on the glycolytic enzymes. Strikingly, the *THT1* mRNA, encoding the major glucose transporter in the bloodstream form, was *down*- rather than *up*regulated after inhibition of glucose transport (Fig. 4A). Hence, the parasites adapted, not homeostatically, but in a way that aggravated their situation.

Further analysis of glycolytic gene expression revealed a general downregulation of mRNAs encoding glycolytic enzymes that are normally expressed in bloodstream-form trypanosomes [see, e.g. pyruvate kinase (*PYK*) in Fig. 4A and the complete data set in Fig. 4B]. Procyclic cells have been demonstrated to express the majority of these enzymes at a lower protein level than bloodstream-form cells (Hart *et al.*, 1984; Aman and Wang, 1986). Furthermore, typical procyclic isoforms of the glucose transporter (*THT2*) and of phosphoglycerate kinase (*PGKB*) were upregulated to the detriment of their bloodstream-form counterparts *THT1* and *PGKC* respectively. The expression of *PGKB* was surprising, since this isoform has a subcellular localization different from that of *PGKC* and its expression is normally toxic in bloodstream-form trypanosomes (Blattner *et al.*, 1998). It is unlikely that the increased mRNA levels of *THT2* can compensate for the decreased expression of *THT1*: the absolute change is much larger for *THT1* since its initial level was 40 times higher than that of *THT2* (Bringaud and Baltz, 1993). Moreover, growth of procyclic trypanosomes was inhibited by phloretin (data not shown), suggesting that also the procyclic glucose transporter THT2 is sensitive to this inhibitor. However, this last finding may also be attributed to an unknown side-effect on other targets or to catabolite repression of proline metabolism [as was suggested previously (Lamour *et al.*, 2005)].

Finally we also observed increased mRNA levels for the genes encoding the Krebs' cycle enzyme citrate synthase (CS), as well as pyruvate orthophosphate dikinase (PPDK) and proline dehydrogenase (PRODH). These enzyme activities are absent in bloodstream-form trypanosomes (Jenkins *et al.*, 1988; Priest and Hajduk, 1994; Bringaud *et al.*, 1998). To test whether the mRNA changes were reflected by changes at the level of functional proteins, we measured CS activity. This was low in untreated bloodstream forms, but rose 3.5-fold after 48 h inhibition of glucose transport, to a level that was even higher than that of procyclic trypanosomes (Fig. 4C).

### *Phloretin treatment causes transcriptome changes indicative of partial differentiation*

To characterize the effects of phloretin treatment on the entire transcriptome, we treated exponentially growing bloodstream-form trypanosomes for 24 h with 100 μM phloretin, then extracted RNA. RNA from untreated trypanosomes served as a control. Fluorescently labelled cDNAs were hybridized to *T. brucei* oligonucleotide microarrays (see *Experimental procedures*). We found that 54 RNAs were significantly increased at $P < 0.05$, 45 of these being altered by 1.5-fold or more. A total of 276 RNAs were significantly decreased after the treatment, 153 of them at least 1.5-fold (see Table S1). For mRNAs that were analysed with both techniques, the microarray results corresponded qualitatively with those of the qPCR analysis, although, as expected, the latter tended to yield somewhat larger changes in expression (Table S1).

We have previously shown that during differentiation of *in vitro* cultured pleomorphic trypanosomes, 1113 mRNAs showed significant changes in abundance, with detailed time-courses that could be classified according to 62 groups with different patterns of regulation. (Queiroz *et al.*, 2009). The 62 patterns fell into four broad categories: highest expression in bloodstream forms; highest

A

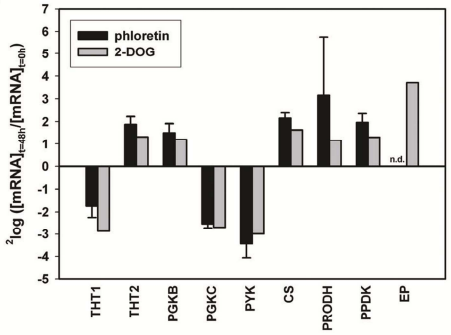


B

| | Phloretin | | | | | | 2-DOG | |
|---|---|---|---|---|---|---|---|---|
| | 24 | | | 48 | | | 24 | 48 |
| | average | SEM | sig | average | SEM | sig | | |
| THT1 | 0.25 | 0.10 | * | 0.34 | 0.11 | * | 0.84 | 0.14 |
| THT2 | 1.22 | 0.42 | | 3.89 | 0.90 | | 2.27 | 2.48 |
| HXK | 0.35 | 0.12 | * | 0.38 | 0.10 | * | 0.91 | 0.27 |
| PGI | 0.32 | 0.07 | * | 0.37 | 0.06 | * | 0.50 | 0.23 |
| PFK | 0.29 | 0.11 | * | 0.19 | 0.07 | * | 0.81 | 0.22 |
| ALD | 0.35 | 0.14 | * | 0.25 | 0.11 | * | 0.28 | 0.28 |
| TIM | 0.34 | 0.15 | * | 0.40 | 0.12 | * | 0.64 | 0.64 |
| G3PDH | 0.24 | 0.08 | * | 0.26 | 0.07 | * | 0.75 | 0.26 |
| GK | 0.32 | 0.11 | * | 0.41 | 0.11 | * | 1.14 | 0.43 |
| AOX | 0.56 | 0.20 | | 0.73 | 0.30 | | 1.32 | 0.85 |
| GAPDH | 0.26 | 0.12 | * | 0.17 | 0.06 | * | 0.46 | 0.13 |
| PGKB | 1.34 | 0.47 | | 3.05 | 0.77 | | 2.26 | 2.30 |
| PGKC | 0.27 | 0.11 | * | 0.17 | 0.02 | * | 0.57 | 0.16 |
| PGAM | 0.77 | 0.26 | | 1.26 | 0.31 | | 1.92 | 1.57 |
| ENO | 0.31 | 0.11 | * | 0.35 | 0.11 | * | 0.44 | 0.40 |
| PYK | 0.17 | 0.07 | * | 0.11 | 0.04 | * | 0.30 | 0.13 |
| CS | 2.82 | 1.17 | | 4.59 | 0.70 | | 4.08 | 3.08 |
| PRODH | 13.11 | 10.46 | | 17.11 | 20.68 | | 2.91 | 2.23 |
| PPDK | 2.48 | 1.08 | | 4.18 | 1.05 | | 2.97 | 2.46 |
| EP1 | n.d. | | | n.d. | | | 1.56 | 13.06 |

C

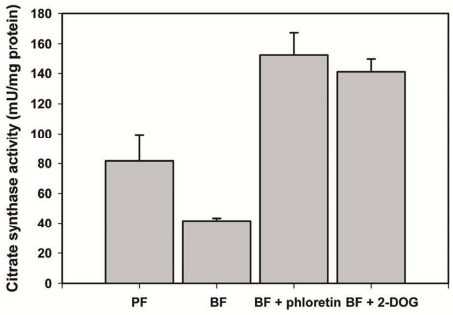


**Fig. 4.** Effect of phloretin and 2-DOG on gene expression
A. mRNA levels in bloodstream-form trypanosomes after 48 h inhibition by 100 μM phloretin or 12.5 mM 2-DOG as compared with expression before inhibition. For phloretin the error bars indicate the SEM of three independent experiments. For PRODH, the error was not SEM, but a standard deviation of two experiments. *EP* was only measured in the 2-DOG-treated cultures.
B. mRNA fold changes for cultures treated with 100 μM phloretin or 12.5 mM 2-DOG compared with uninhibited cultures after 24 or 48 h. Colour coding: green = twofold or more upregulated; red = twofold or more downregulated; yellow = less than twofold change. n.d., not determined. An asterisks in the column 'sig' (for significance) indicates a $P < 0.05$ in a one-sided Student's *t*-test comparing the measurements to a value of 1 (for no change in expression).
2-DOG, 2-deoxy-D-glucose; ALD, aldolase; AOX, alternative oxidase; CS, citrate synthase; ENO, enolase; EP, EP procyclin; HXK, hexokinase; G3PDH, glycerol-3-phosphate dehydrogenase; GAPDH, glyceraldehyde-3-phosphate dehydrogenase; PGAM, phosphoglycerate mutase; PGK, phosphoglycerate kinase; PFK, phosphofructokinase; PGI, phosphoglucose isomerase; PYK, pyruvate kinase; PPDK, pyruvate orthophosphate dikinase; PRODH, proline dehydrogenase; THT, trypanosome hexose transporter; TIM, triosephosphate isomerase.
C. Citrate synthase activity was measured in procyclic cultures (PF; $n = 2$), in ethanol-treated (control) bloodstream-form cultures (BF; $n = 4$) and in bloodstream forms exposed for 48 h to a (sublethal) dose of either 100 μM phloretin ($n = 2$) or 12.5 mM 2-DOG ($n = 4$).

expression in procyclic forms; and either increased, or decreased, expression during differentiation. The gene-expression patterns between 1 and 12 h after initiation of differentiation were indicative of growth arrest and partial induction of a stumpy-like phenotype, with surface-coat switching initiating at around 12 h (Queiroz *et al.*, 2009). We compared our microarray data after phloretin treatment with the previous differentiation data set (Fig. 5 and Tables S1 and S2). When we examined the 153 mRNAs that were at least 1.5-fold downregulated after phloretin treatment, we found that less than 10% were preferentially expressed in procyclic forms. In contrast, a quarter of them were preferentially expressed in bloodstream forms, and another quarter decreased in level during differentiation (Fig. 5A). The category preferentially expressed in bloodstream forms included, as expected, 20 proteins involved in glucose metabolism, including glycolytic and other glycosomal enzymes, and glycosome assembly proteins. The mRNAs that were decreased during differentiation, and also decreased after phloretin, included no fewer than 24 genes encoding components of the flagellum (Fig. 5B): flagellar biosynthesis halts in non-dividing cells.

The 45 mRNAs that increased at least 1.5 times after phloretin treatment fell into more groups, but RNAs that are preferentially expressed in procyclics, or are

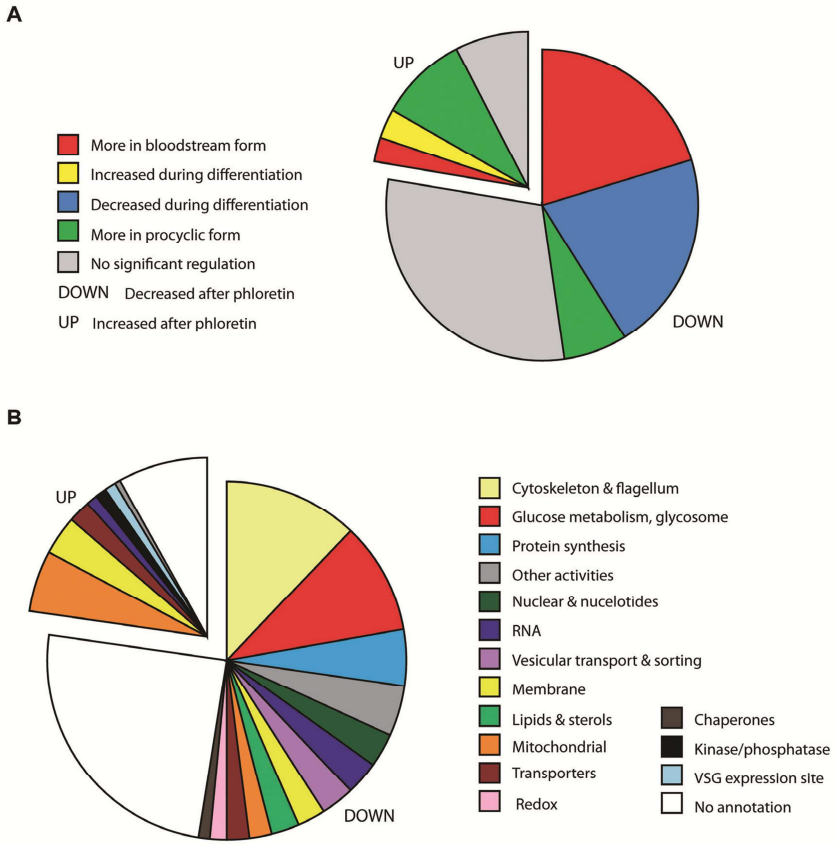


**Fig. 5.** Effects of phloretin treatment on the bloodstream-form transcriptome. Exponentially growing bloodstream-form trypanosomes (density $6 \times 10^5$ cells $ml^{-1}$) were treated with 100 µM phloretin for 24 h and subsequently their RNA was prepared for microarray analysis using untreated cells as a control, exactly as described in Queiroz *et al.* (2009). Results shown are for five slides including three biological replicates, with dye-swap, and include all spots showing significant $P < 0.05$ differences of at least 1.5-fold. The colour key is in the figure.
A. Regulated RNAs classified according to regulation during differentiation, as seen in Queiroz *et al.* (2009).
B. Regulated mRNAs classified according to the function of the encoded protein [automated and manual annotation, as in Queiroz *et al.* (2009)].

increased during differentiation, predominated (Fig. 5A). They included mitochondrial proteins and procyclic-specific membrane proteins (Fig. 5B). Notably, the upregulated mRNAs included those that encode two citrate/*cis*-aconitate transporters involved in differentiation, PAD1 and PAD2. PAD1 is a marker of growth-arrested stumpy forms (Dean *et al.*, 2009).

The overlap between the phloretin and differentiation data sets was only partial: just 124 RNAs were both affected by phloretin (at least 1.5-fold) and significantly regulated during differentiation. Using the phloretin data for just these 124 mRNAs, we calculated correlation coefficients with data from the different differentiation time points. The best correlation coefficients, i.e. 0.72 and 0.79, were for the 1 and 12 h time points respectively. These results indicated that our phloretin treatment had caused a subset of transcriptome changes similar to those seen during the early stages of differentiation to procyclic forms, when the parasites undergo growth arrest and initiate the switch from bloodstream-form to procyclic-form gene expression.

We also compared the phloretin microarray results with a data set generated using a tiling array (Fig. S2). The populations tested included stumpy trypanosomes

 *Molecular Microbiology*, **79**, 94–108

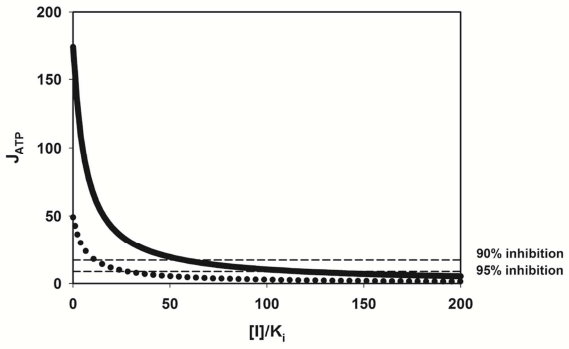


| | gene-expression adaptation | |
|---|---|---|
| | No | Yes |
| [I]/$K_i$ 90% inhibition | 56 | 11 |
| [I]/$K_i$ 95% inhibition | 118 | 28 |

**Fig. 6.** The impact of gene-expression adaptation on the reduction of the glycolytic flux. The steady-state ATP synthesis flux was calculated as a function of the concentration [I] of a competitive inhibitor of glucose transport across the plasma membrane. The concentration [I] was normalized with respect to the inhibition constant $K_i$, which equals the dissociation constant of the inhibitor from the transport protein. Calculations were performed for the original model as described in Albert *et al.* (2005) (solid line) and when the $V_{max}$ values were altered with the same factor as the corresponding transcript levels as measured (dotted line). The glucose concentration was 5 mM, like the blood glucose concentration. Details of the modelling are given in *Experimental procedures*.

generated in mice, as well as comparisons of bloodstream and procyclic forms (Jensen *et al.*, 2009) (Fig. S2A). In addition, we looked at a comparison of bloodstream and procyclic-form transcriptomes generated by cDNA sequencing (Siegel *et al.*, 2010) (Fig. S2B). As before, the mRNAs that were increased by phloretin showed a rather heterogeneous regulation pattern, with a bias towards procyclic-specific mRNAs. The results confirmed that many of the mRNAs that decreased after phloretin-treatment were preferentially expressed in bloodstream forms. Moreover, an even larger group of the mRNAs decreased after phloretin treatment showed expression that was suppressed in the stumpy forms.

We concluded that phloretin induced gene-expression changes characteristic of growth arrest and early differentiation. The next step was to assess the implications of these changes for trypanosome metabolism.

### *Decreased expression of glycolytic enzymes renders trypanosome glycolysis more sensitive to glucose transport inhibition*

We investigated the impact of the altered gene expression on the inhibition of the glycolytic flux, using the previously developed computer model of *T. brucei* glycolysis (Albert *et al.*, 2005). The model takes the enzyme expression (concentration or $V_{max}$) and the kinetic parameters of the enzymes as input. It predicts how the glycolytic flux and the metabolite concentrations respond to substrate availability, enzyme expression or specific inhibitors. We calculated how the (glycolytic) ATP production flux will respond to an increasing concentration of a competitive inhibitor of glucose transport, like phloretin (Fig. 6). In the calculations the inhibitor concentration [I] was normalized against its inhibition constant $K_i$, which equals the dissociation constant of the inhibitor from the transport protein. This was done to generalize the results to any competitive inhibitor of glucose transport.

If gene expression were not taken into account, a flux reduction of 90% would be achieved at an inhibitor concentration that was 56 times the inhibition constant for the transporter. A flux reduction of 95% would require 118 times the inhibition constant (Fig. 6, solid line). Next, the $V_{max}$ values in the model were altered by the same factor as the observed change of the corresponding mRNA after 24 h of phloretin treatment (Fig. 4B). Now, the required inhibitor concentrations for flux reductions of 90% or 95% were only 11 times, or 28 times the inhibition constant respectively (Fig. 6, dotted line). Hence, according to the model the same flux reduction is achieved at a four to five times lower drug dosage when the gene-expression response is included, than when it is not.

Obviously, the assumption that the actual change in protein concentrations equals that in the mRNAs is an approximation. The rationale behind this assumption is that during trypanosome differentiation from the bloodstream to the procyclic form not only mRNAs of glycolytic proteins are downregulated (Jensen *et al.*, 2009; Queiroz *et al.*, 2009; Nilsson *et al.*, 2010), but also protein levels and $V_{max}$ values (Hart *et al.*, 1984; Aman and Wang, 1986). The fact that the phloretin-treated cells are hardly dividing would diminish the changes in protein as com-

pared with those in mRNA, if the proteins were stable. During trypanosome differentiation, however, 'old' glycosomal enzymes are degraded through autophagy of glycosomes (Herman *et al.*, 2008).

Given the uncertainties in the protein response, the above calculations should be considered as an illustration of how the gene-expression response will affect the required drug dosage, rather than as an exact prediction. Nevertheless, the calculations were in surprisingly good agreement with the measured inhibition of the glycolytic flux by phloretin (Fig. 1). The $K_i$ of phloretin for the trypanosome glucose transporter THT1 is 21 μM (Bakker *et al.*, 1999b). In the presence of 20 mM glucose – like in our experiments – the model predicts that 100 μM phloretin will inhibit the flux by 13% without a gene-expression response, and by 75% if the gene-expression adaptation is taken into account. In reality we measure 30% inhibition at 100 μM phloretin (linear fit to the curve in Fig. 1). We have to be aware, however, that the used $K_i$ value for phloretin has been measured in a buffer that differs substantially from the medium used here.

### *Expression of EP procyclins on the surface and sensitivity to Concanavalin A*

Results so far indicated that the phloretin- or 2-DOG-treated cells had entered into a differentiation programme towards the procyclic stage. We therefore next investigated whether the procyclic features expressed by the phloretin- or 2-DOG-treated cells also encompassed the surface coat, since the mRNA encoding EP procyclin came up after glucose-transport inhibition (Fig. 4A and B). In procyclic trypanosomes the glycosylated EP1 and EP3 proteins bind the lectin Concanavalin A (ConA), which then kills the cells via an unknown mechanism (Hwa and Khoo, 2000; Pearson *et al.*, 2000; Morris *et al.*, 2002). Bloodstream-form trypanosomes do not normally express procyclin proteins and are resistant to ConA killing (Fig. 7A). In contrast, 20–30% of the cells died from exposure to ConA after pre-treatment with phloretin (Fig. 7A), suggesting either that some cells had incorporated procyclins into their coats, or else that the surface VSG had undergone unusual carbohydrate modification. However, we were unable to detect EP procyclins by Western blot (Fig. 7B) or flow cytometry (Fig. S3), so if they are expressed, the level must be very low.

More evidence for a functional change to the procyclic life stage came from experiments with procyclic culture conditions. Phloretin-treated bloodstream-form cells survived incubation under procyclic culture conditions (i.e. in a procyclic culture medium at 28°C) for more than 4 days, while untreated bloodstream-form cells died (Fig. 7C and an independent experiment in Fig. S4A). As a control we subjected the untreated bloodstream-form cells to a temperature downshift from 37°C to 28°C. Under those conditions the cells survived, although they almost stopped growing (Fig. S4B). This result excluded the possibility that the death of untreated trypanosomes under procyclic culture conditions was merely a result of the change in temperature. After 72 h under procyclic culture conditions, the phloretin-treated cells were as sensitive to ConA (Fig. 7D and Fig. S4C) as are procyclic cultures (see Fig. 7A) and Western blot analysis revealed a strong signal for EP procyclin proteins (Fig. 7E). This result indicated that the phloretin treatment had potentiated the ability of the trypanosomes to undergo a differentiation programme.

### *Probing the metabolic signal for differentiation*

We did some first experiments to determine the metabolic signal that triggers differentiation in response to glucose transport inhibition. A lowered [ATP]/[ADP] ratio could be excluded, since the [ATP]/[ADP] ratio did not change (Fig. 8A). Conditional knock-down of the next enzyme of the pathway, HXK, led to upregulation rather than downregulation of THT1 in the first 24 h (Fig. 8B). However, after 48 h, *THT1* mRNA levels had returned to initial levels. These results are compatible with intracellular glucose being the molecule that initiates the signal cascade, but more detailed dynamics are required. It is known that changes in the activities of mitochondrial enzymes influence expression of procyclins (Vassella *et al.*, 2004). Phloretin as well as HXK depletion caused upregulation of mitochondrial enzymes in our experiments and therefore one may expect secondary effects on coat protein expression (Vassella *et al.*, 2004).

## Discussion

In a network-based approach to identify and validate a new drug target within trypanosome glycolysis, we have systematically investigated first the metabolic responses (Bakker *et al.*, 1999a,b) and subsequently (this article) the gene-expression responses that follow inhibition of the glucose transporter. Instead of homeostatic adaptation, inhibition of glucose transport initiated a domino effect that rendered the parasite increasingly vulnerable: first a decrease in the glycolytic flux via metabolic control, then a downregulation of the mRNAs encoding the glucose transporter and most other glycolytic enzymes. Results of a transcriptome analysis indicated that the phloretin treatment had caused the trypanosomes to partially undergo the early stages of differentiation, with some changes typical of growth-arrested stumpy forms with early further differentiation. Consistent with this, the phloretin-treated bloodstream cells had an

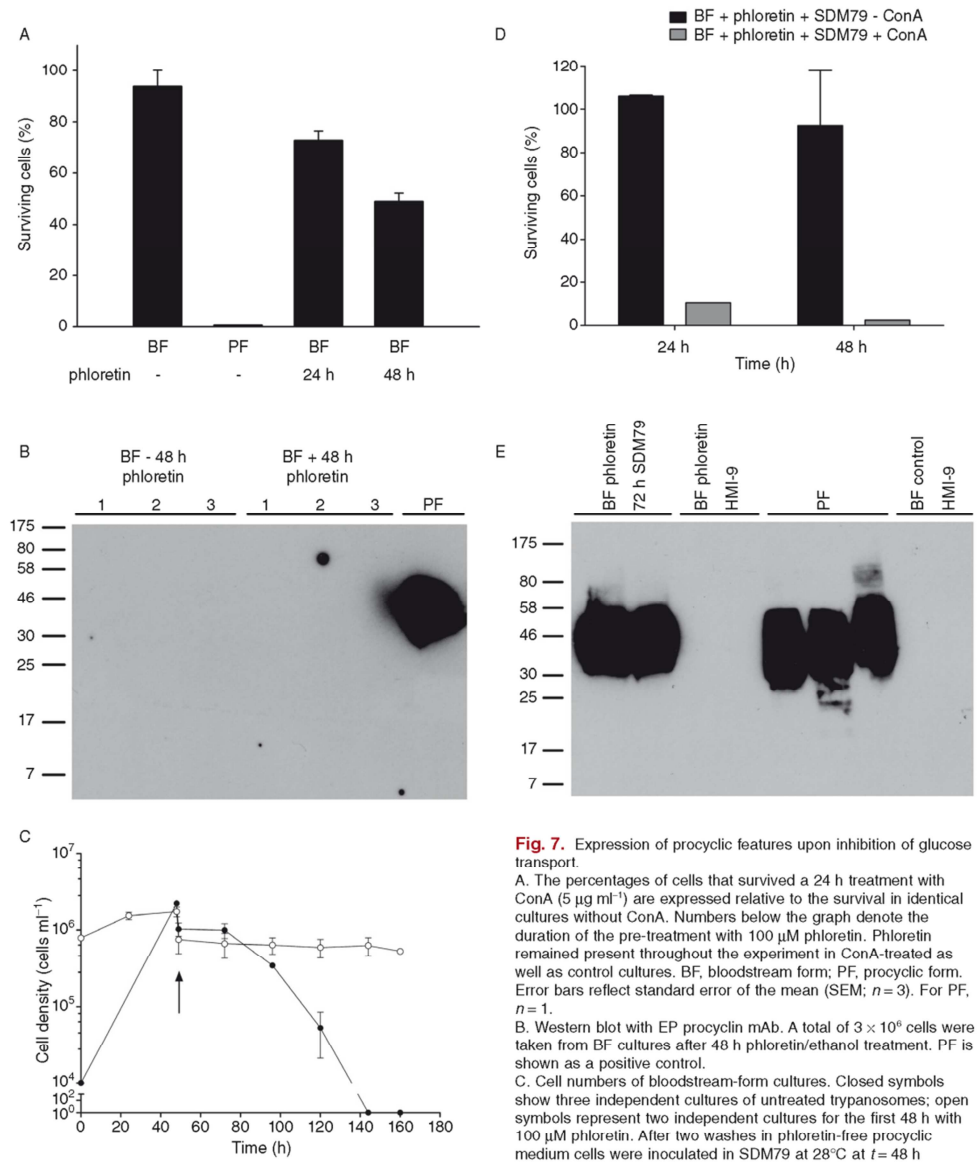


**Fig. 7.** Expression of procyclic features upon inhibition of glucose transport.

A. The percentages of cells that survived a 24 h treatment with ConA (5 μg ml$^{-1}$) are expressed relative to the survival in identical cultures without ConA. Numbers below the graph denote the duration of the pre-treatment with 100 μM phloretin. Phloretin remained present throughout the experiment in ConA-treated as well as control cultures. BF, bloodstream form; PF, procyclic form. Error bars reflect standard error of the mean (SEM; $n = 3$). For PF, $n = 1$.

B. Western blot with EP procyclin mAb. A total of $3 \times 10^6$ cells were taken from BF cultures after 48 h phloretin/ethanol treatment. PF is shown as a positive control.

C. Cell numbers of bloodstream-form cultures. Closed symbols show three independent cultures of untreated trypanosomes; open symbols represent two independent cultures for the first 48 h with 100 μM phloretin. After two washes in phloretin-free procyclic medium cells were inoculated in SDM79 at 28°C at $t = 48$ h (indicated by arrow).

D. After 72 h in procyclic culture medium part of the cell culture was subjected to ConA (5 μg ml$^{-1}$) treatment. The percentages of cells that survived a 24 and 48 h treatment with ConA (5 μg ml$^{-1}$) are expressed relative to the survival in identical cultures without ConA. Error bars indicate standard deviations among two independent experiments.

E. Western blot with EP procyclin mAb. A total of $3 \times 10^6$ cells were taken from cultures after 48 h with phloretin treatment (lanes 3 and 4, $t = 48$ h in C), after 72 h in procyclic medium (lanes 1 and 2, $t = 120$ in C), from untreated procyclic cultures (lanes 5, 6 and 7) and from untreated bloodstream-form cultures (lanes 8 and 9, $t = 48$ h in C). Replicate samples were taken from independent cultures.

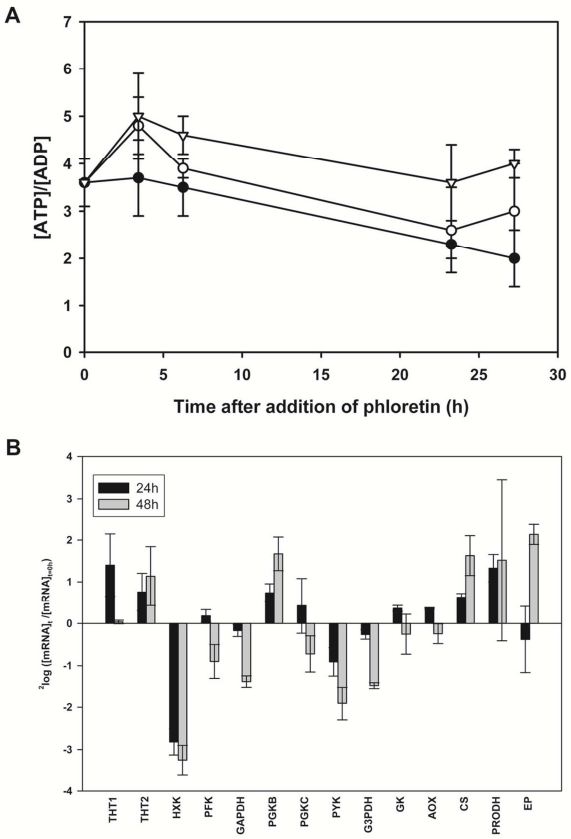


**Fig. 8.** Probing the metabolic signal for differentiation after phloretin treatment.
A. [ATP]/[ADP] ratio in untreated and phloretin-inhibited bloodstream-form trypanosomes. Symbols denote: (●) untreated; (○) 50 μM phloretin; (▽) 100 μM phloretin. Values represent averages ± standard deviations of results obtained from two independent cultures
B. Changes in mRNA levels after HXK RNAi. An inducible HXK RNAi mutant (Albert *et al.*, 2005) was induced by addition of 0.25 μg ml$^{-1}$ tetracycline. mRNA levels at 24 and 48 h were measured by quantitative PCR and compared with levels before induction. Error bars show standard deviations of results from two independent experiments. THT, trypanosome hexose transporter; HXK, hexokinase; PFK, phosphofructokinase; GAPDH, glyceraldehyde-3-phosphate dehydrogenase; PGK, phosphoglycerate kinase; PYK, pyruvate kinase; G3PDH, glycerol-3-phosphate dehydrogenase; AOX, alternative oxidase; CS, citrate synthase; PRODH, proline dehydrogenase; EP, EP procyclin.

enhanced ability to undergo subsequent differentiation steps upon transfer to procyclic culture conditions. The fact that they did not fully differentiate, and were not able to divide under procyclic culture conditions (Fig. 7C), is likely to be due to the fact that we used a monomorphic strain which cannot complete a full life cycle. In addition, glucose transport inhibition might not be sufficient to induce the full spectrum of changes seen in stumpy forms. To address this issue, future studies should be performed with pleomorphic trypanosomes.

As noted in the introduction, alterations of coat-protein expression in glucose-deprived trypanosomes had been observed before, although the resulting transcriptome had not been analysed and the implications for drug treatment were not explored. Is the transcript response to glucose deprivation specific to this particular metabolic challenge, or is it simply a reaction to growth arrest? It has long been known that treatment with dihydrofluoromethyl ornithine, which causes cell-cycle arrest but has no obvious connection to signalling or energy metabolism, can enhance the ability of monomorphic trypanosomes to undergo initial steps of differentiation (Giffin *et al.*, 1986). Growth arrest is known to be important in the differentiation process, and various growth-inhibitory treatments have been shown to induce expression of EP procyclins or their mRNAs (Fenn and Matthews, 2007). We do not really know which of these treatments targeted physiological differentiation control mechanisms, or whether any sort of growth inhibition will do. We therefore examined transcriptome data for bloodstream trypanosomes following treatments that inhibited growth, but had no obvious link to differentiation. None of the treatments caused the differentiation-related gene-expression changes reported in this article. They were: RNAi targeting the small RNA-binding proteins UBP1 and UBP2, or overexpression of UBP2 (Hartmann *et al.*, 2007); RNAi targeting the 14-3-3

proteins (C. Benz and C. Clayton, unpubl. data); knockdown of clathrin expression or treatment with tunicamycin (Koumandou *et al.*, 2008); and treatment with dithiothreitol (Koumandou *et al.*, 2008; Goldshmidt *et al.*, 2010). We cannot rule out the possibility that induction of EP procyclins was missed in all of these experiments because the timing was wrong, or because the parasites were too debilitated to initiate such a response. However, so far, it seems that the transcriptome response to glucose deprivation is not solely a response to growth arrest.

We suggest that trypanosome differentiation can be triggered by a variety of stimuli, but that the intracellular glucose concentration may be a critical intermediate signal. In the case of glucose transport inhibition, the cells seem to be misled by the low glucose influx and respond as if they are in the glucose-poor environment of the tse-tse fly, switching on their differentiation programme. A recently identified phosphatase that is critical for trypanosome differentiation, PIP39, is located inside the glycosome. It is tempting to speculate that this phosphatase is a key player in monitoring glycosomal glucose levels (Szoor *et al.*, 2010).

An anti-trypanosomal drug needs to have a very low cost and to be easy to deliver. It therefore needs to be cheap to manufacture and must be active at low concentrations. It also needs to have as few side-effects as possible, so must be selective for the parasite target. What are the implications of the present study for the use of glucose-transport inhibition against trypanosome infections? To answer this question, we will distinguish two different aspects, namely (i) inhibition of parasite growth and (ii) side-effects on human metabolism.

(i) To cure trypanosomiasis, either all parasites must be killed by the drug, or growth of all of them must be inhibited for a sufficient time to enable elimination of all existing antigenic variants by adaptive immunity. Escape of a single trypanosome with a novel variant surface coat will be sufficient to reinitiate the infection. Ideally therefore we need to attain a drug concentration adequate to kill at least 99% of the parasites (LD99) in the blood and tissues without causing significant side-effects. The LD99 is also influenced by the response of the biochemical network. The high flux control coefficient of the glucose transporter in *T. brucei* will contribute to a low $LD_{99}$, especially since 50% inhibition of glycolytic flux is sufficient to kill the parasite (Fig. 3). On top of this, according to our model calculations, the observed downregulation of glycolytic gene expression upon transporter inhibition led to a four- to fivefold decrease of the inhibitor concentration required to reduce the glycolytic flux. Thus the results of our analyses are favourable to THT1 as a target. If, in line with the results presented here, the few surviving trypanosomes start expressing invariable procyclins this may be an extra, efficient target for the mammalian immune system. The ConA-sensitive mannose residues on the EP proteins (Hwa and Khoo, 2000; Pearson *et al.*, 2000) may be recognized by the mannan-binding lectin of the innate immune system. Whether glucose transporter inhibition is able, by itself, to prompt sufficient surface EP procyclin expression to activate either innate or adaptive immunity is currently unclear: this should be assessed in pleomorphic parasites.

(ii) A low therapeutic drug concentration is of no use if those low levels also kill host cells. And even minor inhibition of glycolysis may be deleterious to some host cell types. Therefore, even if selectivity at the level of molecular recognition is attained, additional selectivity at the network level would be helpful. Simulations with a detailed model of erythrocyte glycolysis (Schuster and Holzhutter, 1995) showed that glucose transport hardly controls erythrocyte glycolysis at all (B. M. Bakker *et al.*, in preparation). This implies that erythrocytes will be less vulnerable to glucose transport inhibition than bloodstream-form trypanosomes. However, a quantitative analysis of potential side-effects on other cell types – including potential homeostatic adaptations – is required.

In the present study, phloretin and 2-DOG were used to inhibit glucose transport in *in vitro* cultures of *T. brucei*. Phloretin has already been used in *in vivo* studies in rats for its anti-tumour activity (Nelson and Falk, 1993) and the LD50 of phloretin for rat hepatocytes in a 2 h incubation was reported as 400 μM (Sabzevari *et al.*, 2004). The concentrations of phloretin and 2-DOG used against trypanosomes in this study (micromolar range) are too high to use in humans, and even too high to serve as a lead compound. Hexose analogues with anti-trypanosome activity have already been developed (Azema *et al.*, 2004) but the mechanism of action was unclear since in many cases the LD50 for the parasite was lower than the $K_i$ for the transporter. For either phloretin or the analogues, a direct comparison of LD50s between trypanosomes and mammalian cells under similar conditions has, to our knowledge, not been performed. It is clear that if inhibitors are to be found, substantial effort will need to be made in screening and in chemical modification, since viable leads are not yet available.

We conclude that although development of specific and potent inhibitors may be a considerable challenge, glucose transport is a more promising drug target in trypanosomes than was thought based on metabolic control alone (Bakker *et al.*, 1999b). Furthermore, this study may open a new avenue to systems biology-based drug target discovery, aiming at tricking microorganisms into lethal

adaptation strategies. Importantly, our results exemplify the importance of monitoring the adaptations of cellular networks in drug target validation (Hornberg and Westerhoff, 2006). Besides identifying cases where a homeostatic response of the pathogen would incapacitate the drug (enabling an early defocusing from that target), it may also reveal more cases like the present one, in which the cellular response is anti-homeostatic. If such an anti-homeostatic response is absent from the human host, the prospects for enhanced specificity of drugs against such targets are substantial.

## Experimental procedures

### *Strains and cultivation*

Monomorphic bloodstream-form *T. brucei* of cell line 449 [a derivative of strain Lister 427 (Biebinger *et al.*, 1997)] were cultivated in HMI-9 (Hirumi and Hirumi, 1989), supplemented with 10% fetal calf serum (FCS, Invitrogen) and 0.2 μg $ml^{-1}$ phleomycin (Cayla) in a water-vapour-saturated incubator at 5% $CO_2$ and 37°C.

Monomorphic procyclic *T. brucei* 449 cells and bloodstream-form cultures subjected to procyclic culture conditions were cultivated in SDM-79 or SOGG-medium [a non-glucose formulation of SDM-79 (Furuya *et al.*, 2002)], supplemented with 10 mM glucose (v/v), 10% FCS and 0.5 μg $ml^{-1}$ phleomycin at 28°C.

Growth was monitored by counting cell numbers in culture samples with a Burker-Türk haemocytometer. The specific growth rate $\mu$ was determined from the increase of the cell numbers in time, by fitting equation $X(t) = X(0) \cdot e^{\mu t}$ to the data. Here $X(t)$ represents the cell density in the culture at time point $t$.

### *Inhibition*

Phloretin, 2-DOG and ConA were purchased from Sigma.

Phloretin was dissolved in 70% ethanol; 2-DOG and ConA in demineralized water. Final concentrations of ethanol were always below 0.7% and the highest ethanol concentration was used in the control cultures.

Increasing cell densities decreased the sensitivity of the cells to phloretin. At constant cell density ($8{\cdot}10^5$ cells $ml^{-1}$ in our experiments), phloretin treatment gave reproducible effects for a given concentration. We used similar cell densities in 2-DOG experiments.

### *RNA isolation and cDNA synthesis*

Total RNA was isolated from $1–4 \times 10^7$ cells by adding 1 ml of Trizol (Invitrogen) to cell pellets according to the manufacturer's protocol. Isolated RNA was DNase-1 (Finnzymes) treated, purified by phenol/chloroform extraction and 1 μg was used in a cDNA synthesis reaction with random hexamer primers (Finnzymes).

### *Microarray*

Fluorescently labelled cDNA was synthesized and hybridized to oligonucleotide microarrays (NIAID) as previously described (Queiroz *et al.*, 2009). Data analysis was performed using the ExpressConverter and MIDAS software which are freely available at http://www.tm4.org. Files obtained from the scan were transformed into .mev files using the ExpressConverter. Using MIDAS the signal intensities were normalized by locally weighted linear regression and duplicate spots on each slide were merged. $Log_2$ transformed data were exported to SAM as described (Tusher *et al.*, 2001). The complete microarray dataset has been uploaded to NCBI GEO with accession number GSE24275 and can be accessed online via: http://www.ncbi.nlm.nih.gov/geo/query/acc.cgi?acc=GSE24275.

### *Real-time quantitative PCR*

Amplification, data collection and data analysis were performed in the ABI 7700 Prism Sequence Detector (once 2 min at 50°C; once 10 min at 95°C; and 40 cycles of 15 s at 95°C followed by 1 min at 59°C). The calculated cycle of threshold values (Ct) were exported to and further analysed in Microsoft Excel. Cycles of threshold for the different genes were normalized to the Ct of hypoxanthine-guanine phosphoribosyl transferase (HGPRT) transcript in the same sample (ΔCt). Transcripts of two other housekeeping genes (60S rRNA and β-tubulin) were assayed as an internal check. Subsequently the normalized Ct values of the different time points were, for each transcript, compared with the Ct of that transcript at time point zero to calculate the fold changes of the mRNA concentrations according to: $mRNA_t/mRNA_{t=0} = 2^{(\Delta Ct(0)-\Delta Ct(t))}$. Dissociation curves proved that only a single-sized product was formed in every qPCR reaction. Primers used in the qPCR are listed in Table S3 in *Supporting information* of this article and were tested for efficiency.

### *Metabolite assays*

Glucose, pyruvate, glycerol, succinate and acetate were measured by HPLC (Rossell *et al.*, 2005). ATP and ADP levels were measured with a luciferase assay as described previously (Rohwer *et al.*, 1996).

### *CS activity assay*

Approximately $3 \times 10^8$ cells were washed twice in ice-cold PBS (140 mM NaCl, 2.7 mM KCl, 10.1 mM $Na_2HPO_4$, 1.8 mM $KH_2PO_4$) and resuspended in 0.5 ml of PBS. Cells were lysed using 0.6 g $ml^{-1}$ acid-washed glass beads (425–600 μm, Sigma) in a Thermo Savant FastPrep FP120 Homogenizer (four cycles of 5 s, speed 6.0, with cooling on ice between cycles for at least 1 min). Cell lysate was transferred to a new tube, centrifuged (maximum speed, at 4°C) and supernatant was used to measure CS activity. CS (E.C. 2.3.3.1) was measured in an automated spectrophotometer (Cobas FARA, Roche) at 412 nm, with an assay modified from Morgunov and Srere (1998). Final concentrations in the assay mixture were 100 mM Tris-HCl (pH 8.0), 0.1 mM oxaloacetic acid; 0.1 mM 5,5′-dithio-bis(2-nitrobenzoic acid (DTNB) and 40 mM KCl. The reaction was started by addition of 0.5 mM acetyl-CoA and the increase in $A_{412}$ (due to conversion of DTNB to TNB) was followed in time. Activities

were determined from the linear part of the $A_{412}$ curves, based on an extinction coefficient for DTNB at 412 nm of 13.6 $mM^{-1}$ $cm^{-1}$. Enzyme activities were normalized to the protein contents of the cell extracts, based on a BCA protein assay (Pierce).

### *Modelling*

The modelling was performed with the most recent version of the glycolysis model (Albert *et al.*, 2005) in the open-source software Jarnac (Sauro, 2000; Sauro *et al.*, 2003). To calculate the effect of phloretin, a competitive inhibitor [I] which only binds to the outside (Bakker *et al.*, 1999b) with an inhibition constant $K_i$ was included in the rate equation for glucose transport across the plasma membrane. To this end, the $K_m$ for extracellular glucose was multiplied with a factor $1 + [I]/K_i$. This yielded the following equation:

$$v_{THT} = \frac{V^{f}_{max}}{K^{Glc}_{m}\cdot\left(1+\frac{[I]}{K_i}\right)}\cdot \frac{[Glc]_{out}-[Glc]_{in}}{1+\frac{[Glc]_{out}}{K^{Glc}_{m}\cdot\left(1+\frac{[I]}{K_i}\right)}+\frac{[Glc]_{in}}{K^{Glc}_{m}}+\alpha\cdot\frac{[Glc]_{out}}{K^{Glc}_{m}\cdot\left(1+\frac{[I]}{K_i}\right)}\cdot\frac{[Glc]_{in}}{K^{Glc}_{m}}}$$

In the version in which gene expression was ignored (solid line in Fig. 6) the original $V_{max}$ values were used (Albert *et al.*, 2005). When altered gene expression was taken into account the $V_{max}$ values were multiplied with the fold change of the transcript levels as measured by qPCR after 24 h (dashed line Fig. 6). In the case of glucose transport, for which two transport proteins exist, we made use of earlier findings that THT1 represented 97.5% and THT2 2.5% of the total THT mRNA pool (Bringaud and Baltz, 1993). This gave rise to the following $V_{max}$ values [in nmol $min^{-1}$ (mg protein)$^{-1}$]:

THT: 108.9·(0.975·0.25 + 0.025·1.22); HXK: 1929·0.35; PGI: 1305·0.32; PFK: 1708·0.29; ALD: 560·0.35; TIM: 999.3·0.34; G3PDH: 465·0.24; GK: 200·0.32; AOX: 368·0.56; GAPDH 720.9·0.26; PGKC: 2862·0.27; PGAM: 225·0.77; ENO: 598·0.31; PYK: 1020·0.17.

### *Western blotting*

For Western blot analysis, $3 \times 10^6$ parasites were harvested by centrifugation, washed in PBS, resuspended in 30 µl of Lämmli buffer and stored at −80°C before analysis. Samples were boiled for 10 min at 95°C and 20 µl was separated on SDS-PAGE (Novex 4–20% Tris-glycine, Invitrogen or 12.5% Tris-glycine) at 125 V and transferred to a nitrocellulose membrane (Hybond-ECL, Amersham) at 150 mA for 4 h. Membranes were blocked for 2 h at room temperature with 5% milk in PBS-T (PBS with 0.05% Tween-20), washed three times with PBS-T, and probed with primary antibody (anti-*Trypanosoma brucei* procyclin mAb, Cedarlane) diluted 1:2000 in 1% milk in PBS-T overnight at 4°C. After three washes with PBS-T, the membrane was incubated with secondary antibody (goat anti-mouse IgG peroxidase conjugate, Calbiochem) 1:2000 in 1% milk in PBS-T for 2 h at room temperature. After five washes with PBS-T, horseradish peroxidase activity was measured with SuperSignal HRP substrate (Novagen).

## Acknowledgements

We thank Professor A.B. Smit and Dr S. Spijker for the use of the qPCR and Dr J. van Hellemond, Professor A. Tielens and Dr Th. Geijtenbeek for discussions. Support from Nederlandse Organisatie voor Wetenschappelijk Onderzoek-Vernieuwings-impuls and IOP Genomics (grants to B.M.B.) from the Scottish Universities Life Science Alliance (studentship to E.J.K.), from the Fonds de la Recherche Scientifique Médicale (FRSM) and the Interuniversity Attraction Poles – Belgian Federal Office for Scientific, Technical and Cultural Affairs (IAP) to P.A.M.M., and from the Nederlandse Organisatie voor Wetenschappelijk Onderzoek, European Union (FP7; BioSim, NucSys, EC-MOAN, YSBN), AstraZeneca and BBSRC to H.V.W. (BBC0082191, BBD0190791, BBF0035281) is acknowledged.

Martin Wurst is supported by the DFG (Sonderforschungsbereich 544). We thank Rafael Queiroz and other members of the Hoheisel lab for assistance with the microarrays, and NIAID for the free microarray slides.

## References

Alberghina, L., and Westerhoff, H.V. (2005) *Systems Biology: Definitions and Perspectives*. Berlin: Springer Verlag.

Albert, M.-A., Haanstra, J., Hannaert, V., Van Roy, J., Opperdoes, F., Bakker, B., and Michels, P. (2005) Experimental and *in silico* analyses of glycolytic flux control in bloodstream form *Trypanosoma brucei*. *J Biol Chem* **280:** 28306–28315.

Aman, R.A., and Wang, C.C. (1986) An improved purification of glycosomes from the procyclic trypomastigotes of *Trypanosoma brucei*. *Mol Biochem Parasitol* **21:** 211–220.

Azema, L., Claustre, S., Alric, I., Blonski, C., Willson, M., Perie, J., *et al.* (2004) Interaction of substituted hexose analogues with the *Trypanosoma brucei* hexose transporter. *Biochem Pharmacol* **67:** 459–467.

Bakker, B.M., Michels, P.A., Opperdoes, F.R., and Westerhoff, H.V. (1999a) What controls glycolysis in bloodstream form *Trypanosoma brucei*? *J Biol Chem* **274:** 14551–14559.

Bakker, B.M., Walsh, M.C., ter Kuile, B.H., Mensonides, F.I., Michels, P.A., Opperdoes, F.R., and Westerhoff, H.V. (1999b) Contribution of glucose transport to the control of the glycolytic flux in *Trypanosoma brucei*. *Proc Natl Acad Sci USA* **96:** 10098–10103.

Barrett, M.P., Burchmore, R.J., Stich, A., Lazzari, J.O., Frasch, A.C., Cazzulo, J.J., and Krishna, S. (2003) The trypanosomiases. *Lancet* **362:** 1469–1480.

Biebinger, S., Wirtz, L.E., and Clayton, C.E. (1997) Vectors for inducible over-expression of potentially toxic gene products in bloodstream and procyclic *Trypanosoma brucei*. *Mol Biochem Parasitol* **85:** 99–112.

Blattner, J., Helfert, S., Michels, P., and Clayton, C.E. (1998) Compartmentation of phosphoglycerate kinase in *Trypanosoma brucei* plays a critical role in parasite energy metabolism. *Proc Natl Acad Sci USA* **95:** 11596–11600.

Borst, P., and Ulbert, S. (2001) Control of VSG gene expression sites. *Mol Biochem Parasitol* **114:** 17–27.
Bringaud, F., and Baltz, T. (1992) A potential hexose transporter gene expressed predominantly in the bloodstream form of *Trypanosoma brucei*. *Mol Biochem Parasitol* **52:** 111–121.
Bringaud, F., and Baltz, T. (1993) Differential regulation of two distinct families of glucose transporter genes in *Trypanosoma brucei*. *Mol Cell Biol* **13:** 1146–1154.
Bringaud, F., Baltz, D., and Baltz, T. (1998) Functional and molecular characterization of a glycosomal PPi-dependent enzyme in trypanosomatids: pyruvate phosphate dikinase. *J Biol Chem* **95:** 7963–7968.
Caceres, A.J., Michels, P.A., and Hannaert, V. (2010) Genetic validation of aldolase and glyceraldehyde-3-phosphate dehydrogenase as drug targets in *Trypanosoma brucei*. *Mol Biochem Parasitol* **169:** 50–54.
Clayton, C., and Shapira, M. (2007) Post-transcriptional regulation of gene expression in trypanosomes and leishmanias. *Mol Biochem Parasitol* **156:** 93–101.
Cross, G.A. (1975) Identification, purification and properties of clone-specific glycoprotein antigens constituting the surface coat of *Trypanosoma brucei*. *Parasitology* **71:** 393–417.
Dean, S., Marchetti, R., Kirk, K., and Matthews, K.R. (2009) A surface transporter family conveys the trypanosome differentiation signal. *Nature* **459:** 213–217.
Ebikeme, C.E., Peacock, L., Coustou, V., Riviere, L., Bringaud, F., Gibson, W.C., and Barrett, M.P. (2008) *N*-acetyl D-glucosamine stimulates growth in procyclic forms of *Trypanosoma brucei* by inducing a metabolic shift. *Parasitology* **135:** 585–594.
Fenn, K., and Matthews, K.R. (2007) The cell biology of *Trypanosoma brucei* differentiation. *Curr Opin Microbiol* **10:** 539–546.
Furuya, T., Kessler, P., Jardim, A., Schnaufer, A., Crudder, C., and Parsons, M. (2002) Glucose is toxic to glycosome-deficient trypanosomes. *Proc Natl Acad Sci USA* **99:** 14177–14182.
Giffin, B.F., McCann, P.P., Bitonti, A.J., and Bacchi, C.J. (1986) Polyamine depletion following exposure to DL-alpha-difluoromethylornithine both *in vivo* and *in vitro* initiates morphologival alterations and mitochondrial activation in a monomorphic strain of *Trypanosoma brucei brucei*. *J Protozool* **33:** 238–243.
Goldshmidt, H., Matas, D., Kabi, A., Carmi, S., Hope, R., and Michaeli, S. (2010) Persistent ER stress induces the spliced leader RNA silencing pathway (SLS), leading to programmed cell death in *Trypanosoma brucei*. *PLoS Pathog* **6:** e1000731.
Groen, A.K., Wanders, R.J., Westerhoff, H.V., van der Meer, R., and Tager, J.M. (1982) Quantification of the contribution of various steps to the control of mitochondrial respiration. *J Biol Chem* **257:** 2754–2757.
Gruszynski, A.E., van Deursen, F.J., Albareda, M.C., Best, A., Chaudhary, K., Cliffe, L.J., *et al.* (2006) Regulation of surface coat exchange by differentiating African trypanosomes. *Mol Biochem Parasitol* **147:** 211–223.
Haile, S., and Papadopoulou, B. (2007) Developmental regulation of gene expression in trypanosomatid parasitic protozoa. *Curr Opin Microbiol* **10:** 569–577.
Hart, D.T., Misset, O., Edwards, S.W., and Opperdoes, F.R. (1984) A comparison of the glycosomes (microbodies) isolated from *Trypanosoma brucei* bloodstream form and cultured procyclic trypomastigotes. *Mol Biochem Parasitol* **12:** 25–35.
Hartmann, C., Benz, C., Brems, S., Ellis, L., Luu, V.D., Stewart, M., *et al.* (2007) Small trypanosome RNA-binding proteins TbUBP1 and TbUBP2 influence expression of F-box protein mRNAs in bloodstream trypanosomes. *Eukaryot Cell* **6:** 1964–1978.
Heinrich, R., and Rapoport, T.A. (1974) A linear steady-state treatment of enzymatic chains. General properties, control and effector strength. *Eur J Biochem* **42:** 89–95.
Helfert, S., Estevez, A.M., Bakker, B., Michels, P., and Clayton, C. (2001) Roles of triosephosphate isomerase and aerobic metabolism in *Trypanosoma brucei*. *Biochem J* **357:** 117–125.
Hellemond, J.J., Bakker, B.M., and Tielens, A.G. (2005) Energy metabolism and its compartmentation in *Trypanosoma brucei*. *Adv Microb Physiol* **50:** 199–226.
Herman, M., Perez-Morga, D., Schtickzelle, N., and Michels, P.A. (2008) Turnover of glycosomes during life-cycle differentiation of *Trypanosoma brucei*. *Autophagy* **4:** 294–308.
Hirumi, H., and Hirumi, K. (1989) Continuous cultivation of *Trypanosoma brucei* blood stream forms in a medium containing a low concentration of serum protein without feeder cell layers. *J Parasitol* **75:** 985–989.
Hornberg, J.J., and Westerhoff, H.V. (2006) Oncogenes are to lose control on signaling following mutation: should we aim off target? *Mol Biotechnol* **34:** 109–116.
Hwa, K.Y., and Khoo, K.H. (2000) Structural analysis of the asparagine-linked glycans from the procyclic *Trypanosoma brucei* and its glycosylation mutants resistant to Concanavalin A killing. *Mol Biochem Parasitol* **111:** 173–184.
Jenkins, T.M., Eisenthal, R., and Weitzman, P.D. (1988) Two distinct succinate thiokinases in both bloodstream and procyclic forms of *Trypanosoma brucei*. *Biochem Biophys Res Commun* **151:** 257–261.
Jensen, B.C., Sivam, D., Kifer, C.T., Myler, P.J., and Parsons, M. (2009) Widespread variation in transcript abundance within and across developmental stages of *Trypanosoma brucei*. *BMC Genomics* **10:** 482.
Kabani, S., Fenn, K., Ross, A., Ivens, A., Smith, T.K., Ghazal, P., and Matthews, K. (2009) Genome-wide expression profiling of *in vivo*-derived bloodstream parasite stages and dynamic analysis of mRNA alterations during synchronous differentiation in *Trypanosoma brucei*. *BMC Genomics* **10:** 427.
Kacser, H., and Burns, J.A. (1973) The control of flux. *Symp Soc Exp Biol* **27:** 65–104.
Koumandou, V.L., Natesan, S.K., Sergeenko, T., and Field, M.C. (2008) The trypanosome transcriptome is remodelled during differentiation but displays limited responsiveness within life stages. *BMC Genomics* **9:** 298.
Krupka, R.M., and Deves, R. (1980) Evidence for allosteric inhibition sites in the glucose carrier of erythrocytes. *Biochim Biophys Acta* **598:** 127–133.
Lamour, N., Riviere, L., Coustou, V., Coombs, G.H., Barrett, M.P., and Bringaud, F. (2005) Proline metabolism in procyclic *Trypanosoma brucei* is down-regulated in the presence of glucose. *J Biol Chem* **280:** 11902–11910.

Matthews, K.R. (2005) The developmental cell biology of *Trypanosoma brucei*. *J Cell Sci* **118:** 283–290.
Milne, K.G., Prescott, A.R., and Ferguson, M.A. (1998) Transformation of monomorphic *Trypanosoma brucei* bloodstream form trypomastigotes into procyclic forms at 37 degrees C by removing glucose from the culture medium. *Mol Biochem Parasitol* **94:** 99–112.
Morgunov, I., and Srere, P.A. (1998) Interaction between citrate synthase and malate dehydrogenase. Substrate channeling of oxaloacetate. *J Biol Chem* **273:** 29540–29544.
Morris, J.C., Wang, Z., Drew, M.E., and Englund, P.T. (2002) Glycolysis modulates trypanosome glycoprotein expression as revealed by an RNAi library. *EMBO J* **21:** 4429–4438.
Nelson, J.A., and Falk, R.E. (1993) The efficacy of phloridzin and phloretin on tumor cell growth. *Anticancer Res* **13:** 2287–2292.
Nilsson, D., Gunasekera, K., Mani, J., Osteras, M., Farinelli, L., Baerlocher, L., *et al.* (2010) Spliced leader trapping reveals widespread alternative splicing patterns in the highly dynamic transcriptome of *Trypanosoma brucei*. *PLoS Pathog* **6:** pii: e1001037.
Noble, D. (2006) Systems biology and the heart. *Biosystems* **83:** 75–80.
Pearson, T.W., Beecroft, R.P., Welburn, S.C., Ruepp, S., Roditi, I., Hwa, K.Y., *et al.* (2000) The major cell surface glycoprotein procyclin is a receptor for induction of a novel form of cell death in African trypanosomes *in vitro*. *Mol Biochem Parasitol* **111:** 333–349.
Priest, J.W., and Hajduk, S.L. (1994) Developmental regulation of mitochondrial biogenesis in *Trypanosoma brucei*. *J Bioenerg Biomembr* **26:** 179–191.
Queiroz, R., Benz, C., Fellenberg, K., Hoheisel, J.D., and Clayton, C. (2009) Transcriptome analysis of differentiating trypanosomes reveals the existence of multiple post-transcriptional regulons. *BMC Genomics* **10:** 495.
Rohwer, J.M., Jensen, P.R., Shinohara, Y., Postma, P.W., and Westerhoff, H.V. (1996) Changes in the cellular energy state affect the activity of the bacterial phosphotransferase system. *Eur J Biochem* **235:** 225–230.
Rossell, S., van der Weijden, C., Kruckeberg, A., Bakker, B., and Westerhoff, H. (2005) Hierarchical and metabolic regulation of glucose influx in starved *Saccharomyces cerevisiae*. *FEMS Yeast Res* **5:** 611–619.
Sabzevari, O., Galati, G., Moridani, M.Y., Siraki, A., and O'Brien, P.J. (2004) Molecular cytotoxic mechanisms of anticancer hydroxychalcones. *Chem Biol Interact* **148:** 57–67.
Sauro, H.M. (2000) Jarnac: a system for interactive metabolic analysis. In *Animating the Cellular Map: Proceedings of the 9th International Meeting on BioThermoKinetics*. Hofmeyr, J.H.S., Rohwer, J.M., and Snoep, J.L. (eds). South Africa: Stellenbosch University Press, pp. 221–228.
Sauro, H.M., Hucka, M., Finney, A., Wellock, C., Bolouri, H., Doyle, J., and Kitano, H. (2003) Next generation simulation tools: the Systems Biology Workbench and BioSPICE integration. *Omics* **7:** 355–372.
Schuster, R., and Holzhutter, H.G. (1995) Use of mathematical models for predicting the metabolic effect of large-scale enzyme activity alterations. Application to enzyme deficiencies of red blood cells. *Eur J Biochem* **229:** 403–418.
Siegel, T.N., Hekstra, D.R., Wang, X., Dewell, S., and Cross, G.A. (2010) Genome-wide analysis of mRNA abundance in two life-cycle stages of *Trypanosoma brucei* and identification of splicing and polyadenylation sites. *Nucleic Acids Res* **38:** 4946–4957.
Szoor, B., Ruberto, I., Burchmore, R., and Matthews, K.R. (2010) A novel phosphatase cascade regulates differentiation in *Trypanosoma brucei* via a glycosomal signaling pathway. *Genes Dev* **24:** 1306–1316.
Tetaud, E., Barrett, M.P., Bringaud, F., and Baltz, T. (1997) Kinetoplastid glucose transporters. *Biochem J* **325** (Part 3): 569–580.
Tusher, V.G., Tibshirani, R., and Chu, G. (2001) Significance analysis of microarrays applied to the ionizing radiation response. *Proc Natl Acad Sci USA* **98:** 5116–5121.
Urwyler, S., Vassella, E., Van Den Abbeele, J., Renggli, C.K., Blundell, P., Barry, J.D., and Roditi, I. (2005) Expression of procyclin mRNAs during cyclical transmission of *Trypanosoma brucei*. *PLoS Pathog* **1:** e22.
Vassella, E., Acosta-Serrano, A., Studer, E., Lee, S.H., Englund, P.T., and Roditi, I. (2001) Multiple procyclin isoforms are expressed differentially during the development of insect forms of *Trypanosoma brucei*. *J Mol Biol* **312:** 597–607.
Vassella, E., Probst, M., Schneider, A., Studer, E., Renggli, C., and Roditi, I. (2004) Expression of a major surface protein of *Trypanosoma brucei* insect forms is controlled by the activity of mitochondrial enzymes. *Mol Biol Cell* **15:** 3986–3993.
Verlinde, C.L., Hannaert, V., Blonski, C., Willson, M., Perie, J.J., Fothergill-Gilmore, L.A., *et al.* (2001) Glycolysis as a target for the design of new anti-trypanosome drugs. *Drug Resist Updat* **4:** 50–65.

## Supporting information

Additional supporting information may be found in the online version of this article.

Please note: Wiley-Blackwell are not responsible for the content or functionality of any supporting materials supplied by the authors. Any queries (other than missing material) should be directed to the corresponding author for the article.

# 6. References


1. Sogin, M.L., et al., *Phylogenetic meaning of the kingdom concept: an unusual ribosomal RNA from Giardia lamblia.* Science, 1989. **243**(4887): p. 75-7.
2. Renger, H.C. and D.R. Wolstenholme, *Kinetoplast and other satellite DNAs of kinetoplastic and dyskinetoplastic strains of Trypanosoma.* J Cell Biol, 1971. **50**(2): p. 533-40.
3. Liu, B., et al., *Fellowship of the rings: the replication of kinetoplast DNA.* Trends Parasitol, 2005. **21**(8): p. 363-9.
4. Barrett, M.P., et al., *The trypanosomiases.* Lancet, 2003. **362**(9394): p. 1469-80.
5. Vanhollebeke, B., et al., *Human serum lyses Trypanosoma brucei by triggering uncontrolled swelling of the parasite lysosome.* J Eukaryot Microbiol, 2007. **54**(5): p. 448-51.
6. Balogun, R.A., *Studies on the amino acids of the tsetse fly, Glossina morsitans, maintained on in vitro and in vivo feeding systems.* Comp Biochem Physiol A Comp Physiol, 1974. **49**(2A): p. 215-22.
7. Lamour, N., et al., *Proline metabolism in procyclic Trypanosoma brucei is down-regulated in the presence of glucose.* J Biol Chem, 2005. **280**(12): p. 11902-10.
8. Roditi, I. and M. Liniger, *Dressed for success: the surface coats of insect-borne protozoan parasites.* Trends Microbiol, 2002. **10**(3): p. 128-34.
9. Acosta-Serrano, A., et al., *The surface coat of procyclic Trypanosoma brucei: programmed expression and proteolytic cleavage of procyclin in the tsetse fly.* Proc Natl Acad Sci U S A, 2001. **98**(4): p. 1513-8.
10. Engstler, M., et al., *Hydrodynamic flow-mediated protein sorting on the cell surface of trypanosomes.* Cell, 2007. **131**(3): p. 505-15.
11. Cross, G.A., L.E. Wirtz, and M. Navarro, *Regulation of vsg expression site transcription and switching in Trypanosoma brucei.* Mol Biochem Parasitol, 1998. **91**(1): p. 77-91.
12. McCulloch, R., *Antigenic variation in African trypanosomes: monitoring progress.* Trends Parasitol, 2004. **20**(3): p. 117-21.
13. Matthews, K.R., *The developmental cell biology of Trypanosoma brucei.* J Cell Sci, 2005. **118**(Pt 2): p. 283-90.
14. Jensen, B.C., et al., *Widespread variation in transcript abundance within and across developmental stages of Trypanosoma brucei.* BMC Genomics, 2009. **10**: p. 482.
15. Queiroz, R., et al., *Transcriptome analysis of differentiating trypanosomes reveals the existence of multiple post-transcriptional regulons.* BMC Genomics, 2009. **10**: p. 495.
16. Kabani, S., et al., *Genome-wide expression profiling of in vivo-derived bloodstream parasite stages and dynamic analysis of mRNA alterations during synchronous differentiation in Trypanosoma brucei.* BMC Genomics, 2009. **10**: p. 427.
17. Siegel, T.N., et al., *Genome-wide analysis of mRNA abundance in two life-cycle stages of Trypanosoma brucei and identification of splicing and polyadenylation sites.* Nucleic Acids Res, 2010.
18. Bringaud, F. and T. Baltz, *Differential regulation of two distinct families of glucose transporter genes in Trypanosoma brucei.* Mol Cell Biol, 1993. **13**(2): p. 1146-54.
19. Overath, P., J. Czichos, and C. Haas, *The effect of citrate/cis-aconitate on oxidative metabolism during transformation of Trypanosoma brucei.* Eur J Biochem, 1986. **160**(1): p. 175-82.
20. Dean, S., et al., *A surface transporter family conveys the trypanosome differentiation signal.* Nature, 2009. **459**(7244): p. 213-7.

21. Szoor, B., et al., *A novel phosphatase cascade regulates differentiation in Trypanosoma brucei via a glycosomal signaling pathway.* Genes Dev, 2010. **24**(12): p. 1306-16.
22. Milne, K.G., A.R. Prescott, and M.A. Ferguson, *Transformation of monomorphic Trypanosoma brucei bloodstream form trypomastigotes into procyclic forms at 37 degrees C by removing glucose from the culture medium.* Mol Biochem Parasitol, 1998. **94**(1): p. 99-112.
23. Haanstra, J.R., et al., *A domino effect in drug action: from metabolic assault towards parasite differentiation.* Mol Microbiol, 2011. **79**(1): p. 94-108.
24. Ziegelbauer, K., et al., *Synchronous differentiation of Trypanosoma brucei from bloodstream to procyclic forms in vitro.* Eur J Biochem, 1990. **192**(2): p. 373-8.
25. Martinez-Calvillo, S., et al., *Transcription of Leishmania major Friedlin chromosome 1 initiates in both directions within a single region.* Mol Cell, 2003. **11**(5): p. 1291-9.
26. Siegel, T.N., et al., *Four histone variants mark the boundaries of polycistronic transcription units in Trypanosoma brucei.* Genes Dev, 2009. **23**(9): p. 1063-76.
27. Ullu, E., K.R. Matthews, and C. Tschudi, *Temporal order of RNA-processing reactions in trypanosomes: rapid trans splicing precedes polyadenylation of newly synthesized tubulin transcripts.* Mol Cell Biol, 1993. **13**(1): p. 720-5.
28. Matthews, K.R., C. Tschudi, and E. Ullu, *A common pyrimidine-rich motif governs trans-splicing and polyadenylation of tubulin polycistronic pre-mRNA in trypanosomes.* Genes Dev, 1994. **8**(4): p. 491-501.
29. Chung, H.M., M.G. Lee, and L.H. Van der Ploeg, *RNA polymerase I-mediated protein-coding gene expression in Trypanosoma brucei.* Parasitol Today, 1992. **8**(12): p. 414-8.
30. Gunzl, A., et al., *RNA polymerase I transcribes procyclin genes and variant surface glycoprotein gene expression sites in Trypanosoma brucei.* Eukaryot Cell, 2003. **2**(3): p. 542-51.
31. Mair, G., et al., *A new twist in trypanosome RNA metabolism: cis-splicing of pre-mRNA.* RNA, 2000. **6**(2): p. 163-9.
32. Berriman, M., et al., *The genome of the African trypanosome Trypanosoma brucei.* Science, 2005. **309**(5733): p. 416-22.
33. Haile, S. and B. Papadopoulou, *Developmental regulation of gene expression in trypanosomatid parasitic protozoa.* Curr Opin Microbiol, 2007. **10**(6): p. 569-77.
34. Buttner, K., K. Wenig, and K.P. Hopfner, *The exosome: a macromolecular cage for controlled RNA degradation.* Mol Microbiol, 2006. **61**(6): p. 1372-9.
35. Parker, R. and H. Song, *The enzymes and control of eukaryotic mRNA turnover.* Nat Struct Mol Biol, 2004. **11**(2): p. 121-7.
36. Song, M.G., Y. Li, and M. Kiledjian, *Multiple mRNA decapping enzymes in mammalian cells.* Mol Cell, 2010. **40**(3): p. 423-32.
37. Schwede, A., et al., *A role for Caf1 in mRNA deadenylation and decay in trypanosomes and human cells.* Nucleic Acids Res, 2008. **36**(10): p. 3374-88.
38. Haile, S., A.M. Estevez, and C. Clayton, *A role for the exosome in the in vivo degradation of unstable mRNAs.* RNA, 2003. **9**(12): p. 1491-501.
39. Li, C.H., et al., *Roles of a Trypanosoma brucei 5'->3' exoribonuclease homolog in mRNA degradation.* RNA, 2006. **12**(12): p. 2171-86.
40. Kulkarni, M., S. Ozgur, and G. Stoecklin, *On track with P-bodies.* Biochem Soc Trans, 2010. **38**(Pt 1): p. 242-51.
41. Kramer, S., et al., *Heat shock causes a decrease in polysomes and the appearance of stress granules in trypanosomes independently of eIF2(alpha) phosphorylation at Thr169.* J Cell Sci, 2008. **121**(Pt 18): p. 3002-14.

42. Fan, X.C. and J.A. Steitz, *Overexpression of HuR, a nuclear-cytoplasmic shuttling protein, increases the in vivo stability of ARE-containing mRNAs.* EMBO J, 1998. **17**(12): p. 3448-60.
43. Peng, S.S., et al., *RNA stabilization by the AU-rich element binding protein, HuR, an ELAV protein.* EMBO J, 1998. **17**(12): p. 3461-70.
44. Antson, A.A., *Single-stranded-RNA binding proteins.* Curr Opin Struct Biol, 2000. **10**(1): p. 87-94.
45. Wang, X. and T.M. Tanaka Hall, *Structural basis for recognition of AU-rich element RNA by the HuD protein.* Nat Struct Biol, 2001. **8**(2): p. 141-5.
46. Sandler, H. and G. Stoecklin, *Control of mRNA decay by phosphorylation of tristetraprolin.* Biochem Soc Trans, 2008. **36**(Pt 3): p. 491-6.
47. Sanduja, S., F.F. Blanco, and D.A. Dixon, *The roles of TTP and BRF proteins in regulated mRNA decay.* WIREs RNA, 2010. **2**(1): p. 42-57.
48. De Gaudenzi, J., A.C. Frasch, and C. Clayton, *RNA-binding domain proteins in Kinetoplastids: a comparative analysis.* Eukaryot Cell, 2005. **4**(12): p. 2106-14.
49. Kramer, S., N.C. Kimblin, and M. Carrington, *Genome-wide in silico screen for CCCH-type zinc finger proteins of Trypanosoma brucei, Trypanosoma cruzi and Leishmania major.* BMC Genomics, 2010. **11**: p. 283.
50. Luu, V.D., et al., *Functional analysis of Trypanosoma brucei PUF1.* Mol Biochem Parasitol, 2006. **150**(2): p. 340-9.
51. D'Orso, I. and A.C. Frasch, *TcUBP-1, a developmentally regulated U-rich RNA-binding protein involved in selective mRNA destabilization in trypanosomes.* J Biol Chem, 2001. **276**(37): p. 34801-9.
52. D'Orso, I. and A.C. Frasch, *TcUBP-1, an mRNA destabilizing factor from trypanosomes, homodimerizes and interacts with novel AU-rich element- and Poly(A)-binding proteins forming a ribonucleoprotein complex.* J Biol Chem, 2002. **277**(52): p. 50520-8.
53. Hartmann, C., et al., *Small trypanosome RNA-binding proteins TbUBP1 and TbUBP2 influence expression of F-box protein mRNAs in bloodstream trypanosomes.* Eukaryot Cell, 2007. **6**(11): p. 1964-78.
54. Quijada, L., et al., *Expression of the human RNA-binding protein HuR in Trypanosoma brucei increases the abundance of mRNAs containing AU-rich regulatory elements.* Nucleic Acids Res, 2002. **30**(20): p. 4414-24.
55. Blattner, J. and C.E. Clayton, *The 3'-untranslated regions from the Trypanosoma brucei phosphoglycerate kinase-encoding genes mediate developmental regulation.* Gene, 1995. **162**(1): p. 153-6.
56. Hotz, H.R., et al., *Role of 3'-untranslated regions in the regulation of hexose transporter mRNAs in Trypanosoma brucei.* Mol Biochem Parasitol, 1995. **75**(1): p. 1-14.
57. Estevez, A.M., *The RNA-binding protein TbDRBD3 regulates the stability of a specific subset of mRNAs in trypanosomes.* Nucleic Acids Res, 2008. **36**(14): p. 4573-86.
58. McNicoll, F., et al., *Distinct 3'-untranslated region elements regulate stage-specific mRNA accumulation and translation in Leishmania.* J Biol Chem, 2005. **280**(42): p. 35238-46.
59. Archer, S.K., et al., *Trypanosoma brucei PUF9 regulates mRNAs for proteins involved in replicative processes over the cell cycle.* PLoS Pathog, 2009. **5**(8): p. e1000565.
60. Doller, A., J. Pfeilschifter, and W. Eberhardt, *Signalling pathways regulating nucleo-cytoplasmic shuttling of the mRNA-binding protein HuR.* Cell Signal, 2008. **20**(12): p. 2165-73.

61. Nett, I.R., et al., *The phosphoproteome of bloodstream form Trypanosoma brucei, causative agent of African sleeping sickness.* Mol Cell Proteomics, 2009. **8**(7): p. 1527-38.
62. Szoor, B., et al., *Protein tyrosine phosphatase TbPTP1: A molecular switch controlling life cycle differentiation in trypanosomes.* J Cell Biol, 2006. **175**(2): p. 293-303.
63. Albert, M.A., et al., *Experimental and in silico analyses of glycolytic flux control in bloodstream form Trypanosoma brucei.* J Biol Chem, 2005. **280**(31): p. 28306-15.
64. Bringaud, F. and T. Baltz, *A potential hexose transporter gene expressed predominantly in the bloodstream form of Trypanosoma brucei.* Mol Biochem Parasitol, 1992. **52**(1): p. 111-21.
65. Hannaert, V. and P.A. Michels, *Structure, function, and biogenesis of glycosomes in kinetoplastida.* J Bioenerg Biomembr, 1994. **26**(2): p. 205-12.
66. Colasante, C., et al., *Comparative proteomics of glycosomes from bloodstream form and procyclic culture form Trypanosoma brucei brucei.* Proteomics, 2006. **6**(11): p. 3275-93.
67. Igoillo-Esteve, M., et al., *Glycosomal ABC transporters of Trypanosoma brucei: Characterisation of their expression, topology and substrate specificity.* Int J Parasitol, 2010.
68. Michels, P.A., et al., *Metabolic functions of glycosomes in trypanosomatids.* Biochim Biophys Acta, 2006. **1763**(12): p. 1463-77.
69. Blattner, J., et al., *Compartmentation of phosphoglycerate kinase in Trypanosoma brucei plays a critical role in parasite energy metabolism.* Proc Natl Acad Sci U S A, 1998. **95**(20): p. 11596-600.
70. Bakker, B.M., et al., *Contribution of glucose transport to the control of the glycolytic flux in Trypanosoma brucei.* Proc Natl Acad Sci U S A, 1999. **96**(18): p. 10098-103.
71. Bakker, B.M., et al., *What controls glycolysis in bloodstream form Trypanosoma brucei?* J Biol Chem, 1999. **274**(21): p. 14551-9.
72. Tetaud, E., et al., *Kinetoplastid glucose transporters.* Biochem J, 1997. **325 ( Pt 3)**: p. 569-80.
73. Hirumi, H. and K. Hirumi, *Continuous cultivation of Trypanosoma brucei blood stream forms in a medium containing a low concentration of serum protein without feeder cell layers.* J Parasitol, 1989. **75**(6): p. 985-9.
74. van Deursen, F.J., et al., *Characterisation of the growth and differentiation in vivo and in vitro-of bloodstream-form Trypanosoma brucei strain TREU 927.* Mol Biochem Parasitol, 2001. **112**(2): p. 163-71.
75. Haile, S., et al., *The subcellular localisation of trypanosome RRP6 and its association with the exosome.* Mol Biochem Parasitol, 2007. **151**(1): p. 52-8.
76. Tusher, V.G., R. Tibshirani, and G. Chu, *Significance analysis of microarrays applied to the ionizing radiation response.* Proc Natl Acad Sci U S A, 2001. **98**(9): p. 5116-21.
77. Wurst, M., et al., *An RNAi screen of the RRM-domain proteins of Trypanosoma brucei.* Mol Biochem Parasitol, 2009. **163**(1): p. 61-5.
78. Morris, M.T., et al., *Activity of a second Trypanosoma brucei hexokinase is controlled by an 18-amino-acid C-terminal tail.* Eukaryot Cell, 2006. **5**(12): p. 2014-23.
79. Alsford, S., et al., *High-throughput phenotyping using parallel sequencing of RNA interference targets in the African trypanosome.* Genome Res, 2011.
80. Samuels, M., G. Deshpande, and P. Schedl, *Activities of the Sex-lethal protein in RNA binding and protein:protein interactions.* Nucleic Acids Res, 1998. **26**(11): p. 2625-37.
81. Haanstra, J.R., et al., *Compartmentation prevents a lethal turbo-explosion of glycolysis in trypanosomes.* Proc Natl Acad Sci U S A, 2008. **105**(46): p. 17718-23.

82. Kramer, S., et al., *The RNA helicase DHH1 is central to the correct expression of many developmentally regulated mRNAs in trypanosomes.* J Cell Sci, 2010. **123**(Pt 5): p. 699-711.
83. Cassola, A. and A.C. Frasch, *An RNA recognition motif mediates the nucleocytoplasmic transport of a trypanosome RNA-binding protein.* J Biol Chem, 2009. **284**(50): p. 35015-28.
84. Hafner, M., et al., *Transcriptome-wide identification of RNA-binding protein and microRNA target sites by PAR-CLIP*. Cell, 2010. **141**(1): p. 129-41.